

Satu Peltonen

Development of a Specific Cell-based Platform to Analyze Proteolytic Activity of Cancer Relevant Serine Proteases

Helsinki Metropolia University of Applied Sciences

Bachelor of Engineering

Biotechnology and Food Engineering

Final Thesis

30.05.2015

Abstract

Author(s) Title Number of Pages Date	Satu Peltonen Development of a Specific Cell-based Platform to Analyze Proteolytic Activity of Cancer Relevant Serine Proteases 70 pages + 6 appendices 30 May 2015
Degree	Bachelor of Engineering
Degree Programme	Biotechnology and Food Engineering
Specialization option	Biomedicine
Instructor(s)	Topi Tervonen, PhD Tiina Soininen, Phil. Lic., Lecturer
<p>Serine proteases modify the cell's internal and external environment, whereas their most important role is in activating or inactivating other proteins by cleavage and their dysregulation is one feature of cancer. They are particularly implicated in tumor growth, invasion and metastasis. Serine proteases are associated with diverse cancer types and pathologies, such as ovarian and prostatic cancer, but also inflammatory and viral diseases. Serine proteases are widely studied as biomarkers and drug targets in drug discovery although compounds with good pharmacokinetic properties have been difficult to obtain.</p> <p>The aim of this thesis was to develop an enzymatic assay targeting hepsin, which is associated inter alia with breast cancer. The development project was made for the Cancer Cell Circuitry Laboratory that is investigating oncogenes and tumor suppressors in breast cancer. The Cancer Cell Circuitry Laboratory is part of the Translational Cancer Research Program in Institute of Biomedicine in University of Helsinki. The development project consisted of two assay formats, namely biochemical assay and cell-based assay. The biochemical assay was optimized and further developed from a commercial protocol based on recombinant hepsin by R&DSystems. The development of cell-based assay was based on doxycycline inducible hepsin expressed in non-malignant mammary epithelial MCF 10A cells.</p> <p>Final assay design parameters includes 0.1 nM rhHepsin, 15 μM BOC, 6 μM positive control and 0.3 % DMSO. The functionality of the biochemical assay was verified by signal variability assessment and further ascertained by the compound screening. It should be noted that the compounds are exposed to changes in room temperature during incubation which leads to significant variations in results regarding compounds.</p> <p>The development of the cell-based assay could not be finalized due to the extent of the project and lack of time caused by replacement of the original equipment. Since the time scope was too limited for a thorough experimental design, all results can be considered indicative. The vital point is to ensure cell viability after seeding to 96-well plate as it is the main source of variation. Another aspect is the usage of doxycyclin which may lead to a combined reaction with the substrate.</p>	
Keywords	cancer, serine proteinase inhibitors, proteolysis, screening analysis, drug design

Tiivistelmä

Tekijä(t) Otsikko Sivumäärä Aika	Satu Peltonen Spesifisen solupohjaisen alustan kehitys syövälle oleellisten seriiniproteaasien analysoimiseksi 70 sivua + 6 liitettä 30.5.2015
Tutkinto	insinööri (AMK)
Koulutusohjelma	Bio- ja elintarviketekniikka
Suuntautumisvaihtoehto	Biolääketiede
Ohjaaja(t)	FT, Topi Tervonen FL, lehtori Tiina Soininen
<p>Seriiniproteaasit muokkaavat solun ulkoista ja sisäistä ympäristöä, missä niiden tärkein rooli on muiden proteiinien pilkkominen aktiivisiksi tai inaktiivisiksi, ja niiden säätelyhäiriö on yksi syövän tunnusmerkeistä. Erityisesti ne osallistuvat tuumorin kasvuun, invaasioon ja etäpesäkkeiden leviämiseen. Seriiniproteaasit on liitetty erilaisiin syövän lajeihin ja sairauksiin, kuten munasarjojen ja eturauhasen syöpiin, mutta myös tulehdus- ja virustauteihin. Seriiniproteaaseja on laajalti tutkittu lääkekehityksen kohteina, vaikka hyvien farmakokiineettisten ominaisuuksien omaavia yhdisteitä on ollut vaikea löytää.</p> <p>Opinnäytetyön tavoitteena oli kehittää entsyymaattinen määrittäsalusta, jonka kohteena on hepsin, joka liittyy muun muassa rintasyöpään. Kehittämishanke tehtiin Cancer Cell Circuitry laboratoriolle, joka tutkii rintasyöpään liittyviä onkogeenejä ja tuumorisuppressoreita. Cancer Cell Circuitry laboratorio on osa Biomedicum Biolääketieteen laitoksen Translational syöpätutkimuksen ohjelmaa. Kehittämishanke koostui kahdesta formaatista eli biokemiallisesta määrittäsalustasta ja solupohjaisesta määrittäsalustasta. Biokemiallinen määrittäsalusta optimointiin ja edelleen kehitettiin kaupallisesta protokollasta, joka perustui R&D Systemsin rekombinanttiin hepsiniin. Solupohjaisen määrittäsalustan kehittämisen perustana käytettiin hyvänlaatuista MCF 10A rintaepiteelisolulinjaa, jossa hepsiinin ekspresio indusoitiin doksisykliinillä.</p> <p>Valmis biokemiallinen määrittäsalusta pitää sisällään 0.1 nM rhHepsiiniä, 15 µM BOC substrattia, 6 µM positiivista kontrollia ja 0.3 % DMSO:ta. Biokemiallisen määrittäsalustan toimivuus varmistettiin signaalin vaihtelun arvioinnilla sekä edelleen todentamalla yhdisteiden seulonnan yhteydessä. Huomattavaa on, että yhdisteet altistuvat inkubaation aikana huonelämpötilan vaihteluille, mikä johtaa merkittäviin vaihteluihin tuloksissa yhdisteiden osalta.</p> <p>Solupohjaista määrittäsalustaa ei voitu saattaa päätökseen projektin laajuudesta sekä alkuperäisen laitteiston korvaamisesta johtuvan ajan puutteen vuoksi. Aikarajoituksesta johtuen testisuunnitelmia ei voitu perusteellisesti käydä läpi, joten tuloksia voidaan pitää alustavina. Olennaisinta on varmistaa solujen elinkelpoisuus 96-kuoppalevyllä kylvön jälkeen, sillä tämä on suurin vaihtelun aiheuttaja tuloksissa. Toinen näkökohta on doxycyclinin käyttö, mikä saattaa johtaa yhteisvaikutukseen substratin kanssa.</p>	
Avainsanat	syöpä, seriiniproteinaasin estäjät, proteolyysi, seulonta, lääkesuunnittelu

Table of Contents

Appreviations

1	Introduction	1
2	Introduction to Proteolytic Enzymes	2
2.1	Serine Proteases	3
2.2	Membrane-Anchored Serine Proteases	4
2.3	Human Hepsin	6
3	Biological Role of Membrane-anchored Serine Proteases	7
3.1	Zymogen Cascades	7
3.2	Activation and Regulation	8
3.3	Biological Role of Human Hepsin	9
4	Membrane-anchored Serine Proteases in Pathologies	9
4.1	Membrane-anchored Serine Proteases in Cancer	10
4.2	Dysregulation of Human Hepsin in Cancer	10
5	Methods in Drug Discovery	11
5.1	Proteases as Drug Discovery Targets	12
5.2	Structure of the Protease Active Site	13
5.3	Catalytic Activity of Hepsin	14
6	Objective	15
7	Methodology Including Methods and Materials	15
7.1	Measurement Instrumentation and Data Analysis	16
7.2	Instrumentation Setup	17
7.3	Enzyme Reaction Progress Curve	17
7.3.1	Determination of Initial Velocity Conditions	18
7.3.2	Active Site Titration and Titration Matrix	19
7.3.3	Enzyme Kinetics Model	20
7.3.4	Determination of K_m and V_{max}	21
7.4	Usage of DMSO and DMSO Compatibility	22
7.5	Determination of IC_{50}	22
7.6	Plate Uniformity and Signal Variability Studies	23

7.7	List of Compounds	24
7.8	Cell-based Assay Preparation and Optimization	25
8	Results	26
8.1	Instrument Capacity and System Linearity	26
8.2	Initial Velocity Conditions	28
8.2.1	Active Site Titration	28
8.2.2	Enzyme Kinetics	32
8.2.3	Enzyme Activity	33
8.3	K_m and V_{max}	34
8.4	DMSO Compatibility	34
8.5	IC_{50} for Mid-level Signal	36
8.6	Activity Loss	37
8.6.1	Activity Loss of Positive Control NTH1	38
8.6.2	Activity Loss Screening of Compounds	38
8.6.3	Activity Reducing Factors	50
8.7	Final Assay Design	50
8.8	Plate Uniformity and Signal Variability Assessment	50
8.9	Compound Screening	52
8.9.1	Preliminary Compound Screening	53
8.9.2	Final Compound Screening	56
8.10	Preliminary Experiment Cell-based Assay	61
8.11	Cell Amount and Incubation Time	62
8.12	Kinetics Cell-based	64
8.13	K_m and V_{max} for Cell-based Assay	64
9	Conclusion and Discussion	65
9.1	Biochemical Assay	66
9.2	Cell-based Assay	67
	References	69
	Appendices	
	Appendix 1. Activity Assay Protocol by R&D Systems	
	Appendix 2. Plate Format for Plate Uniform and signal Variability	
	Appendix 3. Adjustment of AMC Standard Reference	
	Appendix 4. Results of System Capacity and Linearity	
	Appendix 5. Best-fit Values for Michaelis.Menten	
	Appendix 6. Experimental Design for Cell Amount and Incubation Time	

Appreviations

AMC	7-Amino-4-methylcoumarin
ANP	Atrial Natriuretic Peptide
BOC	BOC-Gln-Arg-Arg-AMC, fluorogenic substrate
DMSO	Dimethylsulfoxide
DOX	Doxycyclin
EGFR	Epidermal Growth Factor Receptor
ENaC	Epithelial Sodium (Na ⁺) Channel
GPI	Glycosylphosphatidylinositol
HA	Haemagglutinin
HGF	Hepatocyte Growth Factor
<i>HPN</i>	Hepsin, gene encoding hepsin serine protease
HTS	High Throughput Screening
Lkb1	Liver Kinase b1, STK11
MMP	Matrix Metalloproteinases
PAR	Protease Activated Receptor
rhH	Recombinant Human Hepsin
SAR	Structure-Activity Relationship
SP	Serine Proteases

SPD	Serine Protease Domain
SRCR	Scavenger Receptor Cysteine-rich
TPRSS	Transmembrane Protease, Serine
TTSP	Type II Transmembrane Serine Protease
uPA	Urokinase Plasminogen Activator

1 Introduction

This thesis was made for the Cancer Cell Circuitry Laboratory that is part of the Translational Cancer Research Program in Institute of Biomedicine, Biomedicum Helsinki. The Cancer Cell Circuitry Laboratory is studying oncogenes and tumor suppressors in breast cancer.

Proteases are important signaling molecules in pericellular environment and they have been under study for their role in pathologies including cancer. Serine proteases particularly are regularly connected to tumor progression and metastases in diverse cancer types, and their dysregulation is one feature of cancer although their mechanism of action has not been fully elucidated. One of the most studied subtypes are membrane-anchored serine proteases as they have been associated with such cancer types as pancreatic, gastric, colorectal, lung, ovarian and thyroid cancer but also with such pathological diseases as cardiovascular, inflammatory and viral diseases.

Serine proteases have been studied extensively as biomarkers in drug discovery. Although there are several serine protease inhibitors in clinical use, obtaining compounds with good pharmacokinetic properties has been challenging. The first step in developing an enzyme inhibitor is the identification of proteases and their inhibitors in diseases through their differential expression. In case of proteases, the expression profile remains often unchanged.

The aim of the project was to develop an enzymatic assay targeting hepsin, which is a membrane-anchored serine protease. The objective was to develop two different assays for screening compounds with pharmacokinetic properties. Namely, a biochemical assay using recombinant hepsin and a cell-based assay using MCF 10A-pINDUCER-NEO-HPN cells.

2 Introduction to Proteolytic Enzymes

Proteolytic enzymes, also known as proteases, are a family of enzymes that catalyze the cleavage of proteins by hydrolyzing peptide bonds. Proteases have an essential role as signaling molecules that regulate numerous biological processes such as DNA replication, cell-cycle progression, cell proliferation and cell death, tissue remodeling, wound healing, blood coagulation, and the immune response. (Turk 2006)

Proteases are known to regulate diverse processes in the pericellular microenvironment that are essential for cancer biology, including proliferation, adhesion, migration, differentiation, angiogenesis, senescence, autophagy, apoptosis and evasion of the immune system. Thus, it has been demonstrated that proteases contribute to all stages of tumour progression. However, the existence of tumor-suppressive proteolytic enzymes reveals the large structural and functional diversity of proteolytic systems operating in all stages of the disease. (López-Otin et al. 2007)

Although the common feature of proteases is their ability to hydrolyze peptide bonds, they use two fundamentally different mechanisms to catalyze substrate cleavage, non-covalent catalysis and covalent catalysis (Turk 2006). On the basis of mechanism of catalysis, all identified human proteases can be classified into five catalytic classes, aspartic and metalloproteases, serine, cysteine and threonine proteases. The first two classes utilize an activated water molecule as a nucleophile to attack the peptide bond of the substrate (non-covalent catalysis), whereas in the latter three classes the nucleophile is a part of an amino acid residue (Serine, Cysteine, or Threonine respectively) in the active site (covalent catalysis). (López-Otin et al. 2007; Turk 2006)

Proteases of the different classes can be further grouped into families on a basis of amino acid sequence comparison which leads to the human degradome (Figure 1) that presents the proteases produced by human cells consisting of at least 569 proteases and homologues in 69 different families. Hence the human degradome can be seen as the complete set of proteolytic genes encoded by the human genome. (López-Otin et al. 2007)

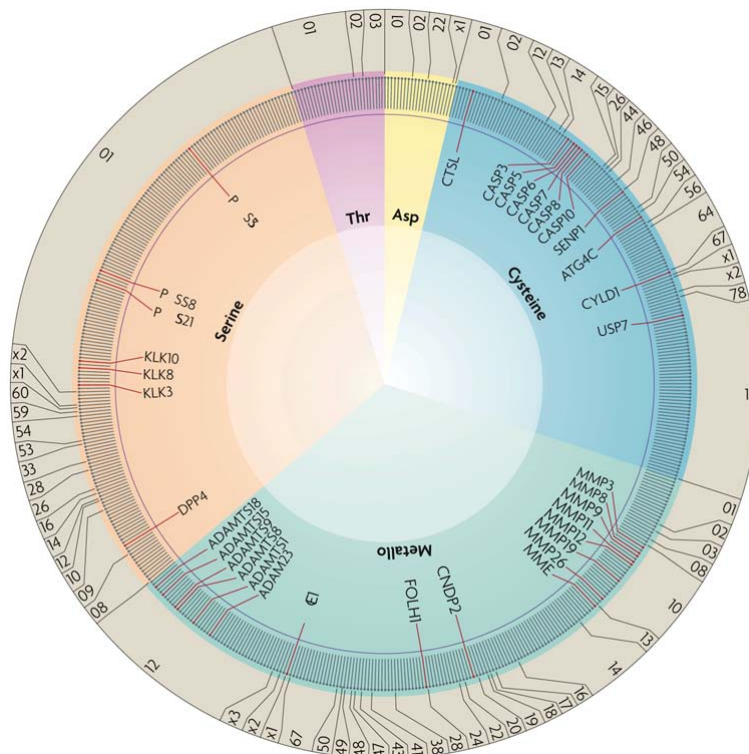


Figure 1. Proteases in the Human Degradome. Grey line presents an individual enzyme, whereas the red line presents an enzyme with tumor-protective properties. (López-Otin C. & Matrisian L.M. 2007)

Each catalytic class consists of both extracellular or pericellular enzymes as well as intracellular or integral-membrane enzymes. Cysteine proteases, for example, consists of five extracellular or pericellular enzymes and 145 intracellular or integral-membrane enzymes, whereas the serine proteases consists of 138 extracellular or pericellular enzymes and 38 intracellular or integral-membrane enzymes. (López-Otin et al. 2007)

2.1 Serine Proteases

Serine proteases are defined by the serine residue within their active site which functions as the primary nucleophile initiating catalysis by attacking the substrate peptide bond (Antalis et al. 2010). Serine proteases are one of the first and most well-studied enzymes due to their ease of isolation and availability in large quantities in a wide range of tissues and biological fluids in mammals. The role of serine proteases in diverse cellular activities such as digestion, blood clotting cascade, inflammation and wound healing and general immune response has been well characterized due to an excessive amount of collected information. Therefore, serine proteases provide an il-

lustrative model for substrate binding specificity and transition state stabilization of proteases. (Copeland 2000)

Serine proteases also have a common structural feature referred to as “*active site triad*” or “*charge relay system*” which means that in order to complete the proteolysis, the nucleophilicity of the serine residue is enhanced by a catalytic triad of histidine, aspartate and serine residues. Virtually, the hydroxyl group of the serine side chain will form a hydrogen-bond with an active site histidine residue side chain, which in turn will form a hydrogen-bond to an active site aspartate side chain. The catalytic triad of histidine, aspartate and serine is included in a tertiary domain structure which has a high sequence homology between serine proteins as the catalytic domain structure is highly conserved. (Copeland 2000; Antalis et al. 2010)

Serine proteases have been further grouped into families based on their amino acid sequence and clans based on their three-dimensional structures and other functional attributes. Some of the most covered serine proteases, including trypsin, chymotrypsin and thrombin, belong to clan PA and subfamily S1A, which is a large group of enzymes representing over 20 % of the known proteases, which, inter alia, participate in the activation of precursors in the pericellular microenvironment. Pericellular microenvironment of the cell contains proteins as inactive precursors including growth factors, cytokines, receptors, enzymes and cell adhesion molecules that will be activated via proteolysis by cell-surface-localized protease receptors, however proteolysis may also be mediated by membrane-anchored protease. (Antalis et al. 2010)

2.2 Membrane-Anchored Serine Proteases

Membrane-anchored serine proteases are a subgroup of thrypsin-like (S1) serine proteases that possess a distinguishing domain which tether them directly to the plasma membrane. These membrane-anchored serine proteases are synthesized with amino- or carboxyl-terminal that allow them to be imbedded directly into the membrane positioning them so that their catalytic serine protease domains lie extracellular. (Netzel-Arnett et al. 2003; Antalis et al 2011)

The structural feature of the amino- or carboxyl-terminal domain allows the membrane-anchored serine proteases to be divided into two subgroups (Figure 2), type I and type

II. The only type I transmembrane serine protease that has been identified is Trypsase γ 1, whereas a total of nineteen TTSPs have been identified. (Antalis et al. 2011)

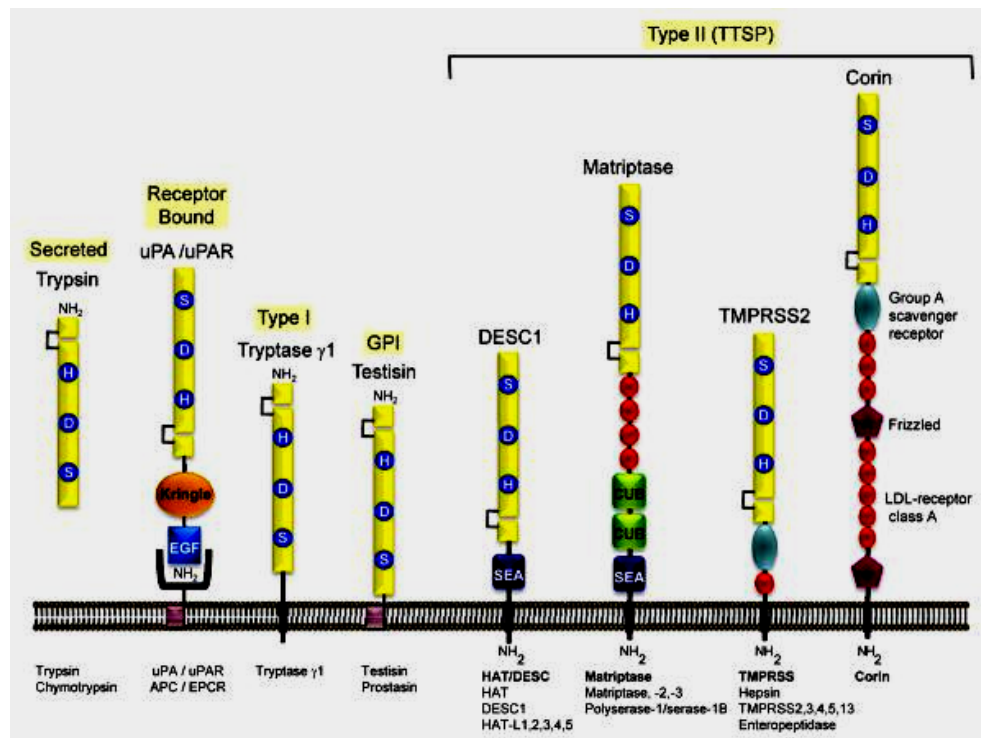


Figure 2. Some of the Well Characterized S1A Serine Proteases. On the left secreted Trypsin following the four subgroups of type II transmembrane serine proteases. (Antalis et al. 2010)

These type II transmembrane serine proteases have been further divided into four subgroups based on their serine protease domains and the domain structure of the extracellular stem region, namely HAT/DESC (human airway trypsin-like protease/differentially expressed in squamous cell carcinoma), Matriptase, TMPRSS (Transmembrane Protease, Serine) and Corin. Type I is tethered to the plasma membrane by hydrophobic C-terminal transmembrane domain via glycosylphosphatidylinositol (GPI) linkage, and it will be synthesized with a classical N-terminal signal peptide that will be cleaved during synthesis. Type II is synthesized and imbedded into the plasma membrane with an N-terminal signal anchor that will not be cleaved during synthesis. Instead, the protease will be positioned into the membrane with a cytoplasmic N-terminus and extracellular C-terminus. (Antalis et al. 2010)

2.3 Human Hepsin

Human hepsin, being part of TMPRSS subfamily, is classified as an integral membrane protein and a TTSP of the trypsin-like (S1) family (Antalis et al. 2010). Hepsin is encoded by human *HPN* gene – has 14 exons and is located on chromosome 19 at q11-13.2 – and is expressed in liver (Figure 3) at higher levels and at lower levels in other tissues, such as kidney, pancreas, stomach, thyroid, testis and prostate. Like other membrane anchored serine proteases, hepsin is linked directly to the plasma membrane consisting of intracellular domain, transmembrane domain and extracellular stem region. (Somoza et al. 2003; Xuan et al. 2006)

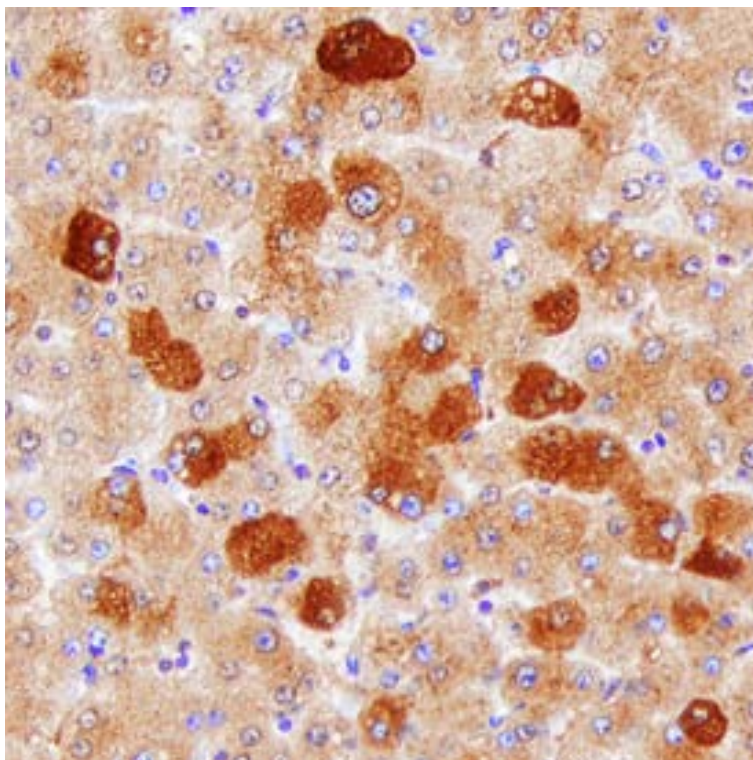


Figure 3. Hepsin in Human Liver. (R&D Systems 2014)

Hepsin was first identified in Earl Davie's laboratory at the University of Washington, by cloning cDNA from a human hepatoma HepG2 cell library based on homology and was named for its hepatic expression. Hepsin is synthesized as single-chain zymogen which is proteolytically activated and its cDNA is ~1.8 kb in length, has a molecular mass of 45 kDa and encodes a polypeptide of 417 amino acids. (Xuan et al. 2006; Antalis et al. 2011)

3 Biological Role of Membrane-anchored Serine Proteases

Membrane-anchored serine proteases, TTSPs particularly, are expressed at the cell surface and are thus ideally located to regulate cell–cell and cell–matrix interactions, participating in a wide range of physiological events through activation, regulation and mediation in many multi-components signaling events. Although many of these biological, physiological and pathological processes *in vivo* remain elusive, they are considered vital for the development and maintenance of homeostasis. (Antalis et al. 2011)

3.1 Zymogen Cascades

Membrane-anchored serine proteases are synthesized as inactive single chain proenzymes, also known as zymogens, and their activation is an integral part of the regulation of cellular signal cascades at the plasma membrane and within the extracellular matrix. Such biological processes as blood coagulation, wound healing, digestion, immune response, fibrinolysis, complement reaction, hormone production, metamorphosis and fertilization are subjected to activation of zymogen cascades. A zymogen cascade consists of sequential irreversible proteolytic reactions, where downstream zymogen is activated by cleavage by another previously activated serine protease or by self-activation. Due to the complexity of the protease signaling cascades the majority of the specific endogenous enzymes that catalyze the activation of the zymogen forms of the proteases *in vivo* are yet to be identified. (Netzel-Arnett et al. 2003; Antalis et al. 2010)

One of the best characterized TTSPs that participate in zymogen activation is enteropeptidase which activates pancreatic trypsinogen into its bioactive form trypsin subsequently converting other pancreatic zymogens to their active forms during digestion. Plasminogen cascade is a key cascade critical for fibrinolysis, cell migration, remodelling of extracellular matrix and activation of matrix metalloproteinases (MMP). Plasminogen cascade can be initiated by several of the TTSPs, including matriptase, hepsin and serase-1B *in vitro* assays, by activating protease zymogen pro-uPA into its catalytically active form. (Netzel-Arnett et al. 2003; Antalis et al. 2010)

3.2 Activation and Regulation

Activation, inhibition and substrate specificity, as well as the cellular localization is determined by the extracellular domains of TTSPs, whereby frequent ectodomain shedding enables the activity of TTSPs in the pericellular microenvironment. Regulation is mainly mediated by endogenous inhibitors such as serpins and Kunitz-type inhibitors by endogenous protease inhibitors in which the main role is by Kunitz-type inhibitors and serpins. (Bugge et al. 2003)

G-protein coupled signaling receptors on the cell surface known as protease activated receptors (PARs) include four family members, PAR₁₋₄ respectively. Each family member of the PAR family is activated either directly or indirectly through proteolytic cleavage by different membrane-anchored serine proteases initiating various intracellular signal transduction pathways. (Antalis et al. 2010.) PAR₂, for example, can be activated by matriptase inducing the release of pro-inflammatory cytokines in endothelial cells including IL (interleukin)-6 and IL-8 (Netzel-Arnett et al.2003; Antalis et al. 2010).

The activation and availability of growth factors are processed through proteolytic cleavage by membrane-anchored serine proteases such as the modulation of epidermal growth factor receptor (EGFR) (Netzel-Arnett et al. 2003; Antalis et al. 2010). For example, both matriptase and hepsin has been shown to activate growth factors functioning as ligands for receptors MET/HGF and RON/MST-1 associated with epithelial cell motility, migration and proliferation (Antalis et al. 2010).

Atrial natriuretic peptide known as ANP is a cardiac hormone, essential in regulating blood pressure and cardiac function by regulating systemic salt and water balance through natriuresis, diuresis and vasodilation. ANP is synthesized as cell-associated precursor molecule pro-ANP. The inactive pro-ANP is released and activated by proteolytic cleavage which is catalyzed by TTSP corin in a sequence-specific manner converting pro-ANP into its bioactive form on the surface of cardiomyocytes. (Bugge et al. 2009; Antalis et al. 2011)

The sodium and water flux across high resistance epithelium of airway, bladder, kidney, colon and skin is regulated by epithelial sodium (Na⁺) channel known as ENaC which is activated and regulated through proteolytic processing. ENaC has been found to be activated by membrane-anchored serine proteases when co-expressed in heter-

ologous expression systems, although implications of non-catalytic protease mechanism involving ENaC activation has also been found. Furthermore, there is evidence implying that membrane-anchored serine proteases may regulate ENaC both positively and negatively. (Antalis et al. 2011)

3.3 Biological Role of Human Hepsin

Hepsin has been implicated in cell growth and maintaining cell morphology, whereas it has been shown that hepsin is not essential for either embryonic development or vital adult functions (Somoza et al. 2003; Xuan et al. 2006). Hepsin is known to activate or cleave pro-HGF (hepatocyte growth factor), liver microsomal glutathione transferase, matriptase, prostaticin, EGFR, laminin and blood clotting factors VII, IX, and XII *in vitro*. Nonetheless, the physiological targets of hepsin *in vivo* remain largely elusive. (Antalis et al. 2011)

Hepsin is one of the TTSPs that have demonstrated autocatalytic activation *in vitro* suggesting it may function as initiator in proteolytic cascades. The physiological mechanism of autoactivation is not well understood, but it is associated with oligomerization. (Bugge et al. 2009.) Hepsin has been implicated in zymogen activation by intercepting the blood coagulation cascade and plasminogen cascade. In blood coagulation cascade hepsin activates protease zymogen Factor VII into its bioactive form Factor VIIa, initiating a coagulation pathway on the cell surface leading to thrombin formation. On the other hand, *in vitro* assays have demonstrated that hepsin catalyses the activation of pro-uPA (urokinase plasminogen activator) to its active form in plasminogen cascade. (Antalis et al. 2010)

4 Membrane-anchored Serine Proteases in Pathologies

Mutations in several genes, encoding TTSPs has been found to entail in missing or truncated serine protease domains (SPDs) in TTSPs and alter enzyme expression and activity. For instance, chromosomal rearrangements together with altered expression of TTSP genes contributes to human carcinogenesis, whereas missense mutations in SPD of matriptase entail in catalytically inactive protease resulting to human skin dysfunction. In addition, autosomal recessive genetic disorders in humans have been re-traced to mutations in five TTSP genes. (Antalis et al. 2010; Bugge et al. 2009)

Membrane-anchored serine proteases promote viral pathogenicity by activating and replicating viruses. In the pivotal role is haemagglutinin (HA), viral antigenic glycoprotein responsible for binding the virus to the cell that is being infected. Haemagglutinins proteolytic cleavage sites mutational evolution is determinant of viral pathogenicity, as HA is synthesized as precursor protein HA₀ that must be cleaved into subunits HA₁ and HA₂ by the host cellular protease. (Antalis et al. 2010)

4.1 Membrane-anchored Serine Proteases in Cancer

The cellular expression of many membrane-anchored serine proteases appears to be aberrant during tumor development and progression in human cancer, possessing complex role in relation to cancer, as expression of these enzymes have been associated both up- and downregulation (Netzel-Arnett et al. 2003; Antalis et al. 2010). Notably, many of the TTSPs have been causally linked to various cancers. TMPRSS4, for instance, has been associated with pancreatic, gastric, colorectal, lung, and thyroid cancers. Matriptase, on the other hand, exemplifies consistent expression in tumors of epithelial origin, including prostate, ovarian, cervical, gastric, colon, renal cell, esophageal, oral squamous cell carcinoma, and malignant pleural mesothelioma. In case of prostasin, a downregulation is documented with tumor progression. (Antalis et al. 2011)

4.2 Dysregulation of Human Hepsin in Cancer

Hepsin attracted interest in epithelial carcinogenesis after several analyses supported the role of hepsin encoding *HPN* gene in prostate cancer. Reportedly overexpressed *HPN* has induced metastasis in prostate epithelium in a non-metastatic murine model of prostate cancer, whereas catalytically active hepsin has promoted the progression of ovarian carcinoma cell lines. As previously mentioned, hepsin is known to cleave *in vitro* such proteins as pro-HGF, laminin 332 and pro-uPA many of which have been associated in carcinogenesis. (Bugge et al. 2009)

In contrast to suggestion in early literature, hepsin having a role in human tumor cell proliferation, the recent studies support role for hepsin in tumor progression and metastases (Xuan et al. 2006; Chevillet et al. 2008; Antalis et al. 2011). As demonstrated in studies by Klezovitch et al. 2004, whereby transgenic mice imitating hepsin overexpression in prostate cancer entailed to altered basement membrane structures in mice,

whereas prostate cell proliferation remained normal. After crossing the mice with non-metastasizing cancer model the mice demonstrated invasive prostate cancer cells inducing metastasis in the liver, lung and bone. (Xuan et al. 2006; Chevillet et al. 2008; Antalis et al. 2011)

Furthermore, recent studies have found that hepsin mediates epithelial integrity and basement membrane defects as well as transformation in Lkb1-deficient (Liver kinase b1, STK11) 3D acini, wherein deregulated expression of hepsin is sufficient to disrupt epithelial integrity. In conclusion, hepsin seems to be released from junctional complexes by loss of Lkb1, wherein hepsin-deregulating lesions generally promote Myc-driven tumorigenesis as Myc does not alter the position or level of hepsin. Although the deregulation of hepsin by Myc coupled with Lkb1 is yet to be demonstrated in mouse breast cancer models, the overexpression of hepsin is implicated as a common genetic alteration in prostate and breast cancer. Hence, hepsin may be a potential therapeutic target in breast cancer. (Partanen et al. 2012)

5 Methods in Drug Discovery

High-Throughput Screening (HTS) is a method for drug discovery that is widely used in pharmaceutical industry. In HTS, a large number of biological modulators and selectors are assayed against specific targets by screening different types of biological and chemical libraries. (Szymański et al. 2012) Virtual screening is a computer-aided method used in drug discovery to align and score ligands based on their shape, wherein similar molecules are assumed to have similar binding characteristics. Prerequisite for virtual screening based on shape is the generation of the 3D structure of the molecule. (Sastry et al. 2011) On the other hand, Structure-Activity Relationship (SAR) analysis measures the relationship between chemical or 3D structure of the molecule with its biological activity, which is also used in toxicology (McKinney et al. 2000).

High-Throughput Screening assays can be divided into two categories, namely biochemical assays and cell-based assays. Until recently pharmaceutical industry has been mainly utilizing target-based biochemical assays, such as enzyme inhibition and receptor-ligand binding assays in High-Throughput Screening. However, cell-based assays have been gaining interest as they provide an early indication of the compound toxicity characteristics. Furthermore, cell-based assay represents tissue-specific responses of compound activity in a cellular context more accurately compared to bio-

chemical assays that are limited by suitable compound purification and preparation methods. (Zang et al. 2012)

5.1 Proteases as Drug Discovery Targets

In order to prevent improper cleavage of signaling molecules, the protease activity is tightly regulated by differential expression at transcriptional level. During cell and tissue development and organism homeostasis, the protease activity is also regulated by zymogen activation and binding of inhibitors and cofactors at protein level (Figure 4). (López-Otin et al. 2007)

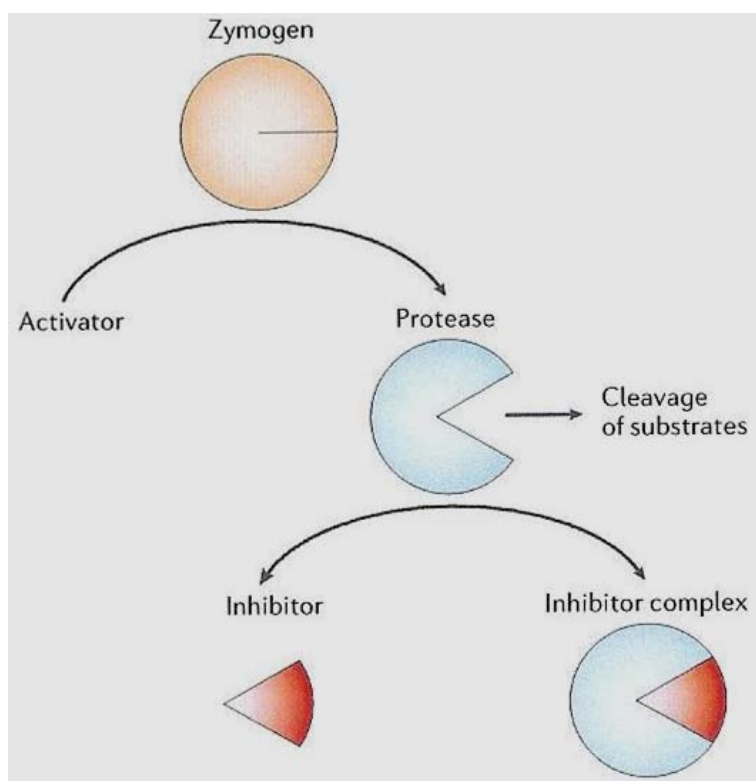


Figure 4. Regulation of Protease Activity. (López-Otin et al. 2007)

However, once dysregulated there is an excessive or insufficient proteolysis at the substrate-cleavage level, mostly resulting from numerous endogenous or exogenous factors. This dysregulation entails to unwanted activation of protease signaling pathways, rather than being a consequence of genetic aberration. (López-Otin et al. 2007)

The first precondition in developing an enzyme inhibitor as drug is the identification of biomarker, meaning the proteases and their inhibitors that are differentially expressed in diseases. Secondly, identification of endogenous substrates, that target the proteases. Nonetheless, it has proven to be complicated as protein target should have altered activity connected to differential expression in the disease of interest. However, in case of proteases the expression profile remains unchanged even by deregulation of activity resulting from increased activation or loss of a key inhibitor. (Katz et al. 2000; Turk 2006)

5.2 Structure of the Protease Active Site

An active enzyme is defined by a binding pocket whose size, shape and charge determine the cleavage specificity of the substrate. The protease surface accommodating a single side chain of a substrate residue is called a subsite, which is numbered S1-Sn towards N terminus of the scissile bond and S1'-Sn' towards C terminus of the scissile bond, the corresponding single side chain of the substrate is numbered P1-Pn and P1'-Pn' respectively (Figure 5). (Copeland 2000; Turk 2006)

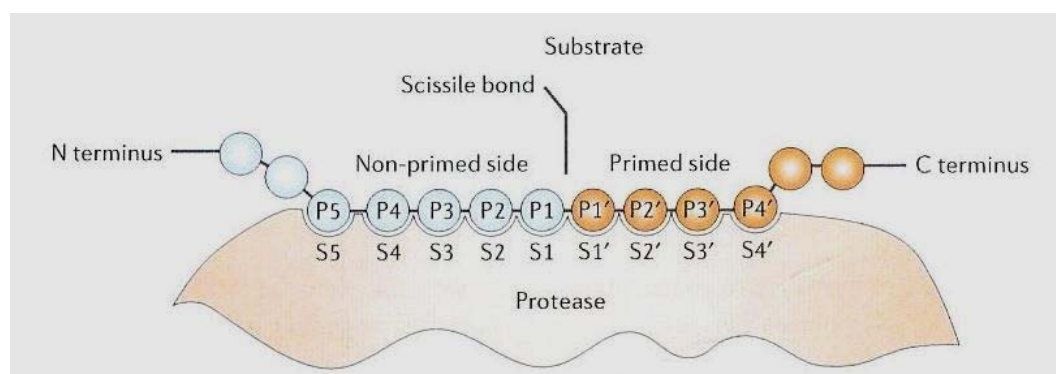


Figure 5. Protein Substrate Binding to Protease. Subsite accommodates a single chain of a substrate residue and they are numbered S1-Sn upwards towards the N terminus non-primed sites and S1'-Sn' towards the C terminus primed sites. (Turk 2006)

In serine proteases, substrates specificity and selectivity of inhibitors is conferred by the combination of the interaction series of inhibitor groups at subsites S3, S2, S1, S1', S2' and S3' binding peptide side chains. Trypsin-like serine proteases possess a S1 binding pocket which has a conserved aspartate residue at position 189 that enable the specificity for non-polar P1 residues. Interactions at the S1 site enable small-molecule

inhibitors to discriminate between protease classes, thus achieving specificity for drug targets. (Copeland 2000; Katz et al. 2000)

5.3 Catalytic Activity of Hepsin

The crystal structure demonstrates how the extracellular component of hepsin might be positioned with respect to the plasma membrane. The extracellular stem region is formed by two domains of which the larger is structurally homologous to the members of the (chymo)trypsin superfamily of serine proteases, and smaller is scavenger receptor cysteine-rich (SRCR) domain. The Pro50 residue of the SRCR domain constrains the spatial relation between the extracellular stem region and the entrance to the membrane (Figure 6). (Somoza et al. 2003; Xuan et al. 2006)

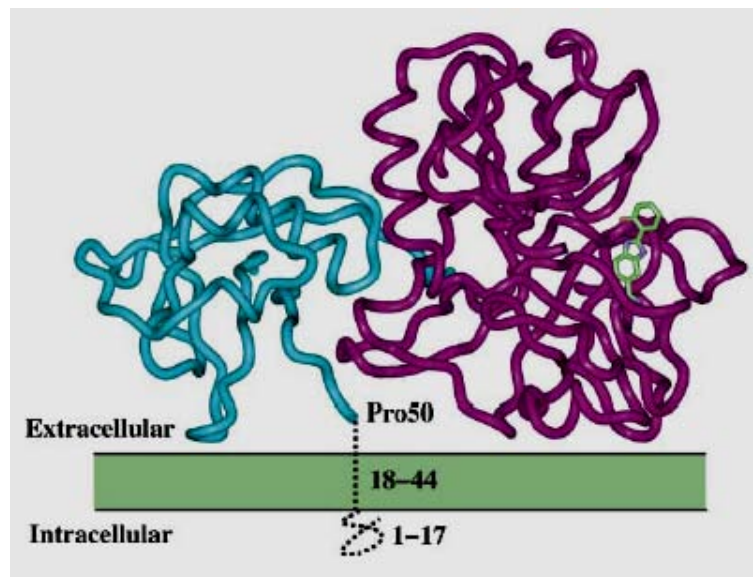


Figure 6. Structure of Human Hepsin. (Somoza et al. 2003)

Since there is no peptide bond linking the two domains, the proteolytic activation step of hepsin requires hydrolyzation of the peptide bond between Arg162 and Ile163, thus separating the serine protease domain from the rest of the protein. The two chains, pro- and catalytic domains, remain covalently bound to each other in activated form through a disulfide bond between Cys277 of the serine protease domain and Cys153 of the non-catalytic chain. The active hepsin possesses a conserved aspartate residue at the bottom of the S1 binding pocket in the activated SPD, which determines the preference for cleavage of substrates with a basic amino acid. (Somoza et al. 2003)

6 Objective

The aim of the thesis was to develop two different enzymatic platforms to use as a compound library screening method for drug discovery assisted by virtual screening. The first platform was a biochemical assay that measures the activity of recombinant hepsin based on commercial protocol. The second platform was a cell-based, measuring the activity of the enzyme produced by the cells (Figure 7).

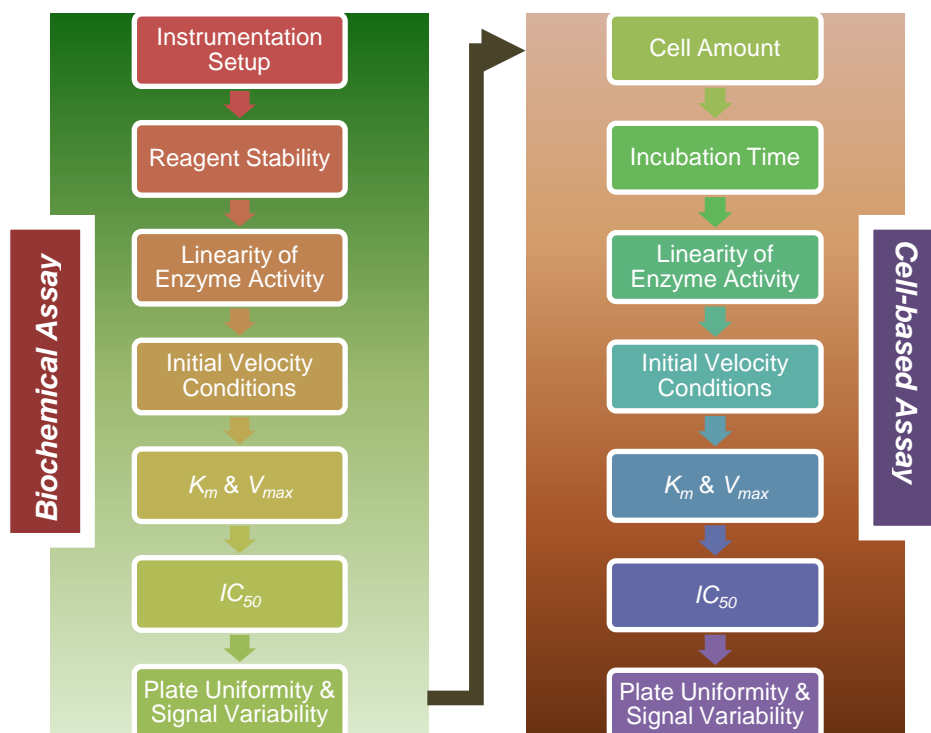


Figure 7. Schematic of Assay Development.

Development was done in two phases: In the first phase, a biochemical activity assay based on commercial protocol was optimized and further developed. In the second phase, a cell-based assay was developed. Both platforms were tested for functionality whereby a compound screening was performed.

7 Methodology Including Methods and Materials

The development of the enzymatic assay was based on the activity assay protocol by R&D Systems (Appendix 1) using recombinant human hepsin (rhHepsin) derived from

mouse myeloma cell line (R&D Systems) and fluorogenic peptide substrate BOC-Gln-Arg-Arg-AMC (BOC). The activity of the recombinant human hepsin is measured by its ability to cleave *tert*-butoxycarbonyl-Gln-Arg-Arg-7-amino-4-methylcoumarin. BOC-Gln-Arg-Arg-AMC is AMC-based substrate for transmembrane serine protease hepsin, which means that 7-Amino-4-methylcoumarin (AMC) can be used as fluorescence reference standard.

Basic Assay procedure contained a 96-well plate (ViewPlate®-96 F TC, Perking Elmer Lot 9508512) used in all measurements, activated rhHepsin (Catalog #4776-SE), fluorogenic peptide substrate BOC (Bachem, Catalog #I-1655) and Assay Buffer 50mM Tris, pH 9.0. Assay Buffer was used as a blank in measurements as well as dilution substance for rhHepsin and BOC, where the dilution ratio was modified according to desired concentration. The requirement for the measurement with 96-well plate included 100 µl substances in the well in total, wherein the pipetting volumes of different substances were modified over the course of experiments in to their final volumes.

In the beginning, the experiments were conducted with extensive limits and ranges in order to gather sufficient data for profound assessment, including measurement time of 55 minutes as well as substance concentrations. In course of experiments these limits and ranges were modified according to the kinetic reaction model of rhHepsin. Development process was iterative; hence measurements had to be repeated in certain order while modifying the parameters.

7.1 Measurement Instrumentation and Data Analysis

Measurements were conducted with Fluostar Omega (BMG Labtech 2014) Multi-Mode Microplate reader using fluorescence intensity detection and top read mode. Fluostar Omega had relatively new features compared to conventional spectrophotometer models such as adjustable gain control that enhances photomultiplier tubes responsiveness to the signal intensity. Hence, measured signal could be optimized to the dynamic range. There were also different modes for well reading as well as amount and intensity of the flashes used in order to enhance the sensitivity. All these features had to be optimized in course of experiments in order to find the best possible parameters for assay measurements.

Data was analyzed with Graph Pad Prism 6 (©2014 GraphPad Software, Inc) statistical data analysis tool which is designed for scientific use. In addition to usual statistical methods, Graph Pad Prism has linear and nonlinear regression curve fitting methods for enzyme kinetics and dose-response models, although using them requires understanding of mathematical models.

7.2 Instrumentation Setup

Before setting up the assay, it was important to establish the range and linearity of instrument performance, in order to determine the linear range of the measurement as described in Assay Guidance Manual: Basics of Enzymatic Assays by Brooks H. B. 2012. This applies particularly to enzymatic reactions where the reaction reaches plateau due to product formation, hence it is important to distinguish progress curve from signal saturation. Signal saturation occurs when upper detection limit is reached and an increase in substance concentration no longer raises the signal levels. Therefore, the detection system becomes non-linear outside of the linear range of the instrument and detected product concentration is less than the total product concentration. The linear range of the measurement system is defined as the linear portion of the dynamic range which is delimited by upper and lower detection limit.

For any subsequent assay analysis and establishing assay parameters, it was essential to perform enzyme reaction conditions within this linear range. Instrument performance and system linearity is closely linked to defining initial velocity conditions as described in the following chapters.

7.3 Enzyme Reaction Progress Curve

All information necessary to analyze an enzymatic reaction can be obtained via reaction progress curve. Analyzing enzymatic reaction is a key feature in establishing assay conditions and basic parameters, such as enzyme and substrate concentrations, as well as K_m and IC_{50} values.

Following sections describe the process in detail as reviewed from Assay Guidance Manual: Basics of Enzymatic Assays for HTS by Iversen H. B. 2012. Methodology to determine initial velocity conditions via active site titration and establishing K_m and V_{max}

were reviewed from *Enzymes: A Practical Introduction to Structure, Mechanism, and Data Analysis* by Copeland R. A. 2000, as well from *Evaluation of Enzyme Inhibitors in Drug Discovery: A Guide for Medicinal Chemists and Pharmacologist* by Copeland R. A. 2013.

7.3.1 Determination of Initial Velocity Conditions

Determining initial velocity conditions of the given enzymatic reaction is considered as a basis in establishing enzyme assay parameters and a first requirement for steady state conditions. Beyond initial velocity conditions, the enzymatic reaction is affected by product inhibition, reverse reaction and substrate limitation as saturation of the enzyme with substrate decreases. These factors contribute to non-linear reaction in proportion to enzyme concentration whereby the substrate concentration remains unknown. Furthermore, there is a greater possibility of saturation of the detection system.

Therefore, the first step in establishing any of the above mentioned assay parameters the initial assay condition had to be determined. Initial velocity is defined as the initial linear portion of the enzyme reaction, when less than 10 % of the initial substrate concentration has been converted to product (Figure 8).

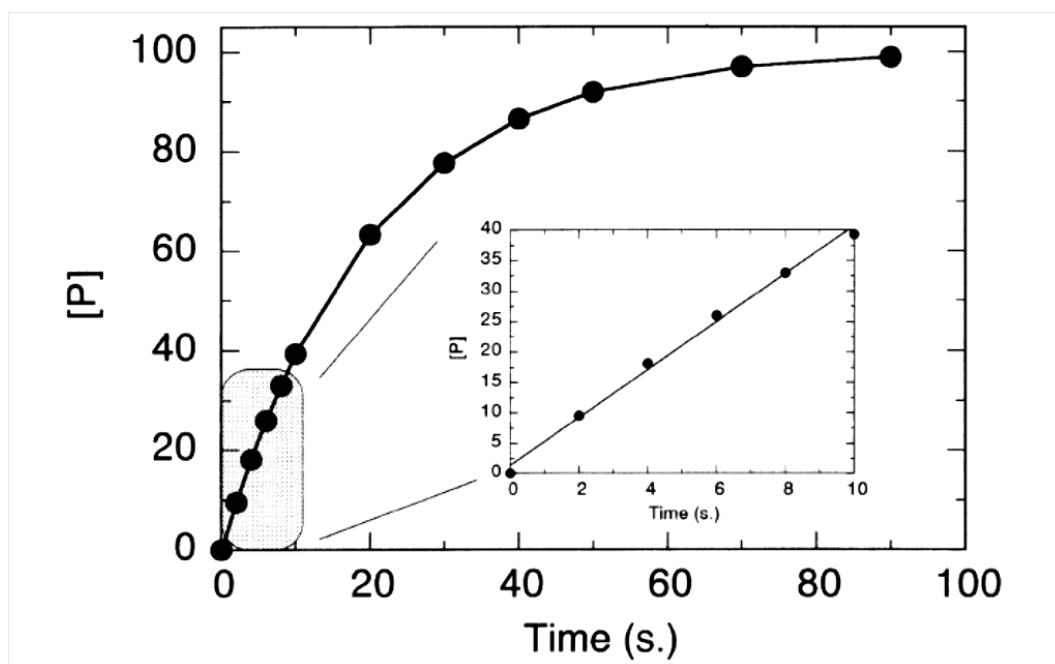


Figure 8. Initial Velocity of the Enzymatic Reaction Progress Curve. (Copeland R. A. 2000)

Initial velocity and reaction time is dependent on the given substrate and enzyme and their concentrations. In order to establish the initial velocity conditions, the enzyme concentration had to be modified to maintain linearity in respect to measurement time. This could be obtained via active site titration.

7.3.2 Active Site Titration and Titration Matrix

The active enzyme concentration can be determined by active site titration for enzymes that demonstrate burst phase kinetics due to covalent intermediate formation, such as serine proteases. In burst phase kinetics, the overall reaction is rate-limited by decomposition of the intermediate species, which leads to rapid build-up of the intermediates before reaching steady state velocity. Therefore, the concentration of active enzyme is identical to that of intermediates and can be determined from the intercept value of a linear fit of the data in the steady state phase.

Enzyme concentration was optimized combining active site titration and two factor design screening into titration matrix (Table 1), since enzyme titration requires multiple concentrations, whereby full level design would be extensive and time-consuming.

Table 1. Titration Matrix.

rhHepsin [nM]	1 st Titration			2 nd Titration		
	50 BOC [μ M]	25 BOC [μ M]	12.5 BOC [μ M]	50 BOC [μ M]	25 BOC [μ M]	12.5 BOC [μ M]
25	X	X	X	-	-	-
12.5	X	X	X	X	X	X
6.25	X	X	X	X	X	X
3.13	X	X	X	X	X	X
1.56	X	X	X	X	X	X
0.781	X	X	X	X	X	X
0.391	X	X	X	X	X	X
0.195	-	-	-	X	X	X
0.098	X	X	X	X	X	X
0.049	X	X	X	X	X	X
0.024	X	X	X	X	X	X

Screening is best suited for fast and approximate determination of possible location of optimum sample point, and is based on bracketing the obtained response surfaces of the sample points close to the optimum. Each enzyme concentration was titrated with

2x, 1x and 0,5x levels of substrate concentration in order to analyze the reaction linearity.

The kinetic reaction model of rhHepsin would indicate that the optimum enzyme concentration is below the concentration of 0.391 nM. Therefore, the bracketing was started between the concentrations of 0.391 nM and 0.098 nM continuing below these values in the titration matrix (Table 2).

Table 2. Titration Matrix After Bracketing.

rhHepsin [nM]	1 st titration			2 nd titration		
	50 BOC [μ M]	25 BOC [μ M]	12,5 BOC [μ M]	50 BOC [μ M]	25 BOC [μ M]	12,5 BOC [μ M]
0.15	X	X	-	X	X	-
0.075	X	X	-	X	X	-
0.0375	X	X	-	X	X	-
0.01875	-	-	-	X	X	-

Lower levels of substrate were excluded as they yielded reaction rates too slow for assessment. Furthermore, a very low enzyme concentration of 0.01875 nM was included for further analysis.

7.3.3 Enzyme Kinetics Model

A detailed enzyme kinetics analysis was performed in order to evaluate possible sources of variation, such as processing time, light and temperature changes. Titration matrix was designed for evenly spaced enzyme concentrations and 4 substrate levels (Table 3).

Table 3. Titration Matrix for Enzyme Kinetics.

rhHepsin [nM]	Titration			
	30 BOC [μ M]	25 BOC [μ M]	15 BOC [μ M]	5 BOC [μ M]
0.8	X	X	X	X
0.7	X	X	X	X
0.6	X	X	X	X
0.5	X	X	X	X

[nM]	30 BOC [μ M]	25 BOC [μ M]	15 BOC [μ M]	5 BOC [μ M]
0.4	X	X	X	X
0.3	X	X	X	X
0.2	X	X	X	X
0.1	X	X	X	X
0.05	X	X	X	X
0.025	X	X	X	X
0.0125	X	X	X	X

Enzyme kinetics model required comparable processing of assay preparation in order to minimize any influences of unwanted factors. Especially, the assessment of these factors became of importance for the functionality of the assay.

7.3.4 Determination of K_m and V_{max}

For an enzymatic reaction, a K_m value is usually defined as the substrate concentration that results in half-maximal velocity of the given enzyme-substrate reaction. K_m can also be defined as a substrate concentration at which half of the enzyme active sites are saturated by substrate molecules in the steady state. Defining K_m concentration for the substrate is of importance so that the enzymatic reaction can be run under steady state conditions. In this way, the reverse reaction will not affect the reaction. The value of K_m is specific to a given enzyme-substrate reaction and to their concentrations.

The value of K_m can be determined accurately only under initial velocity conditions, which is also of importance for identification of competitive inhibitors, the common goal of SAR. Competitive inhibitor activity in a competition experiment that measures IC_{50} values can be identified by a substrate concentration at or below K_m value. In this way the velocity of the reaction is insensitive to changes in substrate concentration. The value of V_{max} describes the maximal reaction rate of the given enzyme-substrate reaction which however will be reached only theoretically.

In order to measure IC_{50} values of competitive inhibitors, a substrate concentration around or below K_m had to be determined as higher substrate concentrations would aggravate the identification of competitive inhibitors. A large excess of substrate over enzyme had to be used in order for steady state conditions to be met, whereby a 2-fold dilution scheme was used covering nine different substrate concentrations varying over

the range of 0.2-5.0 K_m . The measurement had to be repeated 5 times, from which the average K_m was calculated.

Assessment was carried out using Graph Pad Prism 6 software, where each reaction was analyzed using linear regression in order to obtain the slope of the reaction. Slope (v_0), is defined as the change in the product formed divided by the change in time i.e. reaction rate. Subsequently, the obtained slope values of each measurement were analyzed via non linear regression that calculates K_m and V_{max} saturation curve using rectangular hyperbola. Compared to Lineweaver-Burk, rectangular hyperbola is considered more accurate, since an enzymatic reaction that follows Michaelis-Menten kinetics will form a rectangular hyperbola when initial velocity reaction is plotted against substrate concentration, whereas Lineweaver-Burk is a variable of the same equation only that it is subjected to measurement errors and the method of least squares is theoretically no longer applicable.

7.4 Usage of DMSO and DMSO Compatibility

DMSO at a concentration of 100 % were used as a test compound dissolvent and therefore DMSO concentration of the assay had to be determined in the early development phase. DMSO concentrations from 0 % to 5 % were tested under uninhibited assay conditions in order to determine the solvent-compatibility of the assay and reaction inhibition due to DMSO. Furthermore, variability studies had to be performed with the final DMSO concentration. For cell-based assays, it is recommended that the final DMSO concentration should not exceed concentration of 1 % to ensure the cell viability.

7.5 Determination of IC_{50}

The value of IC_{50} is defined as the concentration of substance that provides an inhibition of 50 % of the enzymatic reaction. According to Assay Guidance Manual: Guidance for Assay Development & HTS by Eastwood et al.:

Substantial variation in the methodology used to derive these values exists, and this variation has been shown to substantially impact overall assay variability (Eastwood et al. 2007,p.41).

Although it usually remains unstated, the IC_{50} is commonly defined as relative IC_{50} value instead of absolute IC_{50} value which has its own applications. There are several guidelines for dose-response curve fitting of IC_{50} value that will not be discussed in detail, since the curve fitting as well as data assessment generally were done with Graph Pad Prism.

Relative IC_{50} is recommended in context of assays and there are three methods to fit the curve. For all three methods in common is that it has to be decided how to fit the top and bottom plateau of the curve. The main points of curve fitting from Graph Pad Prism 6 User Guide will be reviewed below:

1. Fit the curve by excluding the Blank and NS control values, i.e. using the data only for curve fitting.
2. The parameter Top is defined as constant equal to the average value of Blanks. The parameter Bottom is defined as constant equal to the average value of NS controls.
3. Blank values are fitted as part of the dose-response curve by entering them as low dose, because zero is not defined on a log-scale. NS controls are fitted as part of the dose-response curve by entering them as a very high concentration of inhibitor.

Nonetheless, all three methods result in a very similar IC_{50} value, where top and bottom plateaus are indistinguishable and a complete dose-response curve is formed. In this case, the first choice was used for dose-response curve fitting as well as Graph Pad Tool Eanything that enabled the inhibition-% analysis of any point along the dose-response curve. Before the actual curve fitting, the concentrations of the data had to be transformed in to a log-scale by transform tool build in Graph Pad Prism.

7.6 Plate Uniformity and Signal Variability Studies

Plate uniformity and signal variability studies are usually done as a part of the validation process of enzymatic assays as described in Assay Guidance Manual: HTS Assay Validation by Iversen P. W. 2012. Although the assay will not be validated in context of this thesis, these studies were selected in order to ensure the functionality of the assay performance. The plate uniformity assessment ensures that the plate format used for measurements has no edge or drift effect or other systematic sources of variability on

the signal. On the other hand, signal variability assessment ensures that the signal separation of raw signals is enough to conduct screening.

The plate uniformity study was performed with Interleaved-Signal format which runs all signals on all plates varying them systematically so that over all plates on a given day each signal is observed in each well. The Interleaved-Signal format can be used in all instances and is run for three days with three plates per day respectively for new invalidated assays (Appendix 2). The signal variability assessment was performed on three types of signals:

1. "Max" Signal measures the maximum signal which consists of negative control including DMSO according to assay design concentrations.
2. "Mid" Signal measures the midpoint signal i.e. IC_{50} concentration of positive control according to assay design concentration.
3. "Min" Signal measures the background signal which consists of assay buffer including DMSO according to assay design concentrations.

Plate acceptance criteria for the assay design were defined as follows: The raw signals are tight and there is enough separation between maximum and minimum signals to conduct screening. The average rate of outliers is less than 2 %. The coefficient of variation of each signal is less than or equal to 20 %. Standard deviation of midpoint signal is less than or equal to 20 on all plates. Signal window is more than or equal to 2 on all plates or Z' factor is more than or equal to 0.4 on all plates. Drift may not exceed 20 % as this is considered to be material drift. Edge effect has no acceptance limit however it may be a helpful troubleshooting technique as it may reveal that the incubation temperature is reached unevenly in the wells across the plate. Universally, no material edge, drift or other spatial effects are allowed. In Inter-plate and Inter-Day tests the normalized average midpoint signal should not translate into a fold shift of more than two within days or more than two across any two days.

7.7 List of Compounds

The name and molecule structure of the compounds were confidential. Therefore, the compounds were identified per Lab No. which was used in laboratory context and per ID in context of traceability (Table 4).

Table 4. List of Compounds.

List of Compounds			
Lab No.	ID	Lab No.	ID
n/a	NTH1	12	1571
1	9128	13	0031
2	6777	14	3560
3	0356	15	7865
4	6934	16	6617
5	2881	17	1908
6	4684	18	2603
7	1595	19	5174
8	3129	20	5657
9	4650	21	3081
10	1907	22	5062
11	5119	23	5975

There were results available from previous compound screenings although with different enzyme and substrate concentration. Unfortunately the screenings in question showed considerable variations and failed to deliver consistent results. Therefore, the development of the assay included also the aspect of tracing down the sources of variation in order to attain reliable results.

7.8 Cell-based Assay Preparation and Optimization

The cell line used for the cell culture was adherent human mammary epithelial cells MCF 10A (ATCC® CRL-10317™) that were lentivirally infected with pINDUCER-NEO-HPN construct. Neo refers to neomycin/G418 selection (Meerbrey et al, 2011). MCF 10A-pINDUCER-NEO-HPN cells were cultured in human mammary epithelial cell basal growths media MCDB 170 (US Biological) supplemented with bovine pituitary extract 70 µg/ml, insulin 5 µg/ml, hydrocortisone 0.5 µg/ml, epidermal growth factor 5 ng/ml, transferrin 5 µg/ml, Isoproterenol 10⁻⁵ M, Amphotericin B 50 µg/ml and Gentamicin 50 µg/ml (all supplements obtained from Sigma). Cells were cultured in 2 cm 6 well plate, as well as 6 cm and 12 cm Petri-dishes (Greiner) and detached from the plates with Trypsin-EDTA (Gibco)

The cells were seeded in a 96-well plate (Perking Elmer) with the density of 50 000 cell per well and incubated 24 hours before the *HPN* gene was activated with 100 ng/ml Doxycyclin using MQ water as a carrier control. After activation of *HPN* gene the cells were incubated for another 24 hours before the measurement.

For the final assay design, the cell amount and incubation time were optimized. The incubation time has to be sufficient enough for the cells to attach at the bottom of 96-well plate, but also sufficiently short so that the cells will not lose their viability during the incubation. Loss of viability by the cells can be seen as uneven measurement results, as well as low fluorescence values during the measurement. The cell amount had to be optimized so that after the incubation the cells covered the bottom of the well in 96-well plate and so that during the measurement there will be enough separation between fluorescence intensity induced by the cells and blank value.

8 Results

The following chapters describe the course of experiments in detail. The results of the experiments during assay development are found in paragraphs and appendices.

8.1 Instrument Capacity and System Linearity

The range and linearity of the instrument performance was determined by using 2-fold dilution scheme of reaction product AMC covering a 1024-fold concentration range. Before the actual calibration testing, the concentration of the AMC standard reference (1 mM stock solution) was adjusted using NanoDrop (Thermo Scientific 2010) in wavelengths of 350 nm and 355 nm (Appendix 3).

In order to assess the decrease in fluorescence intensity, the measurement was set to 55 minutes in five minutes intervals. Results were assessed with Graph Pad Prism 6 using statistical evaluation of linear curve fitting with interpolation function that is designed to recognize outliers, and also calculates the coefficient of variation. Only Blank (assay buffer) corrected values were used for assessment. The fluorescence intensity capacity of the equipment is evaluated up to 100 μ M AMC in the first phase. 95 % confident intervals are marked red (Figure 9).

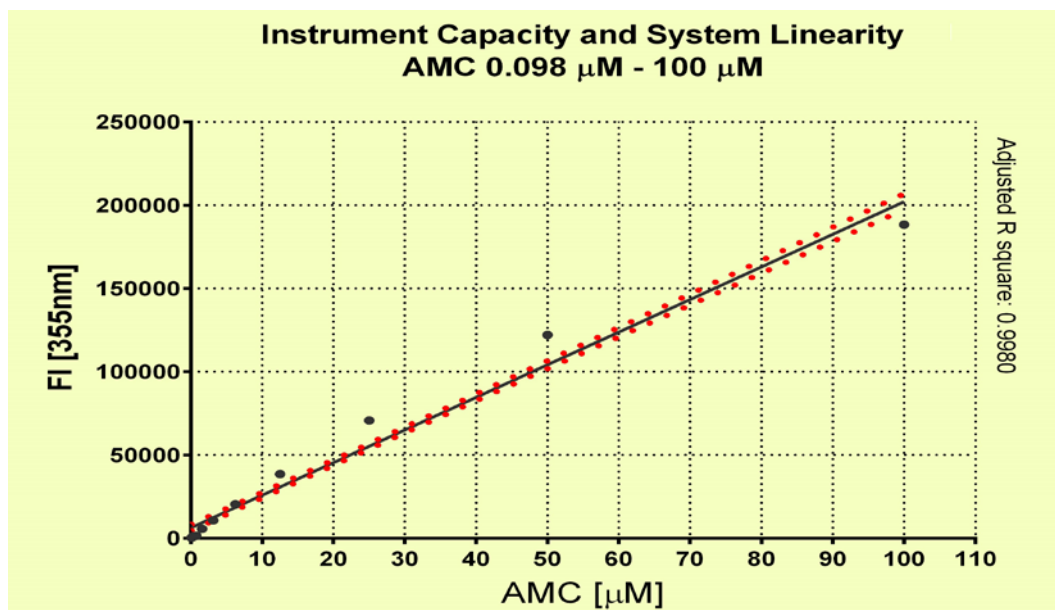


Figure 9. System Capacity and System Linearity 0.098 μM – 100 μM .

Second phase evaluates the linearity up to 6.25 μM AMC, as the preliminary experiments show that the final product formation of the reaction lies around 5 μM AMC. The 95 % confident intervals are marked red (Figure 10).

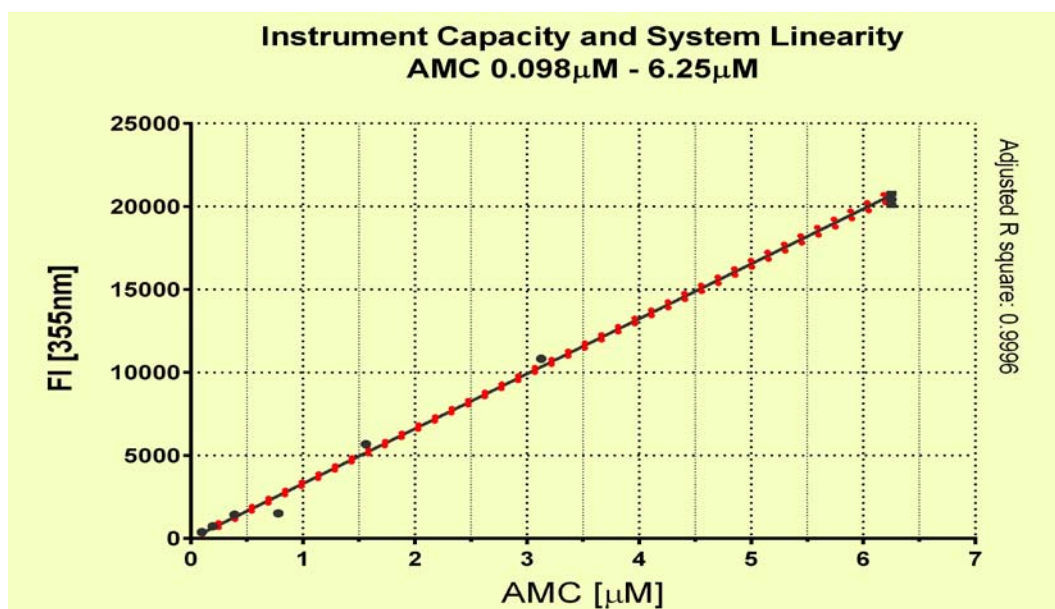


Figure 10. System Capacity and System Linearity 0.098 μM – 6.25 μM .

The enzymatic reaction of rhHepsin and BOC substrate is in the linear portion of the system linearity and detection limits. According to manufacturer's specifications, the sensitivity of the Fluostar Omega corresponds to < 0.2 fmol/well Sodium Fluorescein,

which is below the measured minimum of 0.098 μM AMC standard reference. The equipment is capable of detecting fluorescence intensities up to 100 μM AMC although the linearity decreases above concentrations of 10 μM AMC, as well as during the 55 minutes measurement (Appendix 4).

The signal amplification of the equipment was further optimized by gain adjustment in order to ensure the maximum sensitivity and dynamic range for the conversion of AMC. The AMC reference standard was used for the optimization that resulted in 10 % target value and Gain value of 600.

8.2 Initial Velocity Conditions

The following chapters describe the steps taken to determine initial velocity conditions for the enzymatic reaction of recombinant hepsin and BOC substrate. Determining initial velocity conditions consists of active site titration and enzyme kinetics.

8.2.1 Active Site Titration

Titration matrix was designed for two titrations respectively (Table 1). In order to analyze the reaction progress curves, both titration matrices were assessed parallel according to substrate concentration. For clarity, the higher and lower concentrations were excluded as they do not contribute to the overall assessment.

When analyzing the reaction progress curves of both titration matrices, it becomes noticeable that higher enzyme concentrations convert AMC relatively fast. The linearity, reaction time and plateau between the titration matrices vary greatly. Generally, the first titration with 50 μM BOC entailed shorter reaction times and higher plateaus compared to the second titration, whereby linearity correlated better time-wise in the second titration (Figure 11).

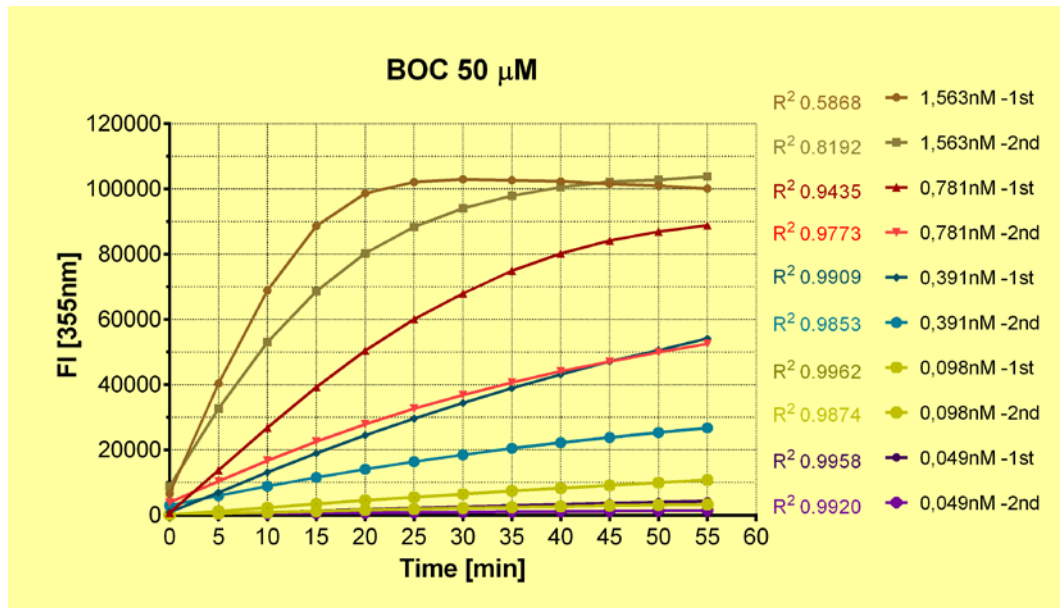


Figure 11. Comparison of 1st and 2nd Titration Matrices 50 µM BOC.

Both titrations with 25 µM BOC resulted in similar phenomena as in the titrations with 50 µM BOC. The first titration resulted in shorter reaction times and higher plateaus compared to the second titration except for second titration with 1.563 nM rhHepsin. Also, the linearity correlated better time-wise in the second titration. (Figure 12).

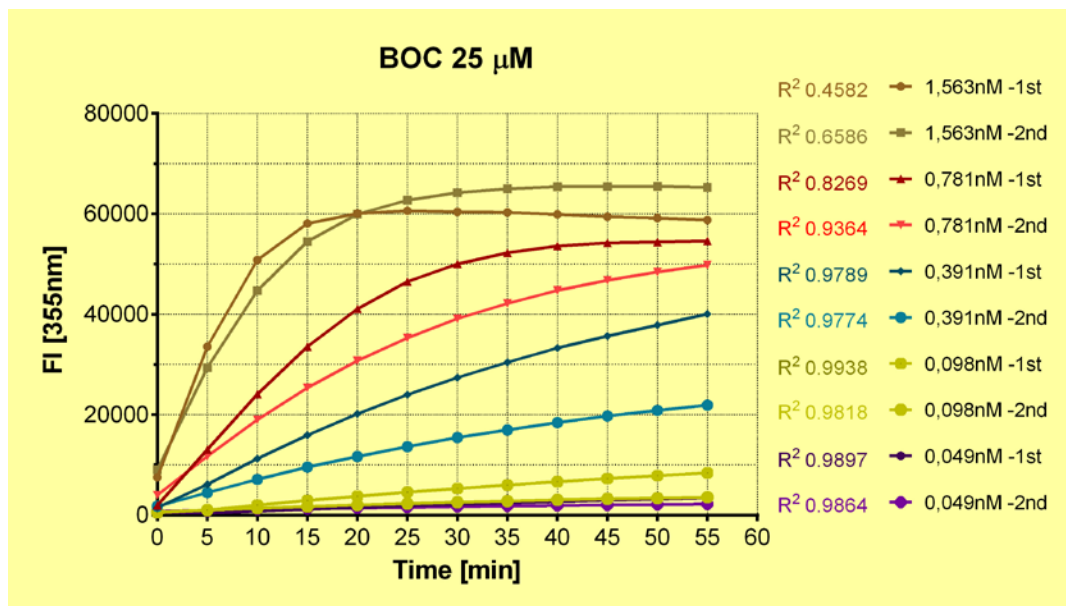


Figure 12. Comparison of 1st and 2nd Titration Matrices 25 µM BOC.

The titrations with 12.5 μM BOC conforms the previous results. The first titration resulted in shorter reaction times and higher plateaus compared to the second titration, wherein linearity correlated better time-wise in the second titration (Figure 13).

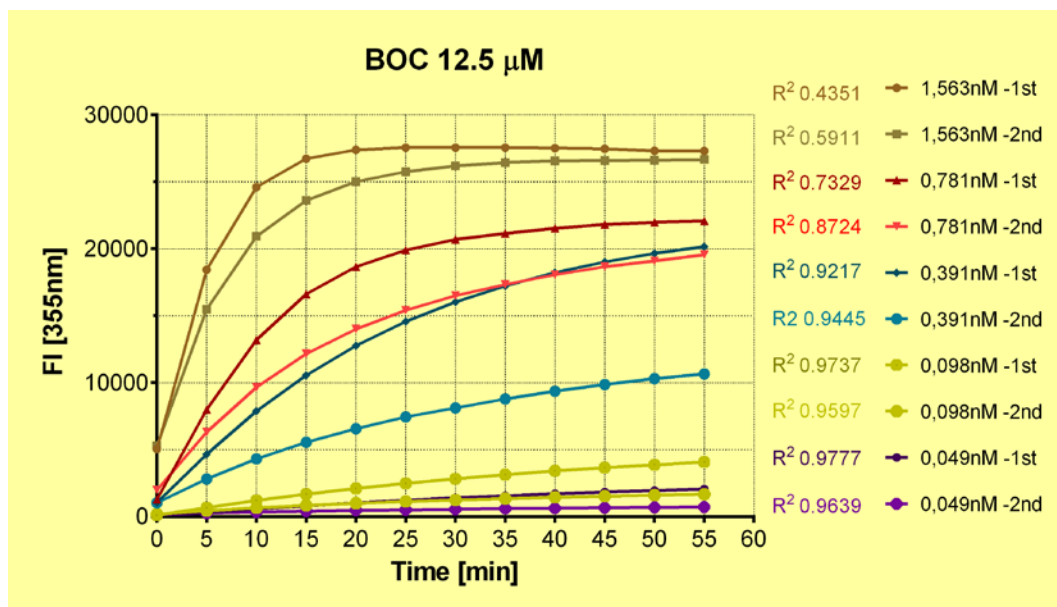


Figure 13. Comparison of 1st and 2nd Titration Matrices 12.5 μM BOC.

The most complex matter is that the reaction progress curves between the enzyme concentrations are not consistent as can be seen with the overlapping enzyme concentrations of 0.781 nM and 0.391 nM with all substrate concentrations. This may indicate to other unknown yet influencing factors in assay processing. Furthermore, the plateaus within a titration do not converge, which is due to decrease in enzyme activity with time.

Same phenomenon as in the previous measurements is particularly outlined in the titration matrices after bracketing (Table 2). The linearity, reaction time and plateau vary greatly between the titrations. The first titration resulted in shorter reaction times and higher plateaus compared to the second titration. The enzyme concentration of 0.15 nM of the second titration is overlapping with the enzyme concentration of 0.075 nM of the first titration as well as the enzyme concentration of 0.075 nM of the second titration is overlapping with the enzyme concentration of 0.0375 nM of the first titration with the substrate concentration of 50 μM BOC (Figure 14).

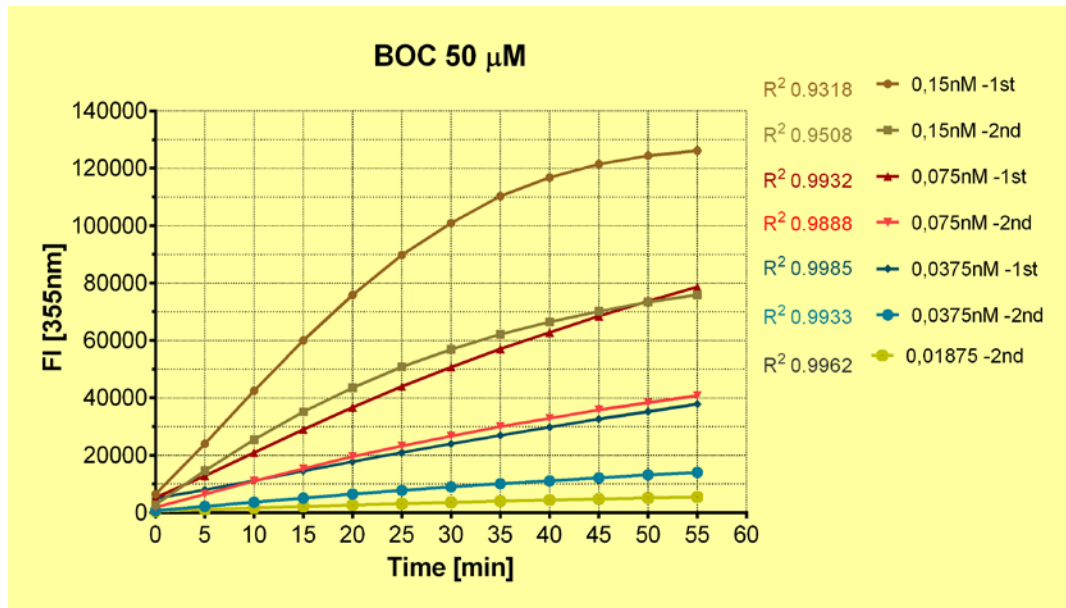


Figure 14. Comparison of 1st and 2nd Titration Matrices 50 μM BOC After Bracketing.

The enzyme concentration of 0.15 nM of the second titration is overlapping with the enzyme concentration of 0.0375 nM of the first titration, wherein the enzyme concentration of 0.075 nM of the second titration is below the enzyme concentration of 0.0375 nM of the first titration with the substrate concentration of 25 μM BOC (Figure 15).

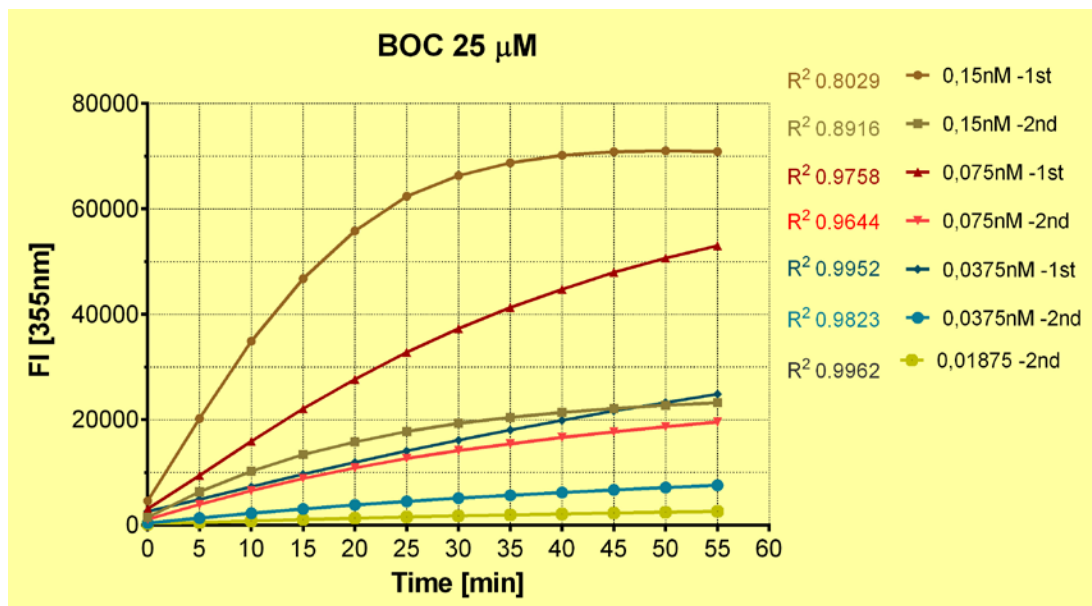


Figure 15. Comparison of 1st and 2nd Titration Matrices 25 μM BOC After Bracketing.

This concludes that the enzyme activity has decreased between the first and the second titration possibly due to inter alia light or higher temperatures during assay pro-

cessing. In order to assess the loss of activity, as well as to determine the optimum enzyme concentration, a series of enzyme kinetics measurements were conducted

8.2.2 Enzyme Kinetics

Only the lowest 5 μM substrate level generated progress curves according to the levels of enzyme concentrations. Meaning, enzyme concentration 0.8 nM yielded the shortest reaction time and the highest plateau, enzyme concentration 0.7 nM yielded the second shortest reaction time and the second highest plateau and so forth (Figure 16a).

In higher substrate levels, this enzyme concentration order is disrupted: Substrate level 15 μM generated progress curves where enzyme concentrations 0.8 nM and 0.7 nM yielded similar reaction times, whereas 0.7 nM reached higher plateau, as well as enzyme concentration 0.5 nM had a shorter reaction time then 0.4 nM, which reached higher plateau nonetheless (Figure 16b).

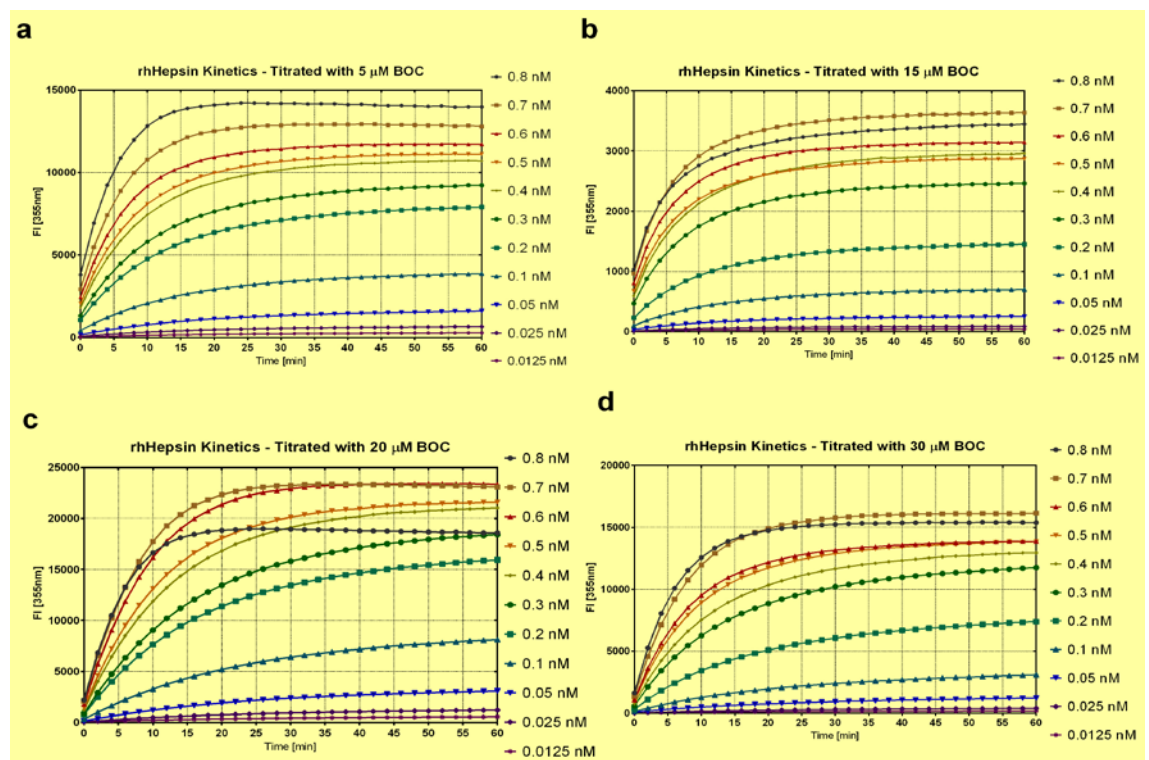


Figure 16. Enzyme Kinetics. a. Substrate level 5 μM . b. Substrate level 15 μM . c. Substrate level 20 μM . d. Substrate level 30 μM .

Similarly, substrate level 20 μM generated progress curves where enzyme concentration 0.8 nM yielded similar reaction time as 0.7 nM. However, the reached plateau of 0.8 nM remained lower than in concentrations of 0.7 nM, 0.6 nM, 0.5 nM and 0.4 nM ending at the same level with the concentration of 0.3 nM (Figure 16c).

The same phenomena are repeated in the progress curves generated with substrate level 30 μM . Enzyme concentration 0.8 nM yields shorter reaction time than 0.7 nM, whereas the reached plateau remains lower than 0.7 nM concentration. The same is repeated with enzyme concentrations 0.6 nM and 0.5 nM (Figure 16d).

In conclusion, the equilibrium of enzyme-substrate reaction is sensitive to concentration changes in either one of the two substances and is influenced by such factors as product inhibition, substrate limitation as well as reverse reaction as observed in the reaction progress curves in figures 16a to 16d. Another interfering factor that can be observed is the enzymes instability over time.

On the basis of the results of enzyme kinetic experiments, the enzyme concentration was modified to 0.1 nM and the measurement time was cut to 30 minutes as the reaction remains linear within this time. Notice: By further development the enzyme concentration may be increased to 0.2 nM as the usage of DMSO inhibits the reaction and the measurement time cut down to 10 minutes or 15 minutes under the condition that the equipment is able to measure the reaction under initial velocity conditions.

8.2.3 Enzyme Activity

In the course of measurements, performed in enzyme kinetics, it became apparent that the enzyme recombinant hepsin shows instability over time. This means that if the enzyme remains stable under the test conditions, the reaction progress curves of each enzyme concentration will converge until they reach similar maximum plateau value of product formation with the same substrate concentration. However, if the enzymes activity decreases during reaction, the progress curves of different enzyme concentrations will not converge and the tested enzyme concentrations do not reach the same maximum plateau value of product formation, as can be seen in figures 16a to 16 d.

8.3 K_m and V_{max}

Initial velocity conditions were predetermined in the measurements described in section 8.2. During the development, the K_m & V_{max} had to be determined several times due to erratic nature of the K_m value, as well as when new enzyme Lot. was taken in use, since enzyme activity differs between batches. With the exception of one, all determined K_m values (Appendix 5) were similar, of which was decided on the latest result 17.76 μM (Figure 17).

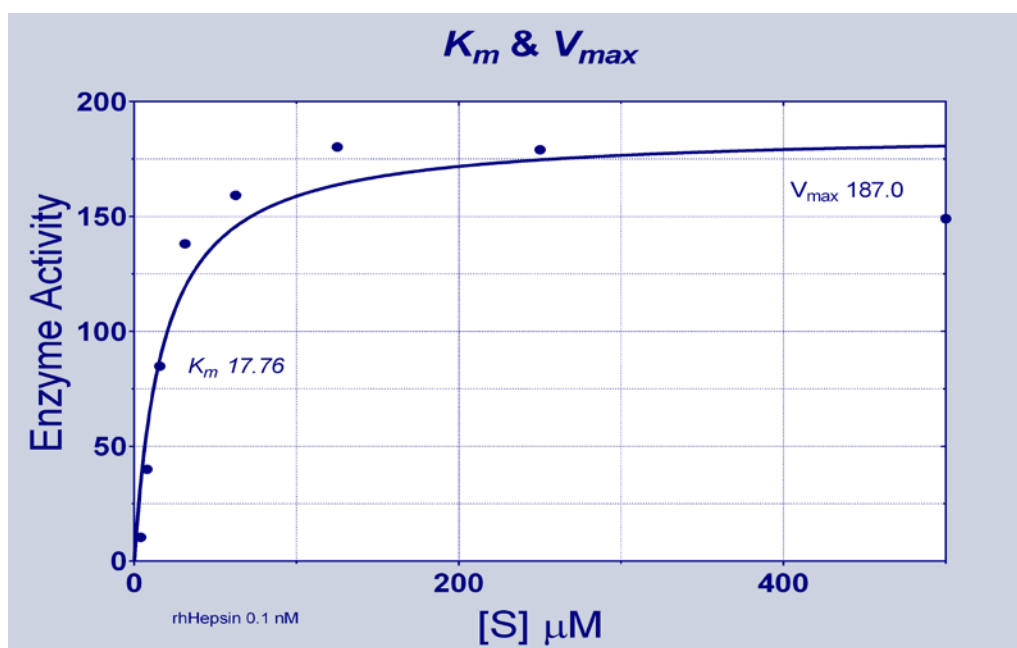


Figure 17. Determination of K_m & V_{max} .

Since a substrate concentration around or below K_m can be used as a guideline in detecting competitive inhibitors, a substrate concentration of 15 μM was used in all subsequent measurements. Recombinant hepsin concentration was set to 0.1 nM (See chapter 8.2.2).

8.4 DMSO Compatibility

DMSO compatibility was assessed with Graph Pad Prism, as well as with Excel calculations in order to gain a better understanding of the inhibition caused by DMSO. The DMSO concentrations above 2 % induce an inhibition of more than 90 %, when DMSO concentrations below 0.50 % induce an inhibition less than 30 % (Table 5).

Table 5. DMSO Compatibility.

DMSO	Inhibition
0,05 %	6,98 %
0,10 %	13,77 %
0,25 %	12,40 %
0,50 %	28,22 %
0,75 %	32,01 %
1 %	84,76 %
2 %	90,46 %
3 %	90,35 %
4 %	91,72 %
5 %	92,78 %

Graph Pad Prism ECanything analysis gave for an inhibition of 5 % in the enzyme-substrate reaction a DMSO concentration of 0.01 % (Figure 18). ECanything F5 (5 % inhibition) was analyzed using 30 minute end-point measurement.

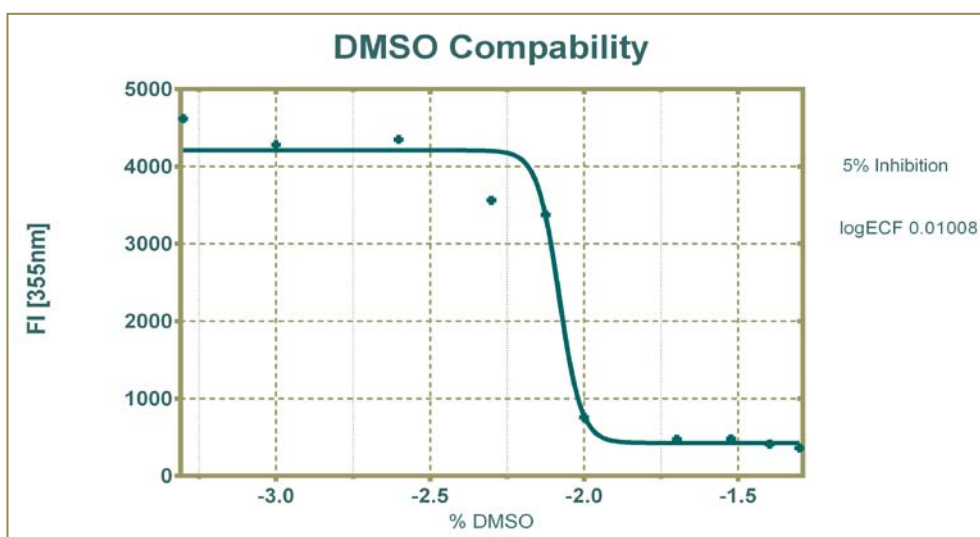


Figure 18. DMSO Compatibility.

In connection with the Excel assessment, it was decided that final assay design should not contain a DMSO concentration above 0.5 %. In addition, a DMSO concentration of 0.5 % causes a 5 % increase in background level. The final DMSO concentration of the compounds will be defined after establishing IC_{50} for Mid-level signal as the DMSO concentration has to be similar in positive control.

8.5 IC_{50} for Mid-level Signal

IC_{50} was determined for compound NTH1, which is used as positive control in enzymatic assay. There were two different NTH1 batches in use: NTH1 and NTH1 “new” which both gave similar IC_{50} values.

IC_{50} was determined by using 3 fold dilution series covering the 50 000-fold concentration range, as well as half-log dilution series parallel that both resulted in similar values in each case. The first NTH1 batch that was in use NTH1 gave an IC_{50} value of 5.458 μM (Figure 19).

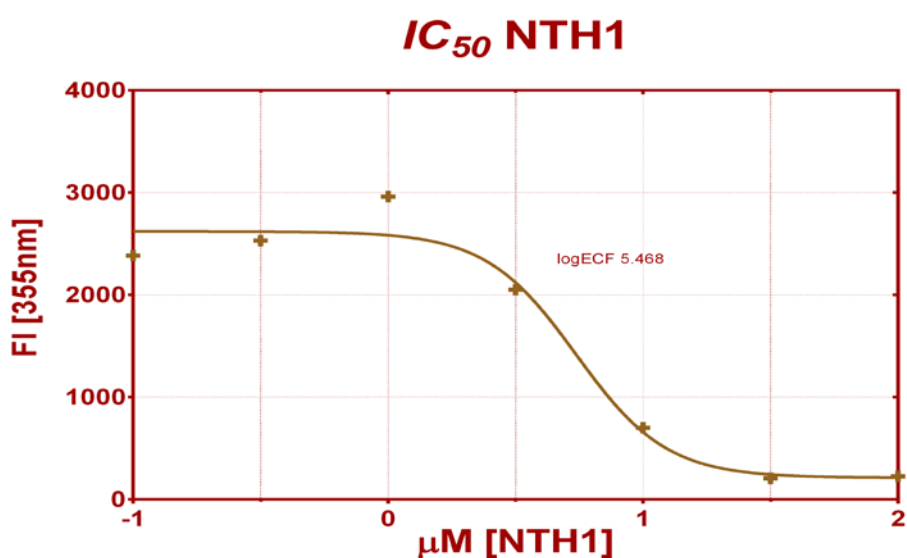


Figure 19. NTH1.

IC_{50} value for the second batch NTH1 “new” was determined in a similar manner using 3-fold dilution series parallel with half-log dilution series. The NTH1 “new” resulted to an IC_{50} value of 5.216 μM (Figure 20).

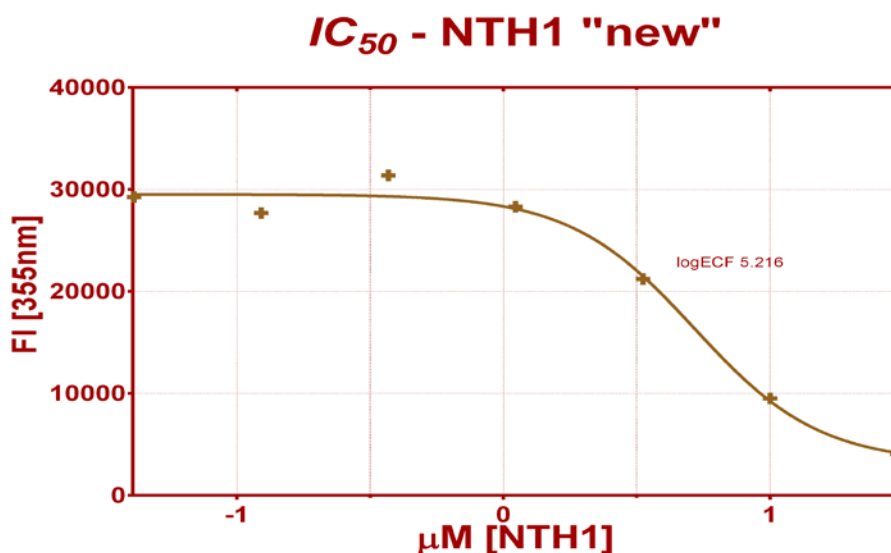


Figure 20. NTH1 "new".

As NTH1 gave an IC_{50} value of 5.458 μM and NTH1 "new" an IC_{50} value of 5.216 μM , the Mid-level signal is set to 6 μM of NTH1. This is due to the guideline that mid-level signal concentration should be above the concentration that causes 50 % inhibition in enzyme-substrate reaction. This concludes as the final DMSO concentration 0.3 % in both compounds and positive control.

8.6 Activity Loss

In addition to enzyme instability, indications of activity loss by both positive control and screened compounds were apparent during preliminary compound screening (See chapter 8.8.2). Therefore, both NTH1 and a set of compounds were tested for activity loss under two different treatment conditions. A percentage difference was calculated between the compounds that underwent different treatment (Equation 1).

Equation 1: Percentage Difference.

$$\text{Percentage Difference} = \left(\frac{\text{Difference (AB)}}{\text{Average (AB)}} \right) * 100$$

There were two different DMSO levels in the experiment: First level (-DMSO) presenting the enzyme-substrate reaction. Second level (+DMSO) presenting the enzyme-substrate reaction including inhibition induced by 0.5 % DMSO. The activity loss exper-

iments were conducted before establishing DMSO compatibility and IC_{50} for mid-level signal.

8.6.1 Activity Loss of Positive Control NTH1

In treatment condition one, the NTH1 “new” was kept frozen (0°C) for one hour before assay processing and preserved in ice during assay processing. In treatment condition two, the NTH1 “old” was allowed to reach room temperature (RT) during one hour before processing and preserved in room temperature during assay processing.

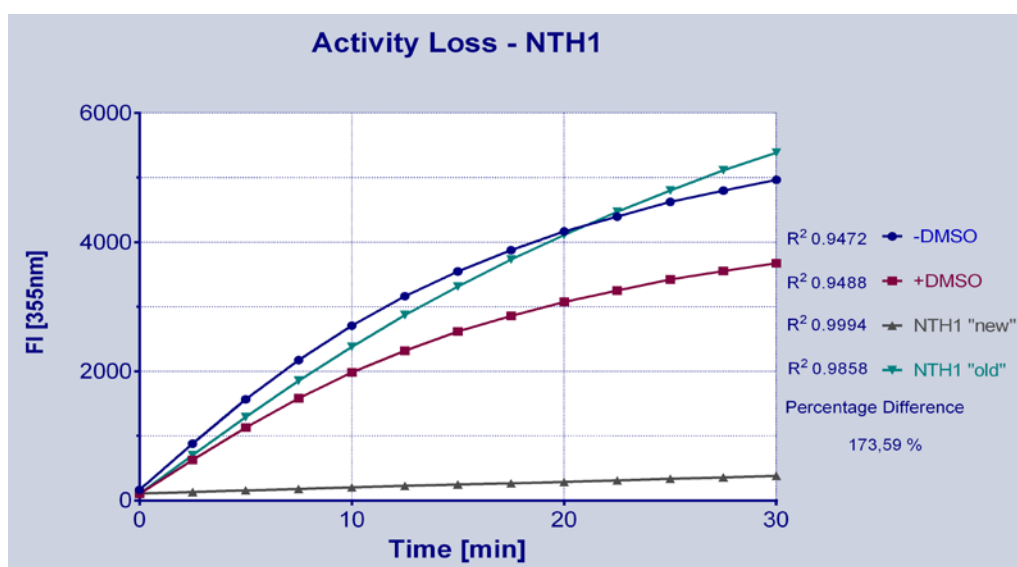


Figure 21. Activity Loss by NTH1. NTH1 “new” was kept in 0°C and NTH1 “old” in RT.

The activity loss of NTH1 was demonstrated, as NTH1 “old” presented no inhibition, in contrast to NTH1 “new”. The percentage difference resulted in 174 % difference in inhibition between the compounds under two treatment conditions “new” (0°C) and “old” (RT). (Figure 21).

8.6.2 Activity Loss Screening of Compounds

In treatment condition one, the compound (A) was kept frozen (0°C) for one hour before assay processing and preserved in ice during assay processing. In treatment condition two, the compound (B) was allowed to reach room temperature (RT) during one hour before processing and preserved in room temperature during assay processing.

For the activity loss screening, ten compounds were selected according to previously measured activity levels. Activity levels were categorized as inhibition, enhancement and within limits, as no inhibition and no enhancement using $\pm 20\%$ cut-off limits. The $\pm 20\%$ cut-off limits were calculated in relation to first DMSO level. Graphical analysis was performed for the second screening only, as in the first screening the used DMSO caused a total inhibition, which was due to the different DMSO Lots used in the laboratory, but in this point of development it had no effect to the evaluation. This complies also to the fact that the mid-level NTH1 concentration was also yet to be defined. Also, the negative fluorescence intensities were due to changes in baseline as the instrumentation automatically corrected the measured values.

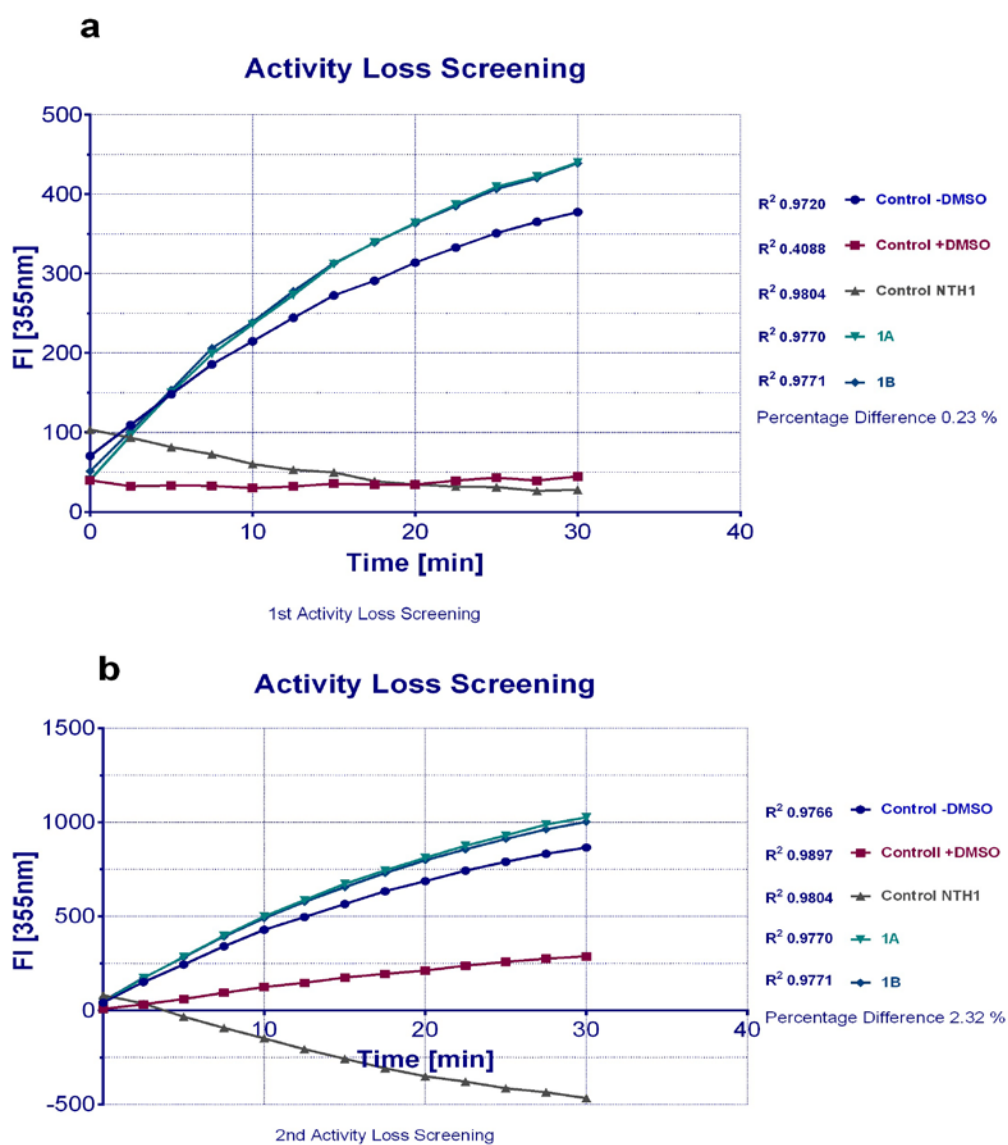


Figure 22. Activity Loss Screening, Compound 9128. a. 1st screening, b. 2nd screening. Compound 1A is kept in condition A (0°C) and compound 1B in condition B (RT).

The compound 9128 remained within limits in both screenings after both treatment conditions A and B. Both screenings presented similar results, giving very low percentage difference between the two treatment conditions with 0.2 % in the first screening and 2 % in the second screening (Figure 22a-b). The graphical analysis of the compound in relation to second level of DMSO (+DMSO) demonstrates enhancement in both treatment A and B.

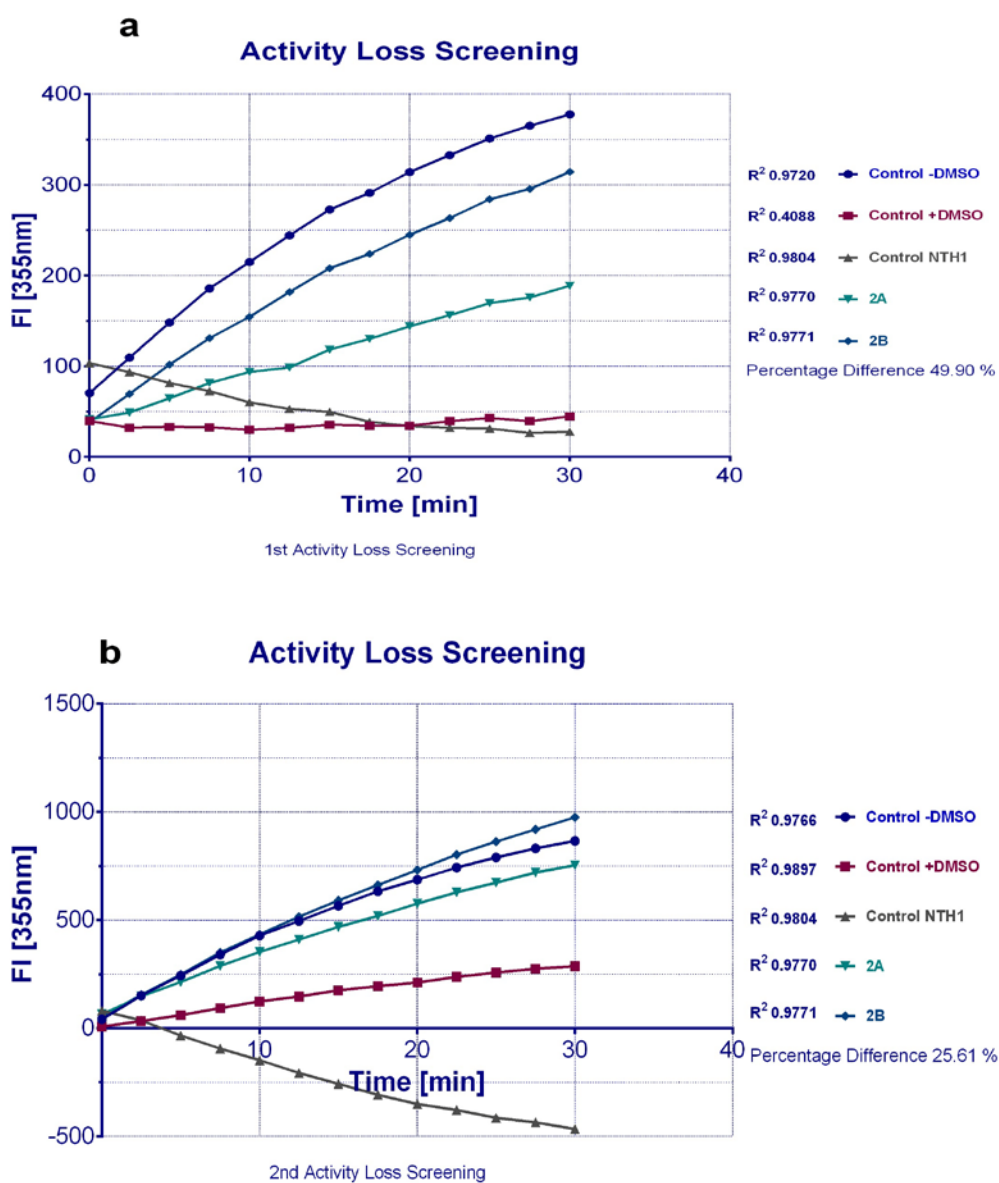


Figure 23. Activity Loss Screening, Compound 6934. a. 1st screening, b. 2nd screening. Compound 2A is kept in condition A (0°C) and compound 3B in condition B (RT).

The compound 6938 induced inhibition after treatment A in the first screening, whereby after treatment B the compound remained within limits (Figure 23a). In the second

screening the compound remained within limits after both treatment A and B (Figure 23b). Percentage difference was relatively high with 49 %, in the first screening when the second screening presented lower 25 % difference between the two conditions. The graphical analysis of the compound in relation to second level of DMSO (+DMSO) demonstrates enhancement in both treatment A and B. The results indicate that the compound is sensitive to interfering factors.

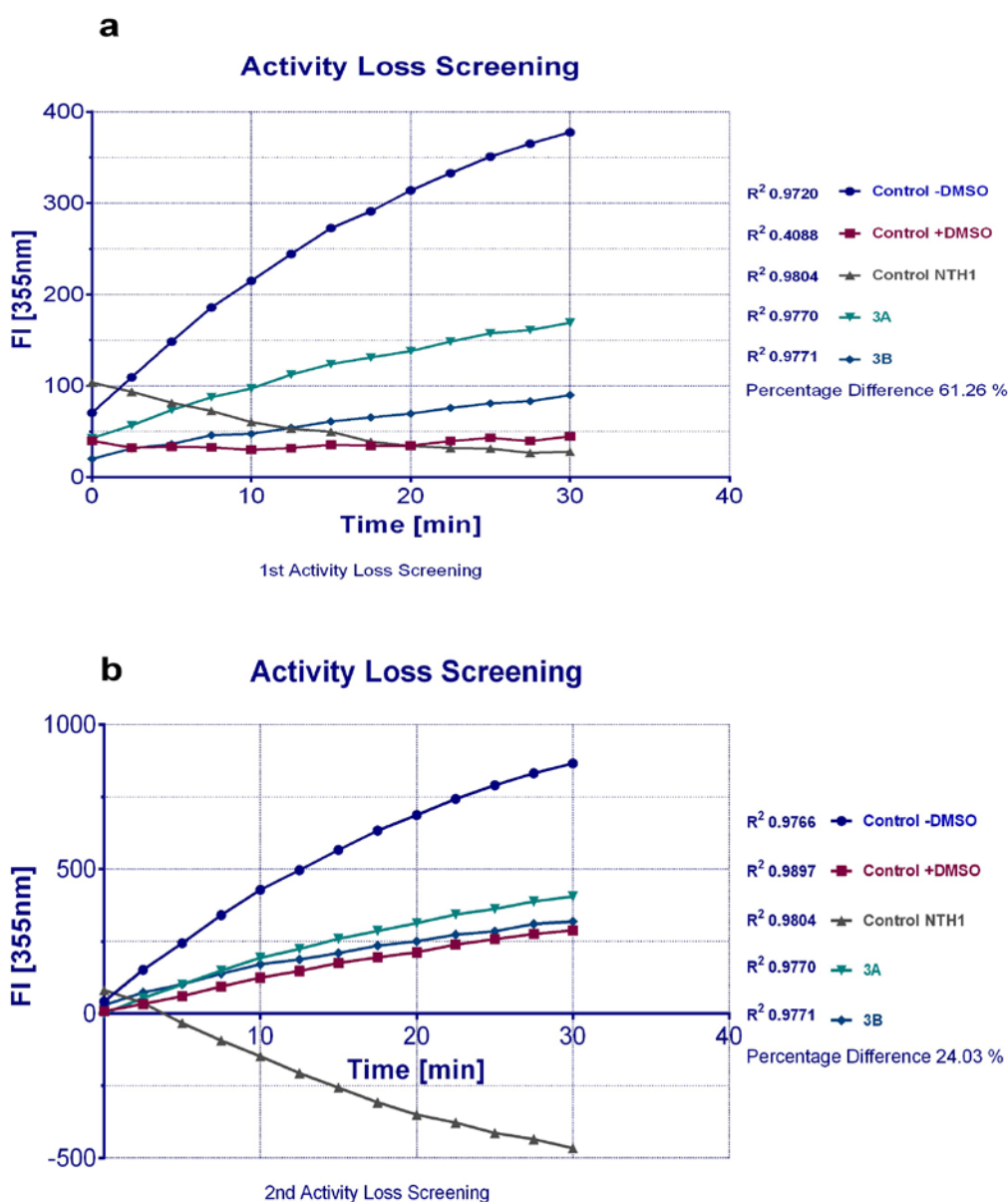


Figure 24. Activity Loss Screening, Compound 2881. a. 1st screening, b. 2nd screening. Compound 3A is kept in condition A (0°C) and compound 3B in condition B (RT).

The compound 2881 induced inhibition after both conditions A and B in both screenings. Percentage difference between the conditions was relatively high with 61 % in the

first screening, whereby the second screening presented lower 24 % difference between the conditions (Figure 24a-b). The graphical analysis of the compound in relation to second level of DMSO (+DMSO) demonstrates slight enhancement in both treatment A and B.

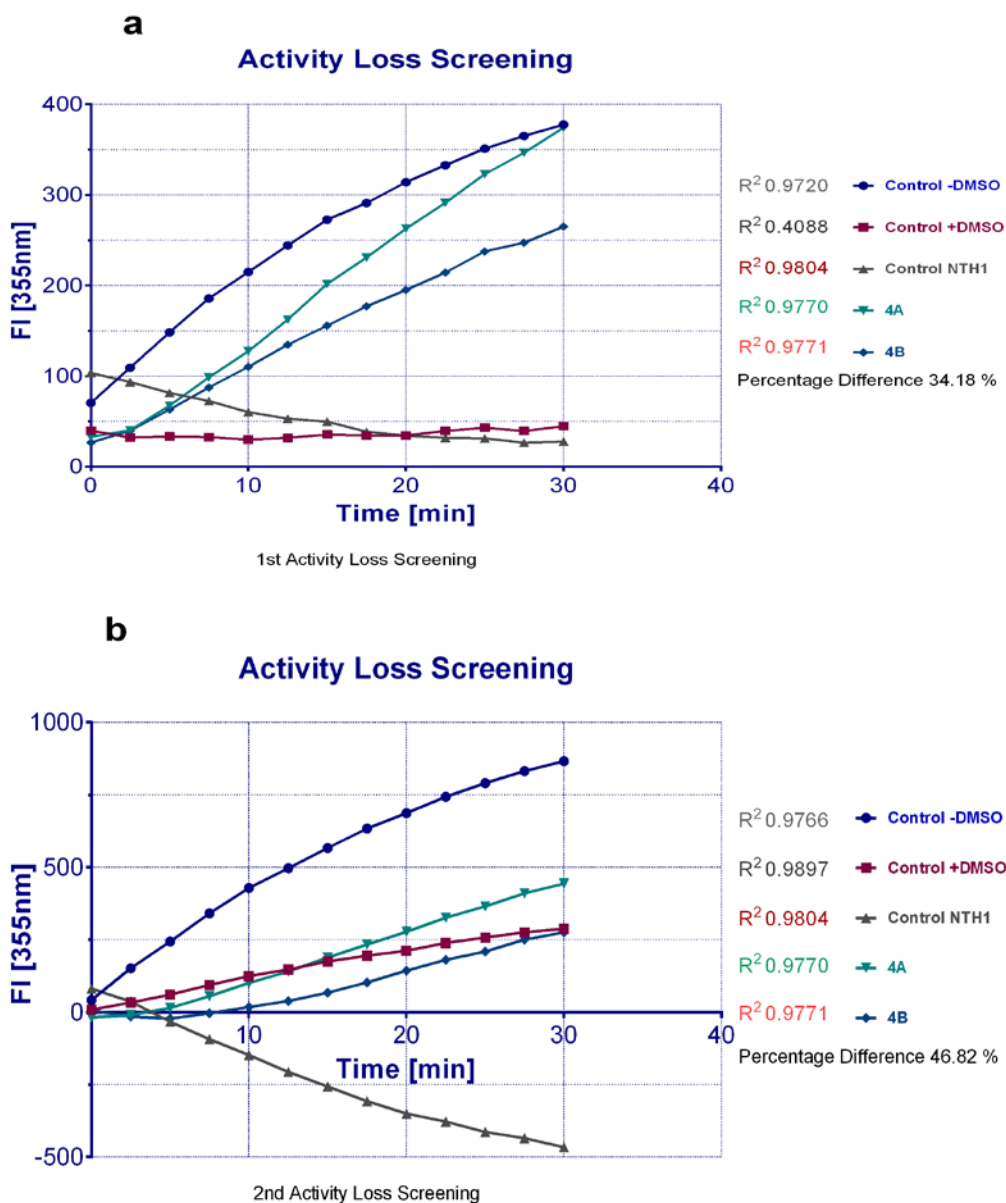


Figure 25. Activity Loss Screening, Compound 3129. a. 1st screening, b. 2nd screening. Compound 4A is kept in condition A (0°C) and compound 4B in condition B (RT).

The compound 3129 induced inhibition after treatment B in the first screening, whereas after treatment A the compound remained within limits (Figure 25a). In the second screening, the compound induced inhibition after both treatment A and B (Figure 25b). Percentage differences in both screenings were relatively high with 34 % in the first

screening and 47 % in the second screening. The graphical analysis of the compound in relation to second level of DMSO (+DMSO) demonstrates slight enhancement in both treatment A and B. Results indicate that the compound is sensitive to interfering factors.

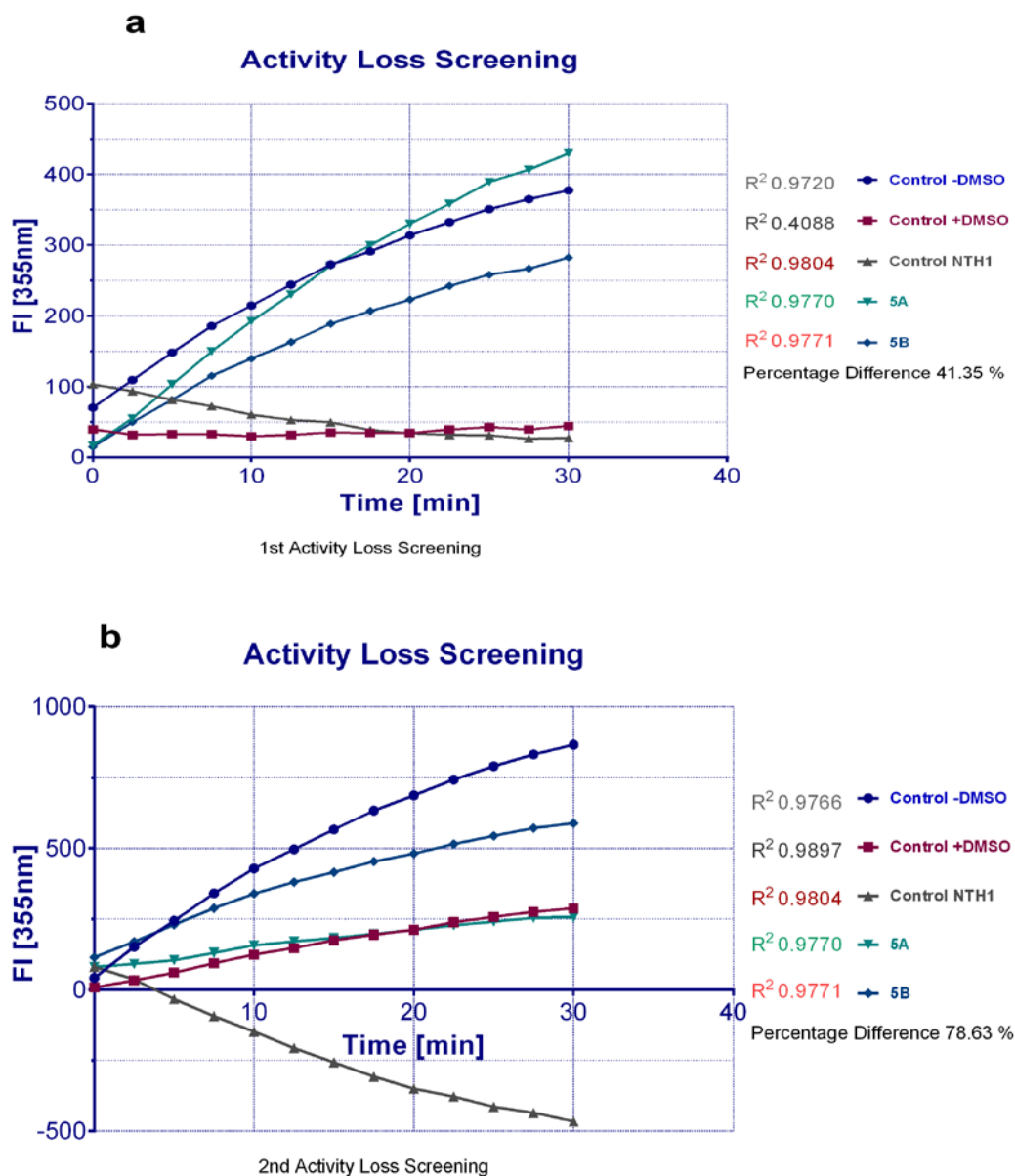


Figure 26. Activity Loss Screening, Compound 1907. a. 1st screening, b. 2nd screening. Compound 5A is kept in condition A (0°C) and compound 5B in condition B (RT).

The compound 1907 induced inhibition after treatment B in the first screening, whereas after treatment A the compound remained within limits (Figure 26a). In the second screening, the compound induced inhibition after both treatment A and B (Figure 26b). Percentage difference in the first screening was relatively high with 41 % and very high

in the second screening with 78 %. The graphical analysis of the compound in relation to second level of DMSO (+DMSO) demonstrates enhancement after treatment B and within limits after treatment A. The results indicate that the compound is sensitive to interfering factors.

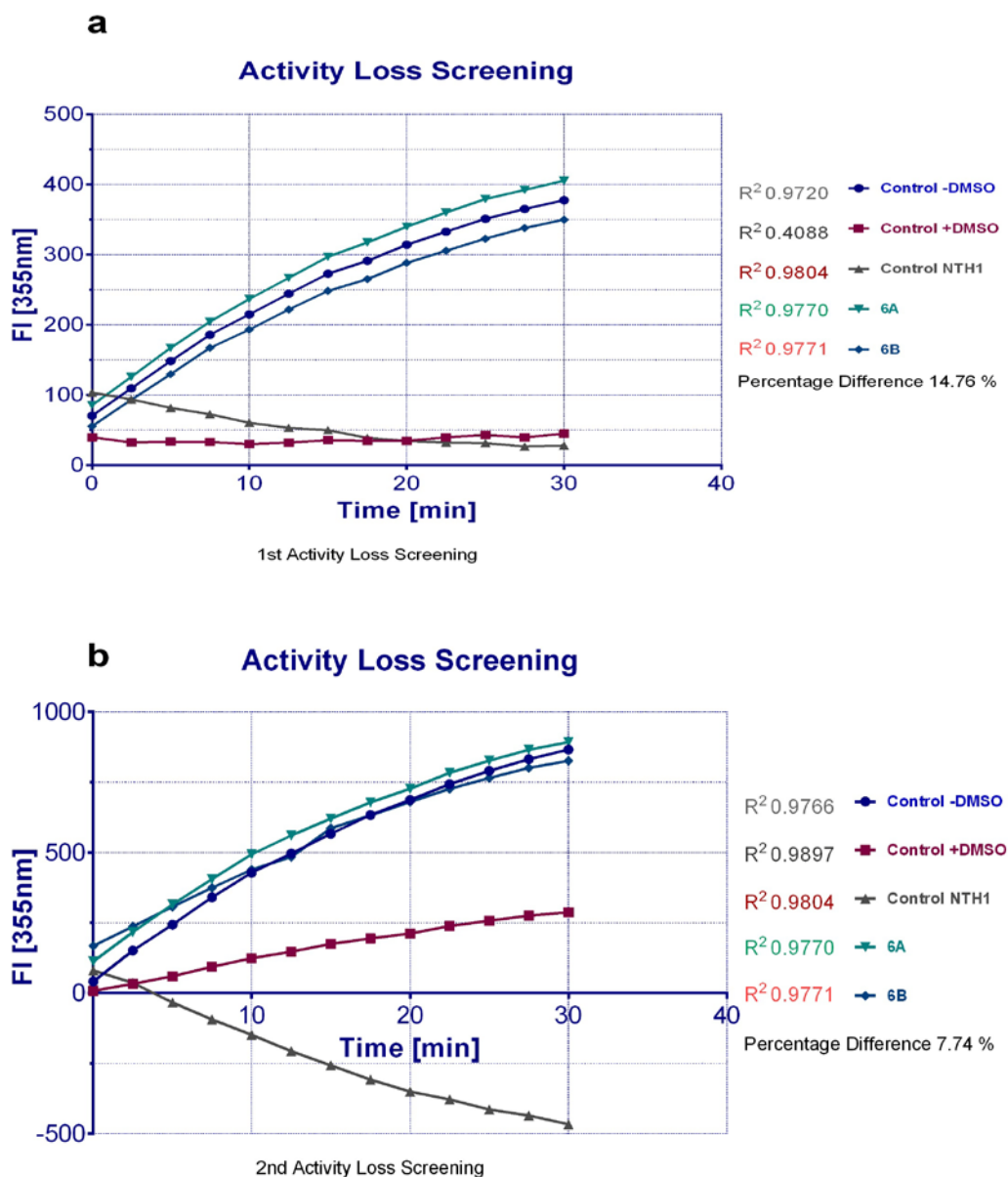


Figure 27. Activity Loss Screening, Compound 5119. a. 1st screening, b. 2nd screening. Compound 6A is kept in condition A (0°C) and compound 6B in condition B (RT).

The compound 5119 remained within limits in both screenings after both treatment conditions A and B. Both screenings presented similar results, giving relatively low percentage difference between the two treatment conditions with 15 % in the first screening and 8 % in the second screening (Figure 27a-b). The graphical analysis of the

compound in relation to second level of DMSO (+DMSO) demonstrates enhancement in both treatment A and B.

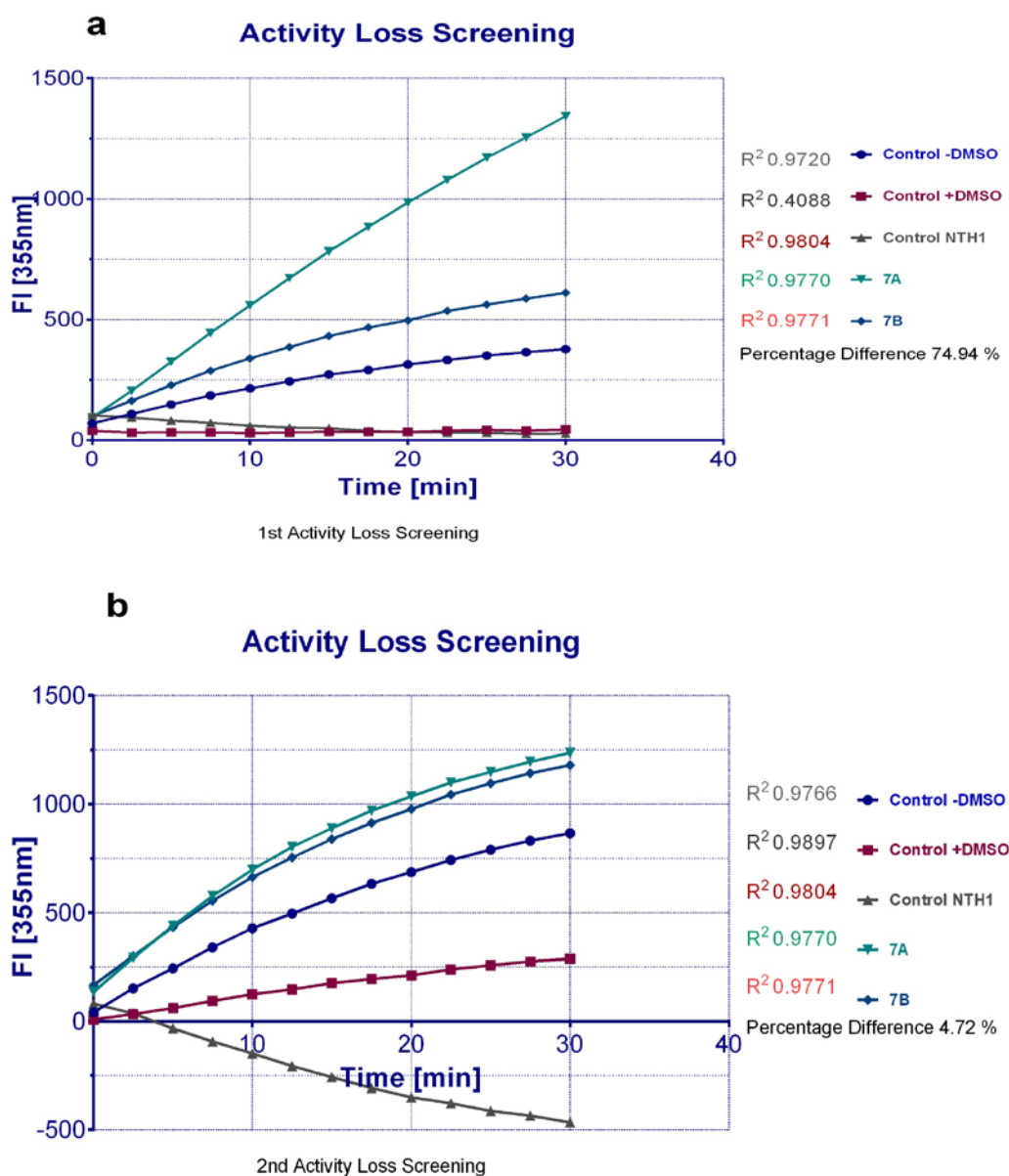


Figure 28. Activity Loss Screening, Compound 1571. a. 1st screening, b. 2nd screening. Compound 7A is kept in condition A (0°C) and compound 7B in condition B (RT).

The compound 1571 enhanced the reaction in both screenings after both treatment conditions A and B. Interestingly, in the first screening, the percentage difference is relatively high with 75 %, whereas in the second screening the percentage difference is low with 5 % between both treatment A and B (Figure 28a-b). The graphical analysis of the compound in relation to second level of DMSO (+DMSO) demonstrates enhancement in both treatment A and B.

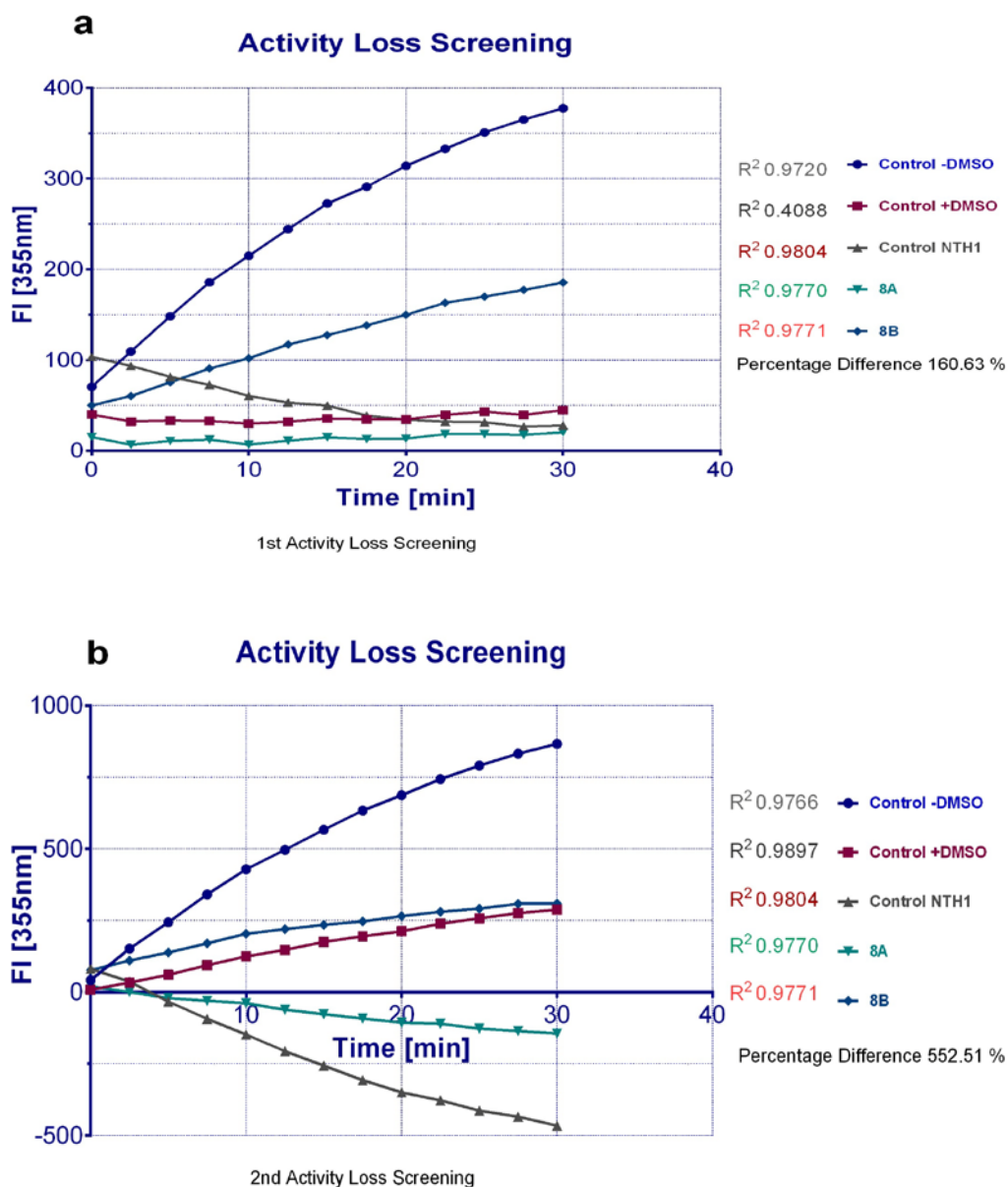


Figure 29. Activity Loss Screening, Compound 1908. a. 1st screening, b. 2nd screening. Compound 8A is kept in condition A (0°C) and compound 8B in condition B (RT).

The compound 1908 induced inhibition after both conditions A and B in both screenings. Percentage difference between the conditions was very high with 161 % in the first screening, and in the second screening with 553 % difference between the conditions (Figure 29a-b). The graphical analysis of the compound in relation to second level of DMSO (+DMSO) demonstrates inhibition after treatment A, whereas the compound remained within limits after treatment B.

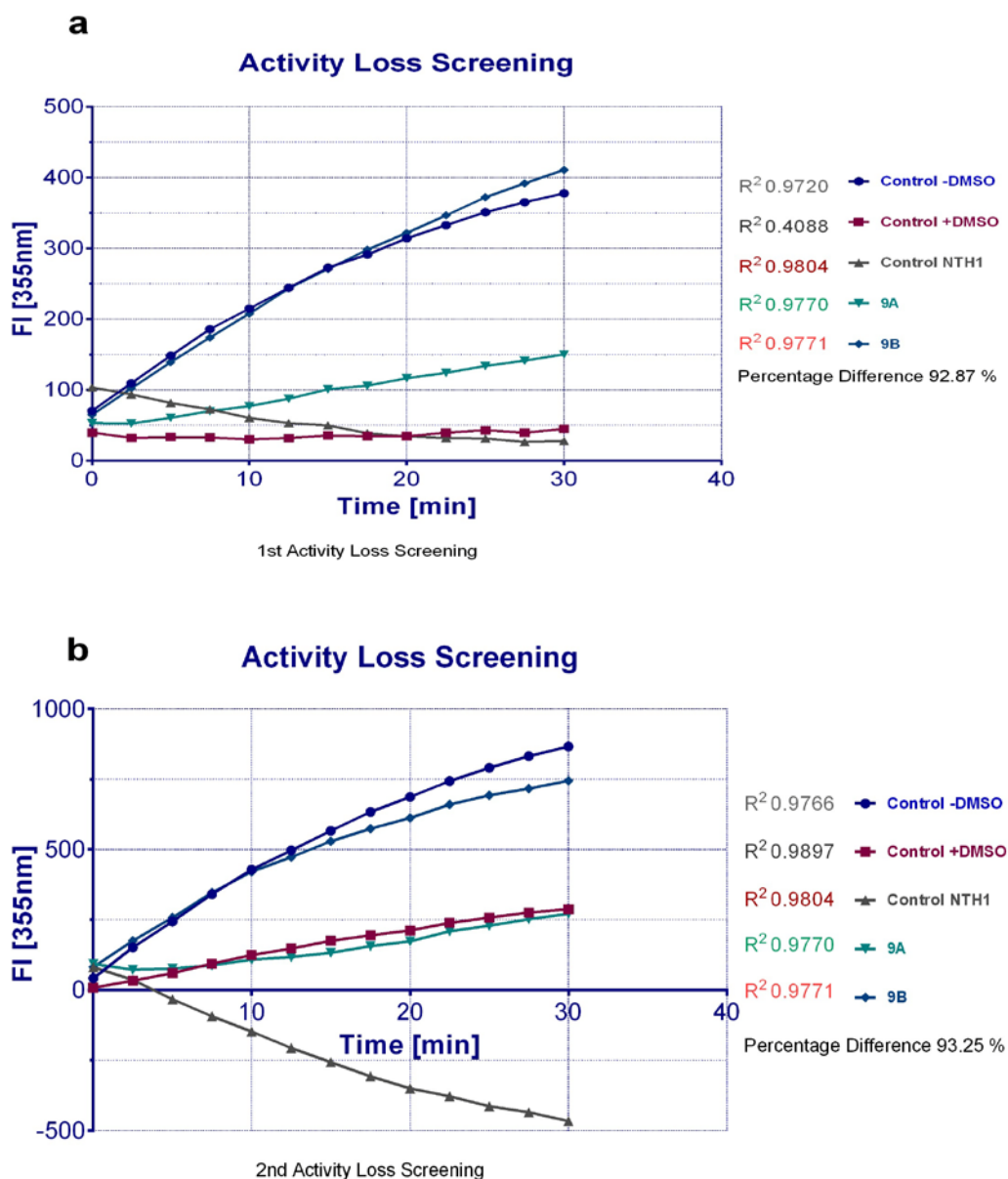


Figure 30. Activity Loss Screening, Compound 5174. a. 1st screening, b. 2nd screening. Compound 9A is kept in condition A (0°C) and compound 9B in condition B (RT).

The compound 5174 induced inhibition after treatment A, whereas after treatment B the compound remained within limits in both screenings (Figure 30a-b). Percentage difference in both screening was similarly high with 93 %. The graphical analysis of the compound in relation to second level of DMSO (+DMSO) demonstrates enhancement after treatment B and within limits after treatment A. The results indicate that the compound is sensitive to temperature.

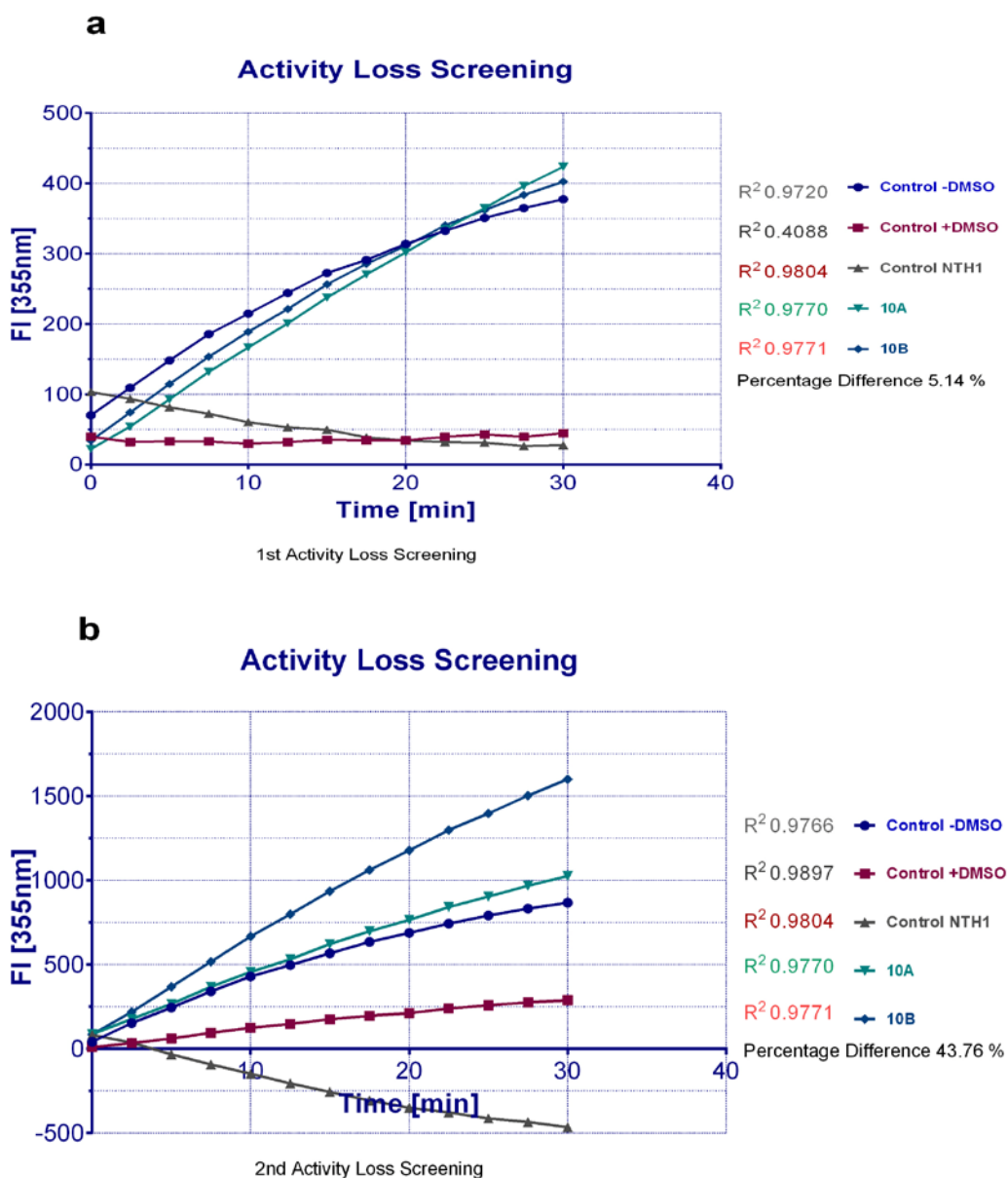


Figure 31. Activity Loss Screening, Compound 5062. a. 1st screening, b. 2nd screening. Compound 10A is kept in condition A (0°C) and compound 10B in condition B (RT).

The compound 5062 remained within limits in the first screening after both treatment A and B (Figure 31a). In the second screening, the compound remained within limits after treatment A, whereas the compound enhanced the reaction after treatment B (Figure 31b). Percentage difference in the first screening was relatively low with 5 % and relatively high in the second screening with 44 %. The graphical analysis of the compound in relation to second level of DMSO (+DMSO) demonstrates enhancement after both treatment A and B. The results indicate that the compound is sensitive to interfering factors.

The activity loss screening demonstrated the contradictory behavior of the screened compounds under two different treatment conditions. The results are outlined below (Table 6).

Table 6. Summary of Activity Loss Screening.

Compound	Code	1st Activity Loss Screening				2nd Activity Loss Screening			
		Inhibition	Within limits	Enhanc.	Percentage	Inhibition	Within limits	Enhanc.	Percentage
9128	1A		x		0.23		x		2.32
	1B		x				x		
6934	2A	x			49.90		x		25.61
	2B		x				x		
2881	3A	x			61.26	x			24.03
	3B	x				x			
3129	4A		x		34.18	x			46.82
	4B	x				x			
1907	5A		x		41.35	x			78.63
	5B	x				x			
5119	6A		x		14.76		x		7.74
	6B		x				x		
1571	7A			x	74.94			x	4.72
	7B			x				x	
1908	8A	x			160.63	x			552.51
	8B	x				x			
5174	9A	x			92.87	x			93.25
	9B		x				x		
5062	10A		x		5.14		x		43.76
	10B		x					x	

Explanatory description of the table:


Inhibition and **enhancement** are calculated using 20% -cut-off limits in relation to negative control.


Within limits states that the compound does not exhibit any inhibition or enhancement in relation to 20% -cut-off limits.


Percentage expresses the difference in activity between compound comparison pair.

Percentage difference = $(\text{difference (AB)} / \text{average(AB)}) * 100$

Comparison pair (A&B) expresses a compound that has undergone two different treatments.

Similar results between activity loss screenings are expressed with the colour: 

Differentiating results between activity loss screenings are expressed with the colour: 

Differentiating results between compound comparison pair are expressed with frame: 

Data analysis excluded five of the compounds as unchanged activity in relation to first DMSO level with $\pm 20\%$ cut-off limits, whereas the other five demonstrated changed activity. However, the percentage difference and graphical analysis show that the compounds have a tendency to enhance the reaction rate rather than inhibit the reaction. Depending on the treatment condition of the compound, the results showed significant variation.

8.6.3 Activity Reducing Factors

Factors that reduce activity could be traced during assay processing and incubation, as temperature during the assay processing caused loss in activity in positive control NTH1 and some of the screened compounds. The 30 minute incubation time seems to be the critical step for successful assay, as during the incubation the compounds are exposed to temperature changes inside the laboratory, as well as light. This can be seen as uneven incubation inside the 96-well plate, wherein the wells in the middle of the plate show significant evaporation in contrast to the wells on the edge.

8.7 Final Assay Design

The final assay design includes two negative control, namely -DMSO that contains only the enzyme-substrate combination and +DMSO that includes 0.3% DMSO. The negative control -DMSO is included as internal control, since during the previous measurements the differences in DMSO batches led to significant variation in results. The concentration of positive control NTH1 is set to 6 μM , wherein the compound concentration must also be 6 μM . Concentration of rhHepsin is 0.1 nM and BOC substrate 15 μM . Measurement time was optimized to 30 minutes and the equipment was optimized to gain value of 600 with 10 % target value. The final assay design is used for plate uniformity and signal variability assessment as well as for final compound screening.

8.8 Plate Uniformity and Signal Variability Assessment

The overall requirement for signal variability and plate acceptance criteria is met to conduct screenings. There were no outliers detected and all plates passed the acceptance criteria for max, mid and min signals, where each signal had a Coefficient of Variation less or equal to 20 %. Furthermore, the raw signals were sufficiently tight and there was enough separation between max and min signals (Figure 32).



Figure 32. Signal Variability, All Signal Levels. Each plate is plotted against fluorescence intensity [FI].

Midpoint percent inhibition for each mid-signal well passes the criteria. Mid-signal wells in each plate had a standard deviation less or equal to 20 %, day 1 plate 3 displaying unusual tight signals (Figure 33).

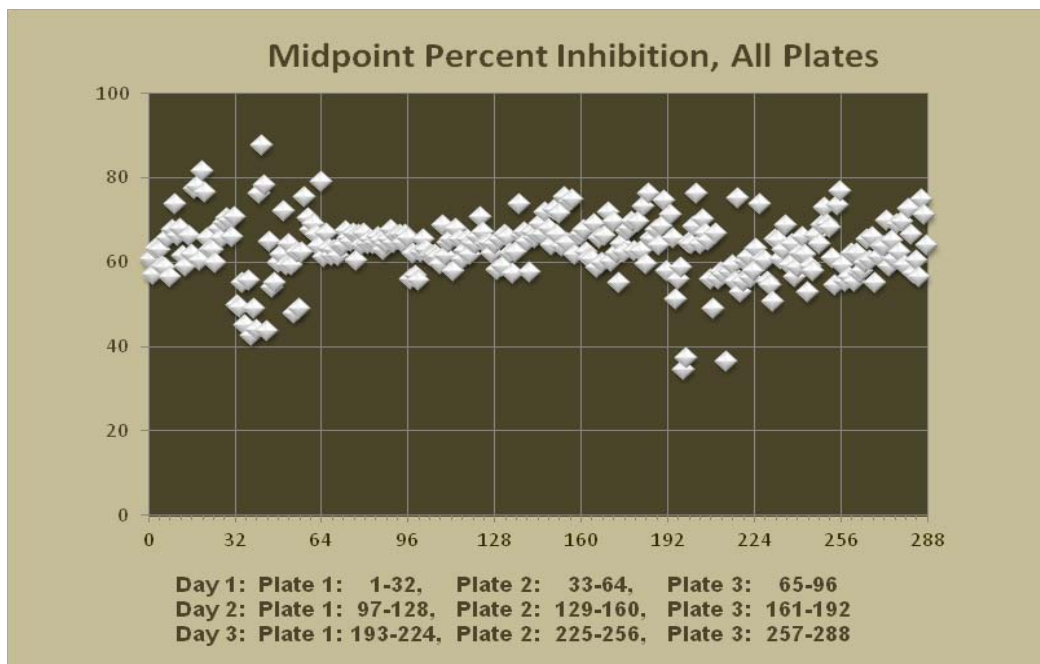


Figure 33. Midpoint Percent Inhibition, All Plates. Each plate is plotted against percentage inhibition [%].

As the validation checklist shows, all criteria for inter-plate tests are met. For intra-plate tests all criteria is met, except for the spatial uniformity assessment containing drift and edge effects (Table 7).

Table 7. Validation Checklist.

<i>Validation Checklist</i>		
Intra-Plate Tests		Meets Criterion ?
1	Check for drift / edge effects in all plates	No
2	All max (HI) signal CV's < 20%	Yes
3	All mid signal (unnormalized) CV's < 20%	Yes
4	All normalized mid signal (mid %) SD's < 20	Yes
5	All min (LO) SD's < Min(max (HI) SD, mid SD)	Yes
6	All SW's > 2	Yes
7	All Z Factors > 0.4 (and < 1 ; must pass one of 6 or 7)	Yes
Inter-Plate Tests		
1	All within-day fold shifts < 2	Yes
2	All Average (between-)Day fold shifts < 2	Yes

Unfortunately, spatial uniformity assessment failed as there were several drift effects and edge effects detected in the plates. In five cases, the max signal displayed drift effect, where the drift was more than 20 % and one case of mid signal displaying drift effect of 30 %. Edge effects were detected as the last column in each plate gave values far below the mean. Systematical source of variation can be seen as each plate displayed values that were decreasing from left to right in each row and from top to bottom in each column.

8.9 Compound Screening

Before the actual and final compound screening, a series of preliminary screenings were performed in order to gain a better understanding of the compound functionality. Preliminary experiments were also necessary for the assessment of assay development as seen in chapter 8.6.

The actual and final compound screening was performed with the final assay design after performing plate uniformity and signal variability assessment (See chapter 8.7). Furthermore, the compound screening was performed three times similarly and assessed together with the preliminary screenings.

8.9.1 Preliminary Compound Screening

The preliminary compound screening was performed in four screenings altogether, using partially different compounds. Each compound was evaluated using $\pm 20\%$ cut-off limits in relation to negative control, namely +DMSO.

In the first screening, from the tested compounds, Compound 1908 resulted in 22 % and Compound 5174 in 18 % inhibition in relation to negative control. All other compounds were within $\pm 10\%$ in relation to negative control. Positive control (NTH1) resulted in 85 % inhibition in relation to negative control (Figure 34).

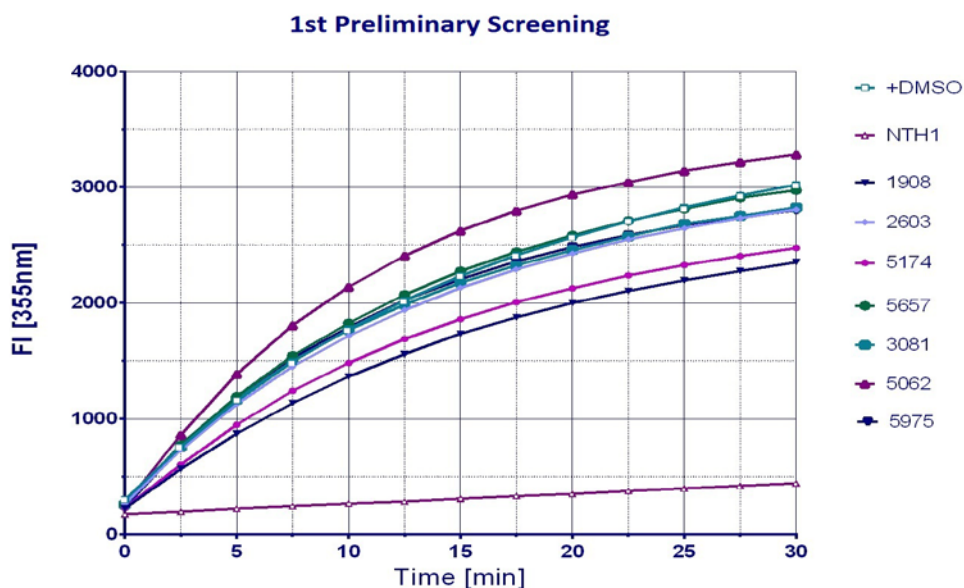


Figure 34. First Preliminary Screening.

In the second screening, several compounds resulted in more than 20 % inhibition in relation to negative control. In the first diagram, Compound 3129 resulted in 18 % inhibition when all other compounds were within $\pm 10\%$ limits. Positive control resulted in 68 % inhibition in relation to negative control (Figure 35).

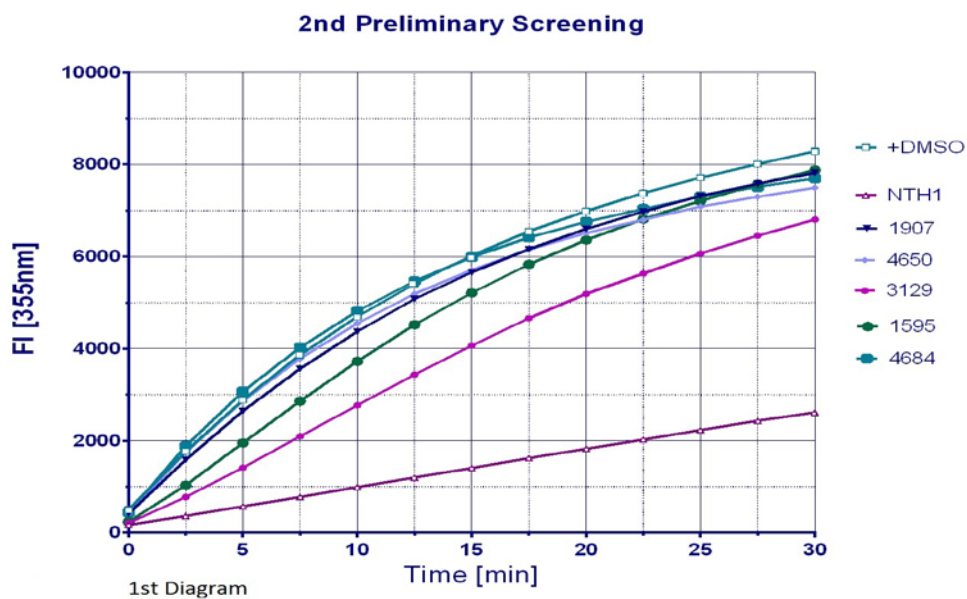


Figure 35. Second Preliminary Screening, 1st Diagram.

In the second diagram, it can be seen how compounds 2881, 6934 and 9128 resulted in over 20 % inhibition in relation to negative control. The two other compounds were within $\pm 20\%$ cut-off limits (Figure 36).

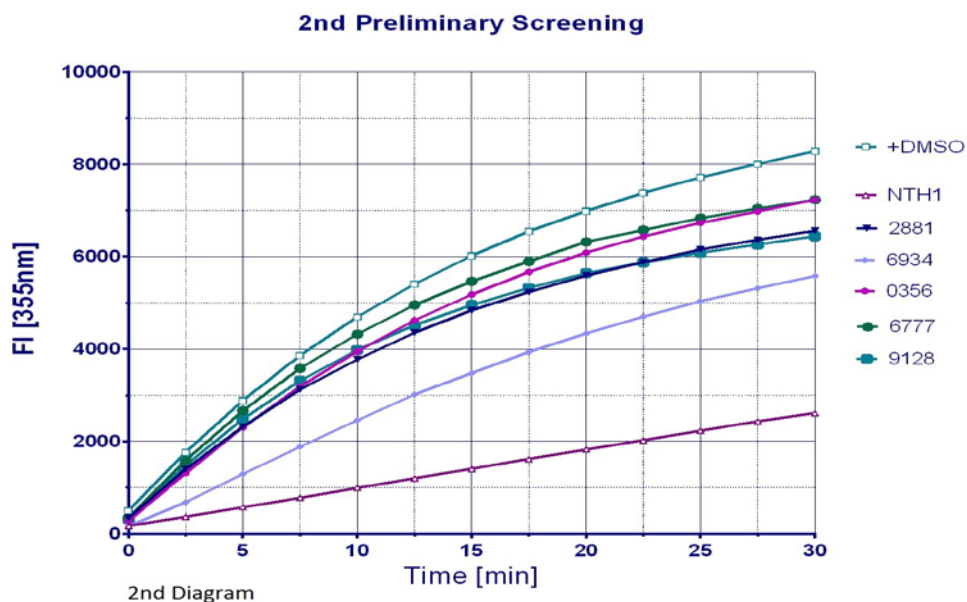


Figure 36. Second Preliminary Screening, 2nd Diagram.

None of the tested compounds inhibited the reaction in the third screening; instead they enhanced the conversion rate of AMC. In the first diagram, the compounds 5062 and

5975 enhanced the reaction with over 75 %, wherein the remaining compounds enhanced the reaction more than 20 % (Figure 37).

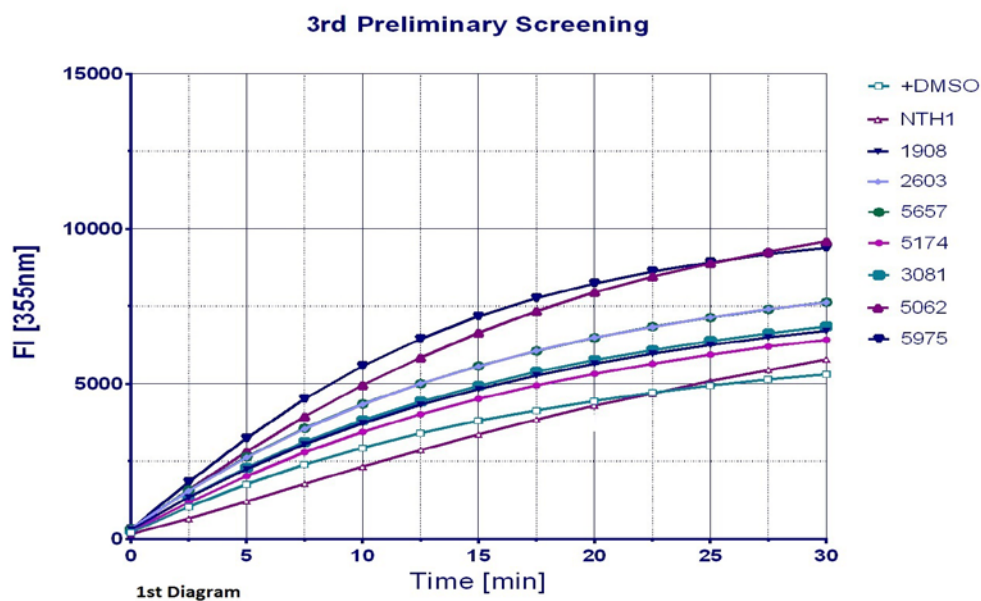


Figure 37. Third Preliminary Screening, 1st Diagram.

In the second diagram, Compound 1907 remained within 10 % limits, wherein all other compounds enhanced the conversion rate more than 20 % in relation to negative control +DMSO. Furthermore, as seen in both diagrams, the positive control NTH1 is not inhibiting the reaction rate and is within 10 % limits (Figure 38).

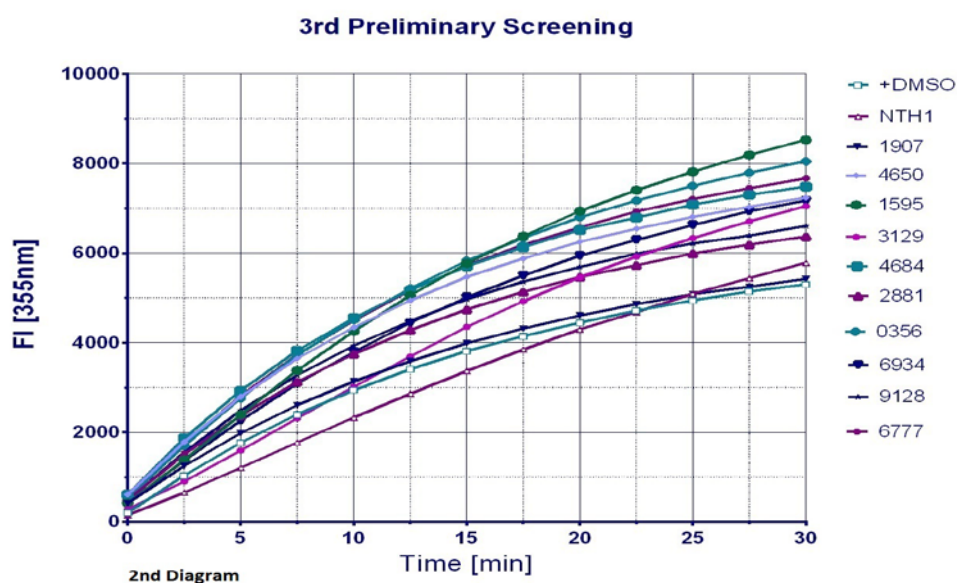


Figure 38. Third Preliminary Screening, 2nd Diagram.

In the fourth screening, the Compound 3560 inhibited the conversion rate by 42 %, wherein from remaining compounds all were within 20 % cut-off limits with the exception of compounds 1571 (68 %) and 6617 (81 %). On a further note, the positive control NTH1 inhibited the reaction rate of AMC conversion only by 13 % (Figure 39).

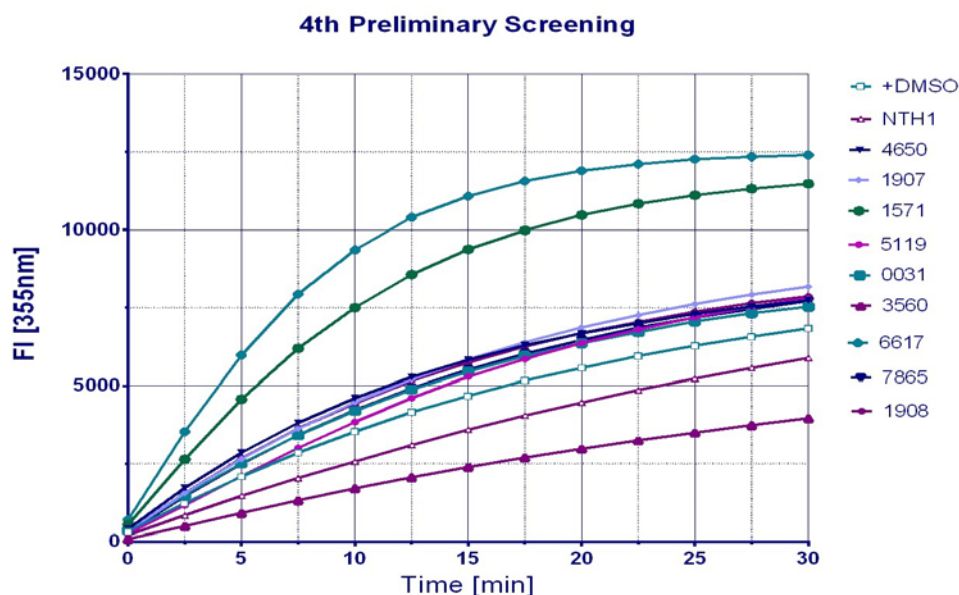


Figure 39. Fourth Preliminary Screening.

During preliminary compound screening, it became apparent that the compounds as well as positive control NTH1 lost their activity during the screening. Furthermore, some compounds enhanced the conversion rate of AMC significantly, although in previous screening they inhibited the conversion rate of AMC.

8.9.2 Final Compound Screening

After finalizing the assay design, the selected compounds were screened three times in a row in order to recognize potential drugs targeting rhHepsin, as well as to ensure the functionality of the assay design.

Compounds were selected based on preliminary screening, including previously reaction inhibiting compounds and one additional NTH1 “Misa” that had proven to inhibit the reaction. For the final screening compounds were kept in 0°C during the assay processing and protected from light during 30 minute incubation. Factors that could not be

influenced during the assay processing and incubation, were changes in room temperature and exposure to light between assay procedures.

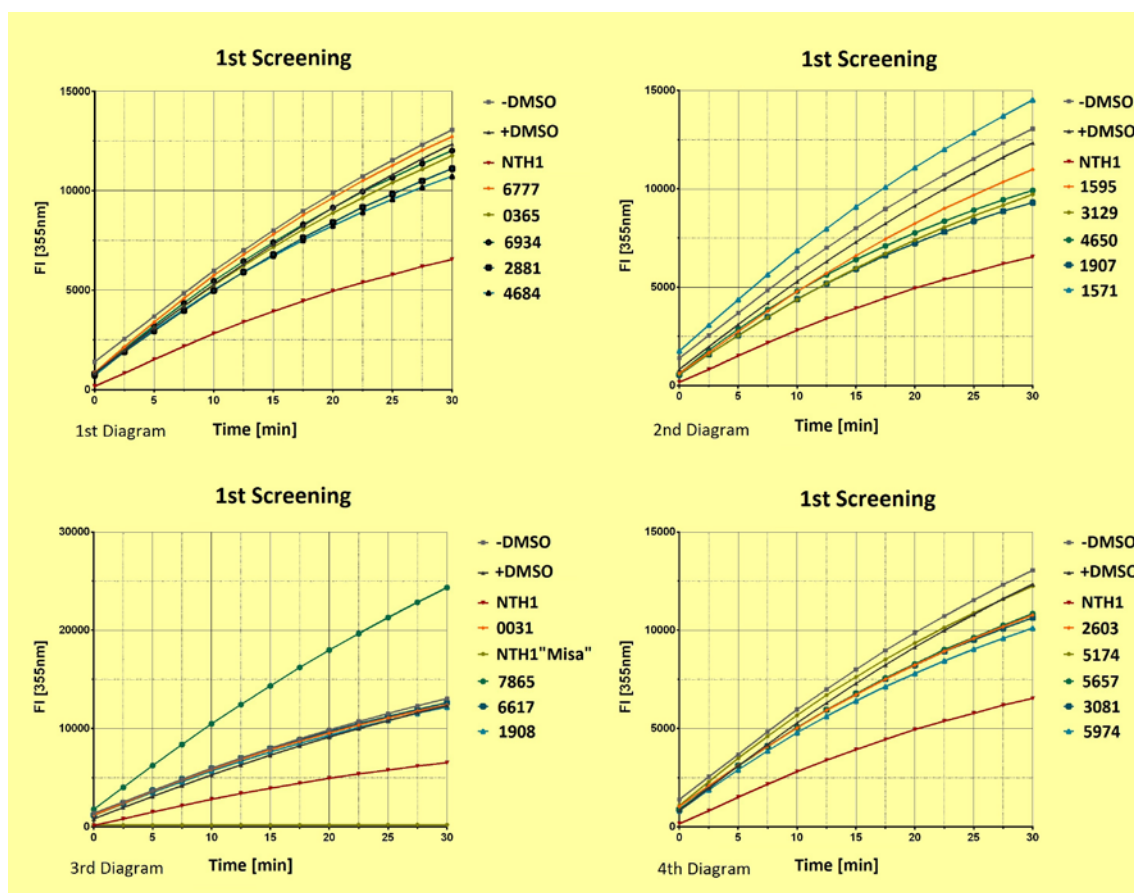


Figure 40. Final Compound Screening, 1st Screening.

In the first screening, compounds 3129 and 1907 inhibited the reaction with more than 20 % (Figure 40, Diagram 2) and NTH1 "Misa" with 98 % (Figure 40, Diagram 3). Remaining compounds were within ± 20 % cut-off limits except, for Compound 7865 that enhanced the reaction with 97 % (Figure 40, Diagram 3).

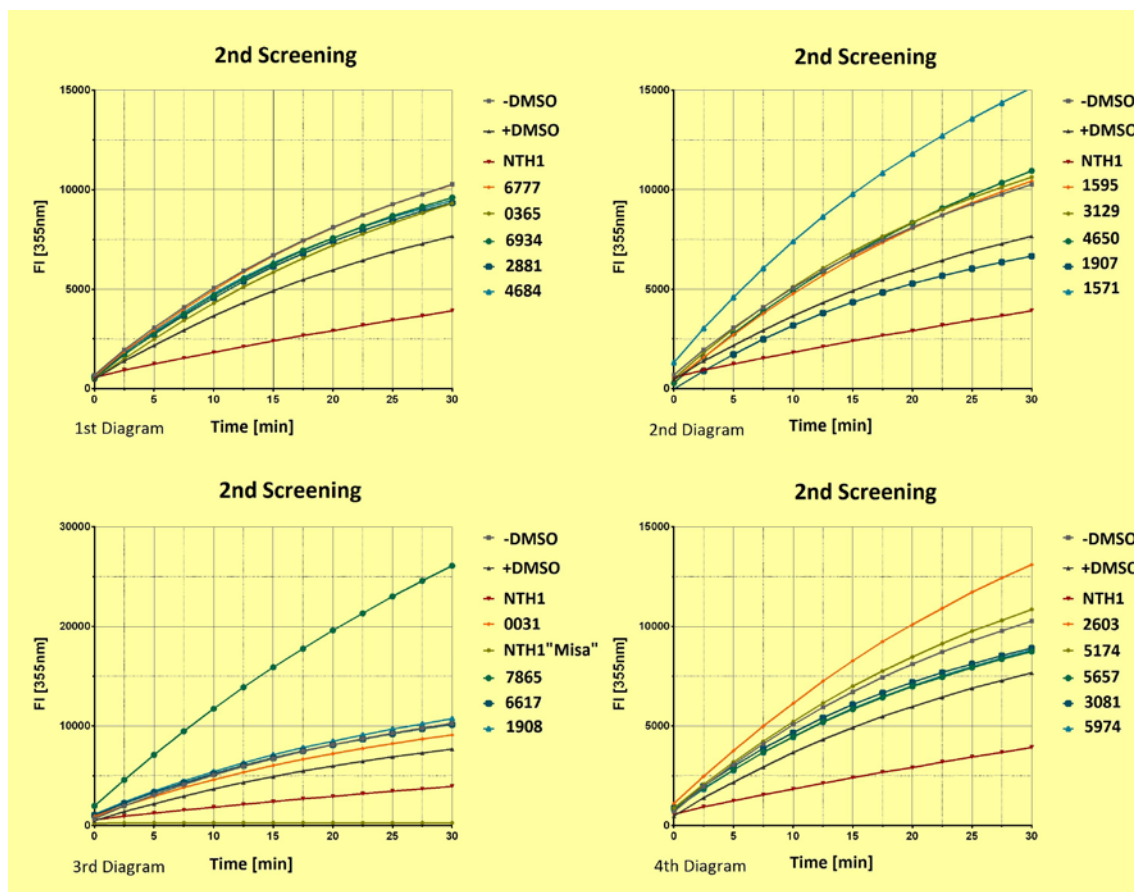


Figure 41. Final Compound Screening, 2nd Screening.

None of the compounds in the second screening inhibited the reaction except for NTH1 "Misa" with 97 % (Figure 41, Diagram 3). Five of the compounds were within ± 20 % cut-off limits, wherein remaining compounds enhanced the reaction i.e. Compound 1571 with 97 % (Figure 41, Diagram 2) and Compound 7865 with 240 % (Figure 41, Diagram 3).

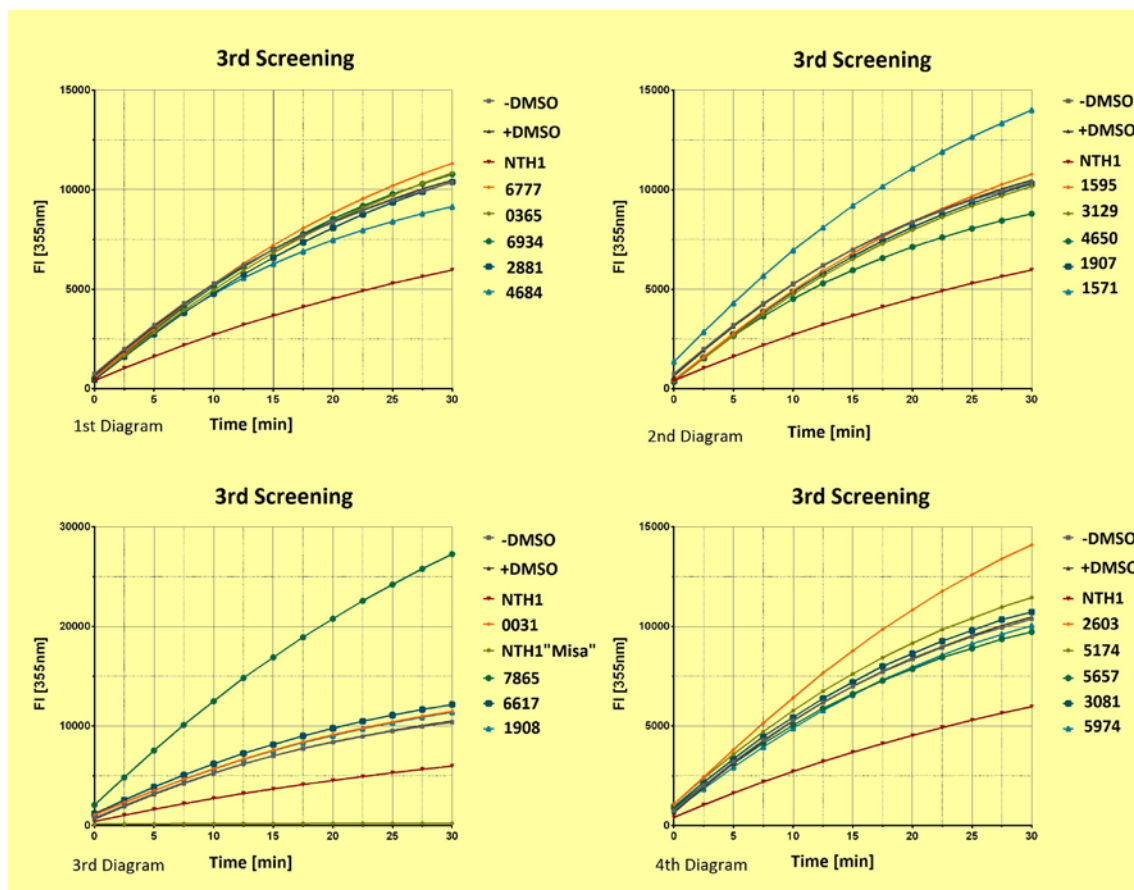


Figure 42. Final Compound Screening, 3rd Screening.

The third screening gave similar results as none of the compounds inhibited the reaction except the NTH1 "Misa" with 98 % (Figure 42, Diagram 3), whereas three of the compounds enhanced the reaction i.e. compound 7865 with 160 % (Figure 42, Diagram 3). Remaining compounds were within ± 20 % cut-off limits (Figure 42).

After summarizing the assessment of preliminary screening and final screening, none of the compounds showed specifically to inhibit, to remain within ± 20 % cut-off limits or to enhance the reaction. On the other hand, each of the screened compounds, with the exception of "NTH1" Misa, demonstrated at least two of three reaction patterns. The results are outlined below (Table 8).

Table 8. Summary of Compound Screening.

Lab No.	Date	ID	Preliminary Screening				Final Screening		
			11.02.2014	11.02.2014	11.02.2014	11.02.2014	27.04.2014	27.04.2014	27.04.2014
			1st Screen	2nd Screen	3th Screen	4th Screen	5th Screen	6th Screen	7th Screen
1		9128		YES	ENH				
2		6777		NO	ENH		NO	ENH	NO
3		0356		NO	ENH		NO	ENH	NO
4		6934		YES	ENH		NO	ENH	NO
5		2881		YES	ENH		NO	ENH	NO
6		4684		NO	ENH		NO	ENH	NO
7		1595		NO	ENH		NO	ENH	NO
8		3129		NO	ENH		YES	ENH	NO
9		4650		NO	ENH	NO	NO	ENH	NO
10		1907		NO	NO	NO	YES	NO	NO
11		5119				NO			
12		1571				ENH	NO	ENH	ENH
13		0031				NO	NO	NO	NO
14		3560				YES			
15		7865				NO	ENH	ENH	ENH
16		6617				ENH	NO	ENH	NO
17		1908	YES		ENH	NO	NO	ENH	NO
18		2603	NO		ENH		NO	ENH	ENH
19		5174	NO		ENH		NO	ENH	NO
20		5657	NO		ENH		NO	NO	NO
21		3081	NO		ENH		NO	NO	NO
22		5062	NO		ENH				
23		5975	NO		ENH		NO	NO	NO
24		NTH1 "Misa"					YES	YES	YES

After analyzing the results using $\pm 20\%$ cut-off limits, it can be concluded that using a broader range of cut-off limits would not influence the overall assessment. It is evident that the screened compounds may either inhibit or enhance the reaction depending on the conditions throughout the assay procedure. The results with obtained values are outlined below (Table 9).

Table 9. Summary of Screenings Values in Percentage.

Date	ID	Preliminary Screening			Final Screening			
		Percentage in relation to negative control (reference value)						
Lab No.		1st Screen	2nd Screen	3th Screen	4th Screen	5th Screen	6th Screen	7th Screen
1	9128		-22,26	24,61				
2	6777		-12,73	44,66		3,12	33,71	8,11
3	0356		-12,73	51,82		-4,65	21,58	3,51
4	6934		-32,66	35,26		-2,63	25,29	2,90
5	2881		-20,84	20,17		-9,97	21,88	-0,81
6	4684		-7,11	41,17		-13,03	23,52	-12,66
7	1595		-4,88	60,89		-10,96	36,14	2,87
8	3129		-17,92	32,91		-21,21	38,70	-2,85
9	4650		-9,54	36,54	13,23	-19,56	42,77	-16,10
10	1907		-5,65	2,30	19,69	-24,57	-13,11	-1,68
11	5119				14,13			
12	1571				67,89	17,76	97,28	33,70
13	0031				10,21	0,67	18,62	9,39
14	3560				-42,05			
15	7865				12,98	97,38	240,34	160,24
16	6617				81,45	2,39	32,42	15,93
17	1908	-22,18		26,49	15,14	-1,15	39,93	8,68
18	2603	-7,04		43,72		-12,64	70,90	34,58
19	5174	-18,05		21,05		-0,73	41,53	9,31
20	5657	-1,54		43,98		-12,07	13,91	-7,18
21	3081	-6,48		29,08		-13,79	16,25	2,39
22	5062	8,62		80,88				
23	5975	-7,25		76,98		-18,06	14,93	-4,17
24	NTH1 "Misa"					-98,09	-96,56	-98,01

Since the negative controls gave similar FI [355] values and the positive control NTH1 inhibited the reaction from 68 % to 43 %, as well as NTH1 "Misa" showing very similar results, the assay design seems to work well.

8.10 Preliminary Experiment Cell-based Assay

The performance of the existing cell-based assay protocol was assessed in a series of preliminary experiments. The experiments were conducted under similar conditions, where each well contained 50 000 cells and -dox and +dox were run parallel. After 48 hour incubation in the 96 well-plate, the conversion of AMC could be measured only in few wells (Figure 43).

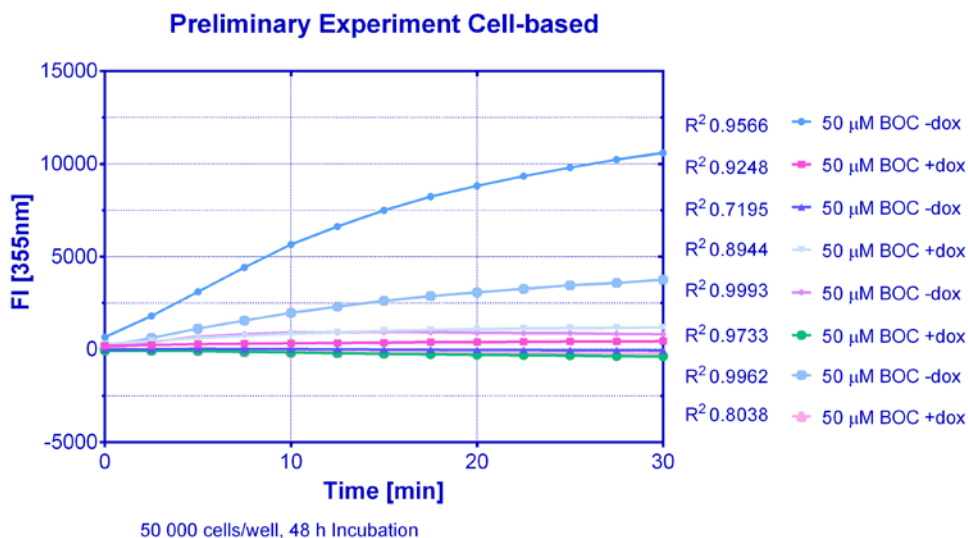


Figure 43. Preliminary Experiment, Cell-based Assay.

As doxycyclin had no influence on the results, possible reasons for large variation can be differences between cell viability in each well after the incubation time. As most wells showed no signs of reaction it can be assumed that the cells had lost their viability.

8.11 Cell Amount and Incubation Time

In order to adjust the cell amount and incubation time for high cell viability, a series of experiments were conducted. The series was performed in three days with three 96 Well-Plate so that the cell were seeded at each plate at the same day with different cell amounts by row and each plate incubated different time (Appendix 6). Before measuring, the 96 well-plates were inspected by microscope in order to ensure the cells fill the wells evenly.

After a 24-hour incubation, the cell viability seems to be good as the reaction rates correlate with the cell amounts in each well (Figure 44). Parallel measurements with doxycyclin gave contradicting results as the higher cell amounts 150 000 cells and 70 000 cells had faster reaction rates with -dox contrary to lower cell amounts where +dox gave higher reaction rates. The differences in results with doxycyclin treatment were not significant except in the 150 000 cell per well.

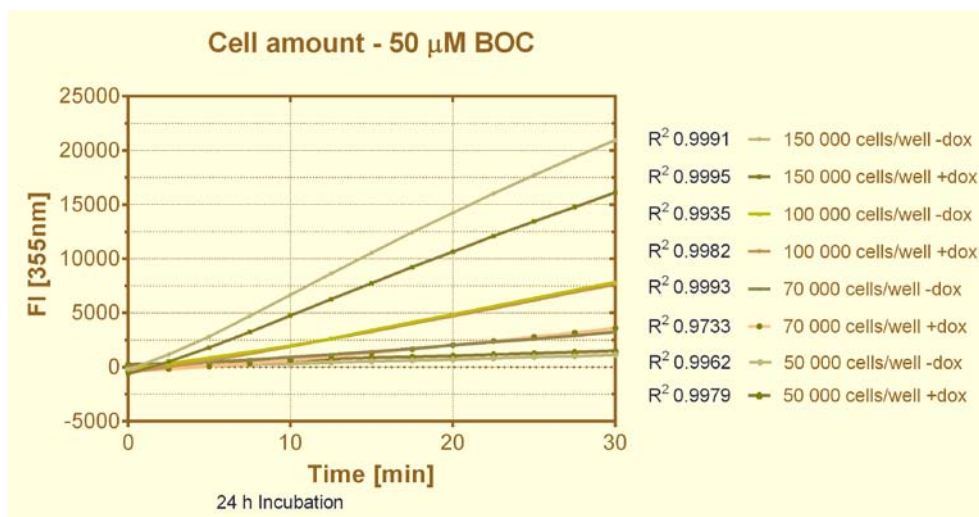


Figure 44. Cell Amount, 24 hours incubation.

After a 48-hour incubation time, the variations between cell amount and doxycyclin treatment became apparent as the reaction rates did not correspond to cell amount. The wells that were not treated with doxycyclin had faster reaction rates with every cell amount, whereas the wells treated with doxycyclin containing 50 000 cells and 70 000 cells resulted in very similar reaction rate being notably lower to 50 000 cells/well -dox (Figure 45).

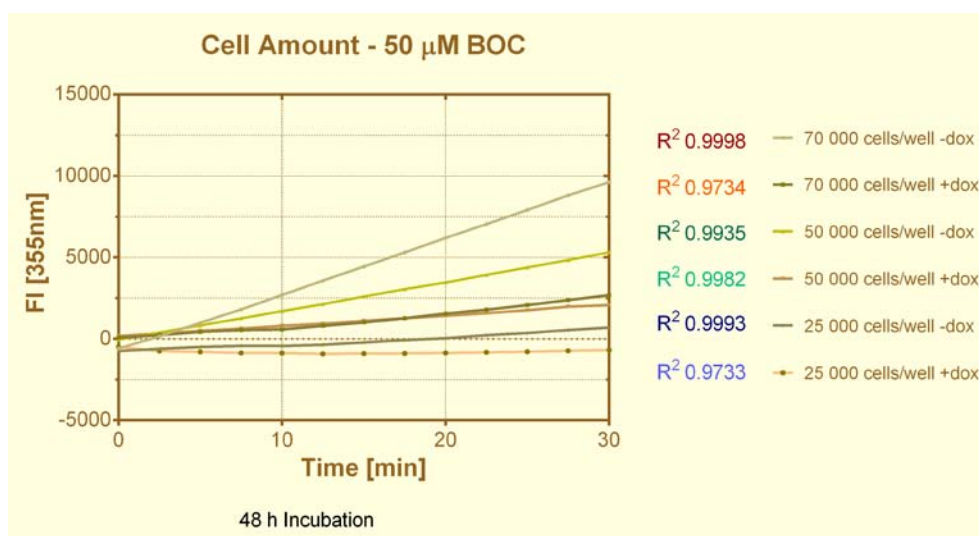


Figure 45. Cell Amount, 48 hour incubation.

After a 72-hour incubation, there could not be measured conversion of AMC in any of the wells, which is most likely due to low cell viability. For cell viability the 24-hour incubation seems to be the best option.

8.12 Kinetics Cell-based

Kinetic model for enzyme in cell-based assay was performed in the same manner as for biochemical assay (See chapter 8.2.2). Only in this case the enzyme measured was produced by the cells and the doxycyclin treated wells were measured parallel with the non-treated wells.

Doxycyclin treated wells resulted in faster reaction rates in all cases except for 30 μM BOC, which gave slow reaction rates with doxycyclin treated and non-treated wells. The lower substrate concentrations resulted in faster reaction rates in all cases (Figure 46).

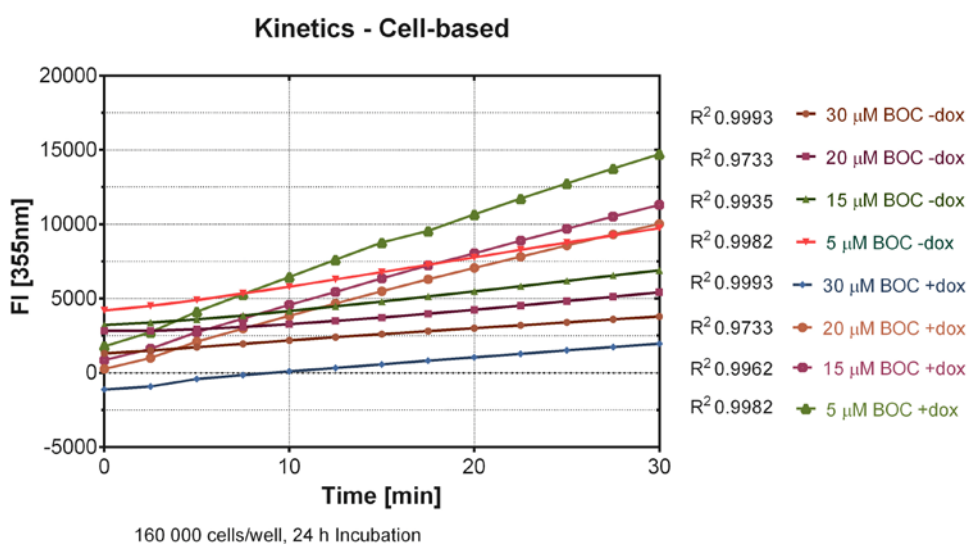


Figure 46. Kinetics, Cell-based Assay.

These results can be considered as indicative due to low and too few substrate concentrations, as the reaction progress curve did not form saturation curve nor did reach plateau. The reaction progress curve also suggest that the cell viability may have been low in the most wells.

8.13 K_m and V_{max} for Cell-based Assay

K_m and V_{max} for cell-based assay was performed in same manner as for biochemical assay (See chapter 8.3). As there were no previous results indicating possible value for

K_m , the substrate concentrations were distributed using 2-fold dilution scheme from 1000 μM covering 1024-fold concentration range.

Whereas the results for K_m in biochemical assay were constant containing only little variation, the results for K_m in cell-based assay were not unambiguous. The average of five measurements gave 36.50 μM for K_m value 1510 (pmol/min/ug) for V_{max} (Figure 47).

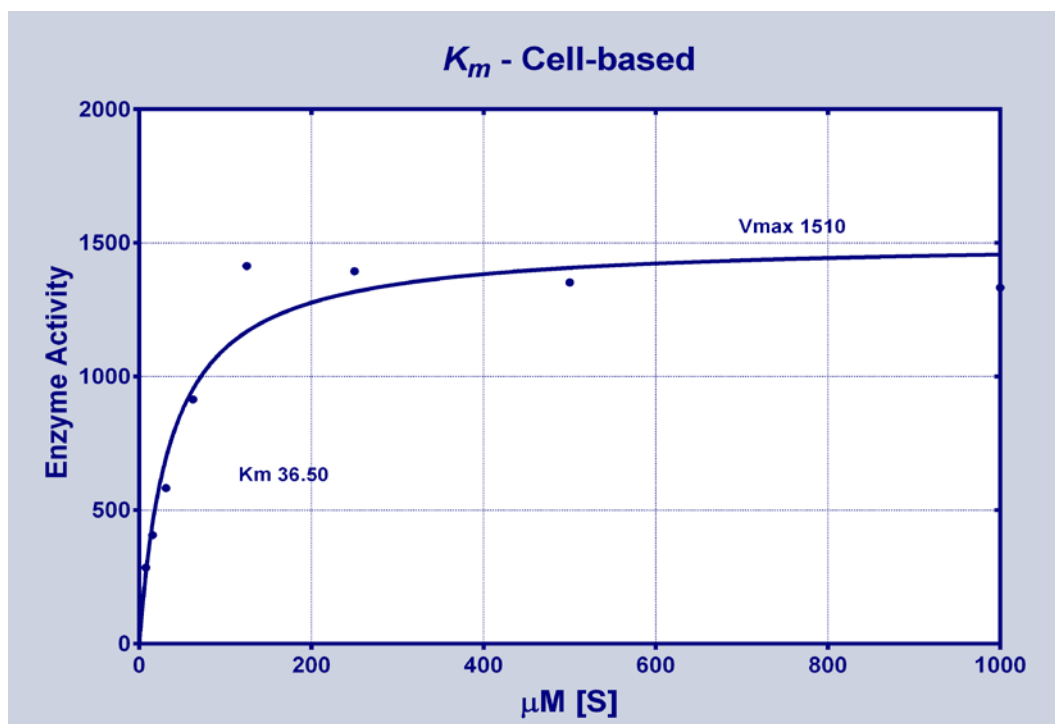


Figure 47. K_m & V_{max} , Cell-based Assay.

These results can be considered as indicative as the results contained large variations and as previous results show, higher than 36.50 μM substrate concentrations will not form saturation curve indicating a higher K_m value. In addition, the cell viability should be further examined as well as the usage of doxycyclin. Running parallel measurements with doxycyclin has displayed contradictory results leading to question if doxycyclin has an additional effect to the enzyme-substrate equilibrium.

9 Conclusion and Discussion

The development of cell-based assay could not be finalized in context of this thesis due to the extent of the project and lack of time caused by replacement of the original

equipment. The biochemical assay could be completed with existing assay parameters and signal variability assessment, whereas the spatial uniformity assessment did not meet criteria due to material effects.

9.1 Biochemical Assay

Before the project began, the existing assay protocol delivered differentiating results as the screened compounds could not be measured twice with similar results. The positive control NTH1 behaved in same manner and the causes of variation could not be traced. Hence, the optimizing of the assay protocol contained the aspect of investigating sources of variation. When defining initial velocity conditions, first indications of the sources of variation could be seen during active site titration as parallel experiments resulted in very different reaction rates. The same phenomena were seen during preliminary compound screening meaning timing and temperature control were necessary for functioning assay processing. In addition, the loss of activity of both the compounds and positive control NTH1 during the preliminary compound screening were significant.

The above mentioned sources of variation can be controlled with the right setting. Factors that cannot be controlled by test set up include enzyme instability as seen in the enzyme kinetics measurement. In addition the enzyme concentration needed to be optimized to 0.1 nM as higher concentrations resulted in product inhibition, reverse reaction and substrate limitation as the conversion of AMC by BOC substrate is fast. The enzyme concentration can be further optimized to 0.2 nM with the prerequisite that the equipment is able to measure the reaction under initial velocity conditions.

The DMSO compatibility limit was set to 0.5 % DMSO as this would cause an inhibition of 7 % in the reaction. The DMSO compatibility was done with the same DMSO used for compound dissolvent, and it would be advisable to verify the compatibility by new batches as there were several DMSO LOTs in use and they delivered differentiating results as seen in the activity loss screening. In addition, the DMSO causes an increase in background level by concentration wise.

The IC_{50} value for mid-level signal was determined as 6 μ M positive control NTH1 as the guideline for IC_{50} is a concentration that causes more than 50 % inhibition in conversion of AMC. In signal variability assessment, all criteria for all signal levels was met

for functioning assay design, wherein the spatial uniformity assessment failed due to material effects.

The final compound screening affirmed the functioning of assay design as all signal levels delivered stable readings, whereas the positive control NTH1 decreased in activity during the screening from 68 % inhibition to 48 % inhibition. The screened compounds delivered differentiating results that was caused by changes in room temperature during 30 minute incubation. The limits for decrease in activity for positive control can be further discussed as the assay design is working with the defined parameters. Another aspect is how to proceed with the temperature during incubation. In case the compound structure is robust, it will inhibit the reaction rate despite changes in room temperature as proved by positive control NTH1 and NTH1 "Misa". Nonetheless, for a congruent assessment of the compounds, it would be recommendable to control the incubation temperature as this would exclude the possibility of non-functioning assay design and false positives.

9.2 Cell-based Assay

All results regarding cell-based assay can be considered indicative as the time scope was too limiting for thorough experimental design. Another aspect is the cell viability that would need further investigation as it is the main source of variation. According to the results, it would be recommendable to set up the assay after the cells have attached to the 96-well plate keeping the incubation time uniform and as short as possible.

As seen in cell amount and incubation time adjustment, the cell amount can be increased if the incubation time is decreased. The experimental design consisted of 25 000 cells per well to 150 000 cells per well as the cells to be seeded were growing too scarce for a larger scale experimental design. It is also possible that the cell viability was affected by scarce cell growth conditions. It would be advisable to run the experiment with larger cell amount and range including several repetitions.

The usage of doxycyclin illustrates another issue. The experiments run parallel with doxycyclin delivered contradictory results to a certain degree, but in this point it cannot be concluded if this is due to cell viability or due to some combined effect by doxycyclin with the substrate.

The development of cell-based assay can be continued by investigating further the above mentioned questions. The vital point is to ensure the cell viability after seeding the cells into a 96-well plate by taking into consideration the maximum amount of cells that can be seeded. Incubation time and the usage of doxycyclin also need further optimization. If these questions are solved, the development can continue by determining K_m and V_{max} , DMSO compatibility and signal levels for signal variability assessment.

References

- Antalis T. M., Bugge T., Wu Q. 2011: Membrane-anchored serine proteases in health and disease. *Progress in Molecular Biology and Translational Science* 99, p. 1–50.
- Antalis T. M., Buzza M. S., Hodge K. M., Hooper J. D., Netzel-Arnett S. 2010: The Cutting Edge: Membrane Anchored Serine Protease Activities in the Pericellular Micro-environment. *Biochemical Journal* 15, p. 325–346.
- Brooks H. B., Geeganage S., Kahl S. D., Montrose C., Sittampalam S., Smith M. C., Weidner J.R. 2012: *Guidance for Assay Development & HTS: Basics of Enzymatic Assays for HTS*. Eli Lilly & Company, Indianapolis, IN, p. 1-13.
- Chevillet J. R., Park G. J., Bedalov A., Simon J. A., Vasioukhin V. I. 2008: Identification and characterization of small-molecule inhibitors of hepsin. *Molecular Cancer Therapy* 7, p. 3343-3351.
- Copeland R. A. 2000: *Enzymes: A Practical Introduction to Structure, Mechanism, and Data Analysis*. Wiley-VCH, Inc., p. 109-186.
- Copeland R. A. 2013: *Evaluation of Enzyme Inhibitors in Drug Discovery: A Guide for Medicinal Chemists and Pharmacologist*. John Wiley & Sons, Inc., Hoboken, New Jersey, p. 25-166.
- Eastwood B. J., Iturria S. J., Iversen P. W., Montrose C., Moore r., Sittampalam S. 2007; *Assay Guidance Manual: Guidance for Assay Development & HTS*, p. 7-18.
- Graph Pad Prism User Guide. 2014 Online Document. Graph Pad Software Inc. < <http://cdn.graphpad.com/docs/prism/6/Prism-6-User-Guide.pdf>> Cited 13.01.2013
- IHC/ICC: Hepsin. 2014. Online Document. R&D Systems, Inc. < http://www.rndsystems.com/ihc_molecule_images.aspx?m=3878> Cited 04.02.2014.
- Iversen P. W., Beck B., Chen Y., Dere W., Devanarayan V., Eastwood B. J., Mark W. Farmen M. W., Stephen J. Iturria S. J., Montrose C., Roger A. Moore R. A., Weidner J. R., Sittampalam S. G. 2012: *Guidance for Assay Development & HTS: HTS Assay Validation*. Eli Lilly & Company, Indianapolis, IN, p. 1-35.
- Katz B. A., Mackman R., Luong C., Radika K., Martelli A., Sprengeler P. A., Wang J., Chan H., Wong L. 2000: Structural basis for selectivity of a small molecule, S1-binding, submicromolar inhibitor of urokinase-type plasminogen activator. *Chemistry and Biology* 7, p. 299-312.
- Lopez-Otín C., Bond J. S. 2008: Proteases: Multifunctional Enzymes in Life and Disease. *The Journal of Biological chemistry* 283, p. 30433–30437.
- Lopez-Otin C., Matrisian L. M. 2007: Emerging roles of proteases in tumour suppression. *Nature reviews. Cancer* 7, p. 800-808.
- McKinney J. D., Richard A., Waller C., Newman M. C., Gerberick F. 2000: The Practice of Stucture Activity Relationship (SAR) in Toxycology. *Toxicological Sciences* 6, p. 8-17.

Meerbrey K., Hu G., Kessler J., Roarty K., Li M., Fang J., Herschkowitz J., Burrows A., Ciccia A., Sun T., Schmitt E., Bernardi R., Fu X., Bland C., Cooper T., Schiff R., Rosen J., Westbrook T., Elledge S. 2011: The pINDUCER lentiviral toolkit for inducible RNA interference in vitro and in vivo. *Proc Natl Acad Sci U S A* 108, p. 3665–3670.

Netzel-Arnett S., Hooper J. D., Szabo R., Madison E. L., Quigley J. P., Bugge T. H., Antalis T. M. 2003: Membrane anchored serine proteases: A rapidly expanding group of cell surface proteolytic enzymes with potential roles in cancer. *Cancer and Metastasis Reviews* 22, p. 237-258.

Partanen J., Tervonen T., Myllynen M., Lind E., Imai M., Katajisto P., Dijkgraaf G., Kovanen P., Mäkelä T., Zena Werb Z., Klefström J. 2012: Tumor suppressor function of Liver kinase B1 (Lkb1) is linked to regulation of epithelial integrity. *PNAS* 109, p. 388–3

Sastry G. M., Dixon S., Sherman W. 2011: Rapid Shape-Based Ligand Alignment and Virtual Screening Method Based on Atom/Feature-Pair Similarities and Volume Overlap Scoring. *Journal of Chemical Information and Modeling* 51, p. 2455-2466

Somoza J. R., Ho J. D., Luong C., Ghatge M., Sprengeler P. A., Mortara K., Shrader W. D., Sperandio D., Chan H., McGrath M. E., Katz B. A. 2003: The Structure of the Extracellular Region of Human Hepsin Reveals a Serine Protease Domain and a Novel Scavenger Receptor Cysteine-Rich (SRCR) Domain. *Structure* 11, p. 1123–1131.

Szymański P., Markowicz M., Mikiciuk-Olasik E. 2012: Adaptation of High-Throughput Screening in Drug Discovery - Toxicological Screening Tests. *International Journal of Molecular Sciences* 13, p. 427-452.

Turk B. 2006: Targeting proteases: successes, failures and future prospects. *Nature reviews. Drug discovery* 5, p. 785-799.

Xuan J., Schneider D., Toy P., Lin R., Newton A., Zhu Y., Finster S., Vogel D., Mintzer B., Dinter H., Light D., Parry R., Polokoff M., Whitlow M., Wu Q., Parry G., 2006: Antibodies Neutralizing Hepsin Protease Activity Do Not Impact Cell Growth but Inhibit Invasion of Prostate and Ovarian Tumor Cells in Culture. *American Association for Cancer Research* 66, p. 3611-3619.

Zang R., Li D., Tang I., Wang J., Yang S. 2012: Cell-Based Assays in High-Throughput Screening for Drug Discovery. *International Journal of Biotechnology for Wellness Industries* 1, p. 31-51.

Klezovitch O., Chevillet J., Mirosevich J., Roberts R. L., Matusik R. J., Vasioukhin V. 2004: Hepsin Promotes prostate cancer progression and metastasis. *Cancer Cell* 6, p. 185-195.

Appendix 1. Activity Assay Protocol by R&D Systems



Recombinant Human Hepsin

Catalog Number: 4776-SE

DESCRIPTION	
Source	Mouse myeloma cell line, NS0-derived Arg45-Leu417 (Asp161Glu & Arg162Lys), with a C-terminal 10-His tag Accession # P05981
N-terminal Sequence Analysis	Arg45
Predicted Molecular Mass	42 kDa
SPECIFICATIONS	
SDS-PAGE	40-43 kDa, reducing conditions
Activity	Measured by its ability to cleave <i>tert</i> -butoxycarbonyl-Gln-Arg-Arg-7-amino-4-methylcoumarin (Boc-QRR-AMC). The specific activity is >20,000 pmol/min/μg, as measured under the described conditions. See Activity Assay Protocol on www.RnDSystems.com
Endotoxin Level	<1.0 EU per 1 μg of the protein by the LAL method.
Purity	>95%, by SDS-PAGE under reducing conditions and visualized by silver stain.
Formulation	Supplied as a 0.2 μm filtered solution in Sodium Acetate and NaCl. See Certificate of Analysis for details.
Activity Assay Protocol	
Materials	<ul style="list-style-type: none"> ● Activation Buffer: 0.1 M Tris, 10 mM CaCl₂, 0.15 M NaCl, 0.05 % Brij-35, pH 8.0 ● Assay Buffer: 50 mM Tris, pH 9.0 ● Recombinant Human Hepsin (rhHepsin) (Catalog # 4776-SE) ● Fluorogenic Peptide Substrate: Boc-Gln-Arg-Arg-AMC (Bachem, Catalog # I-1655), 5 mM stock in 50:50 DMSO:Methanol ● F16 Black Maxisorp Plate (Nunc, Catalog # 475515) ● Fluorescent Plate Reader (Model: SpectraMax Gemini EM by Molecular Devices) or equivalent
Assay	<ol style="list-style-type: none"> 1. Dilute rhHepsin to 100 μg/mL in Activation Buffer. 2. Incubate at 37 °C for 24 hours. 3. Dilute activated rhHepsin to 0.2 ng/μL in Assay Buffer. 4. Dilute Substrate to 200 μM in Assay Buffer. 5. Load 50 μL of the 0.2 ng/μL rhHepsin in a black well plate and start the reaction by adding 50 μL of 200 μM Substrate. Include a Substrate Blank containing 50 μL Assay Buffer and 50 μL of 200 μM Substrate. 6. Read at excitation and emission wavelengths of 380 nm and 460 nm (top read), respectively in kinetic mode for 5 minutes. 7. Calculate specific activity: $\text{Specific Activity (pmol/min/}\mu\text{g)} = \frac{\text{Adjusted } V_{\text{max}}^* \text{ (RFU/min)} \times \text{Conversion Factor}^{**} \text{ (pmol/RFU)}}{\text{amount of enzyme (}\mu\text{g)}}$ <p>*Adjusted for Substrate Blank **Derived using calibration standard 7-Amino, 4-Methyl Coumarin (AMC) (Sigma, Catalog # A-9891).</p>
Final Assay Conditions	Per Well: <ul style="list-style-type: none"> ● rhHepsin: 0.010 μg ● Substrate: 100 μM
PREPARATION AND STORAGE	
Shipping	The product is shipped with dry ice or equivalent. Upon receipt, store it immediately at the temperature recommended below.
Stability & Storage	Use a manual defrost freezer and avoid repeated freeze-thaw cycles. <ul style="list-style-type: none"> ● 6 months from date of receipt, -70 °C as supplied. ● 3 months, -70 °C under sterile conditions after opening.
BACKGROUND	
<p>Hepsin, also known as TMPRSS1, is a Type II membrane protein with an extracellular serine protease domain (1). It is most highly expressed in liver, but is also present in many other tissues, notably lung, kidney, and skeletal muscle (2). A soluble form of Hepsin lacking the transmembrane domain has been identified (3). Hepsin is capable of activating Factor VII, and may initiate blood coagulation at the cell surface (4). Hepsin is overexpressed in various human tumors, including prostate (5), and is considered to be a biomarker for prostate cancer (6). Recombinant human Hepsin was expressed as a secreted, soluble protein lacking its cytosolic and transmembrane domains. The D161E and R162K mutations were introduced into the prosequence to improve expression of the recombinant human Hepsin.</p>	
References:	
<ol style="list-style-type: none"> 1. Leytus, S.P. <i>et al.</i> (1988) <i>Biochemistry</i> 27:1067. 2. Tsuji, A. <i>et al.</i> (1991) <i>J. Biol. Chem.</i> 266:16948. 3. Li, Y. <i>et al.</i> (2005) <i>Biomed. Biochim. Acta</i> 1681:157. 4. Kazama, Y. <i>et al.</i> (1995) <i>J. Biol. Chem.</i> 270:66. 5. Dhanasekaran, S.M. <i>et al.</i> (2001) <i>Nature</i> 412:822. 6. Wu, Q. and Parry, G. (2007) <i>Front. Biosci.</i> 12:5052. 	

Appendix 2. Plate Format for Plate Uniformity and Signal Variation

Interleaved-Signal format for three day three plate signal variation assessment.

Plate 1

	1	2	3	4	5	6	7	8	9	10	11	12
A	H	M	L	H	M	L	H	M	L	H	M	L
B	H	M	L	H	M	L	H	M	L	H	M	L
C	H	M	L	H	M	L	H	M	L	H	M	L
D	H	M	L	H	M	L	H	M	L	H	M	L
F	H	M	L	H	M	L	H	M	L	H	M	L
G	H	M	L	H	M	L	H	M	L	H	M	L
H	H	M	L	H	M	L	H	M	L	H	M	L
I	H	M	L	H	M	L	H	M	L	H	M	L

Plate 2

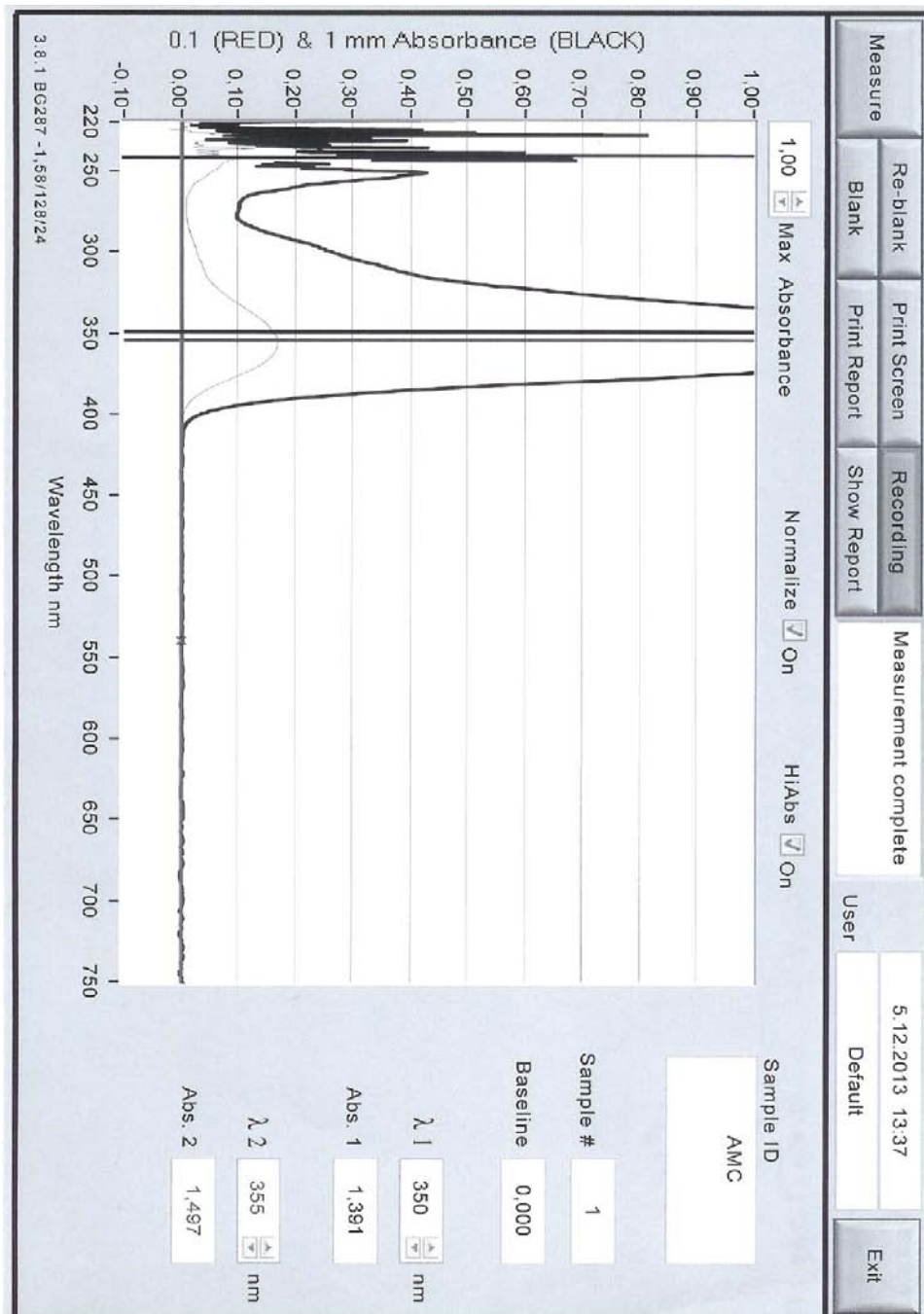
	1	2	3	4	5	6	7	8	9	10	11	12
A	L	H	M	L	H	M	L	H	M	L	H	M
B	L	H	M	L	H	M	L	H	M	L	H	M
C	L	H	M	L	H	M	L	H	M	L	H	M
D	L	H	M	L	H	M	L	H	M	L	H	M
F	L	H	M	L	H	M	L	H	M	L	H	M
G	L	H	M	L	H	M	L	H	M	L	H	M
H	L	H	M	L	H	M	L	H	M	L	H	M
I	L	H	M	L	H	M	L	H	M	L	H	M

Plate 3

	1	2	3	4	5	6	7	8	9	10	11	12
A	M	L	H	M	L	H	M	L	H	M	L	H
B	M	L	H	M	L	H	M	L	H	M	L	H
C	M	L	H	M	L	H	M	L	H	M	L	H
D	M	L	H	M	L	H	M	L	H	M	L	H
F	M	L	H	M	L	H	M	L	H	M	L	H
G	M	L	H	M	L	H	M	L	H	M	L	H
H	M	L	H	M	L	H	M	L	H	M	L	H
I	M	L	H	M	L	H	M	L	H	M	L	H

Appendix 3. Adjustment of AMC standard Reference

The Standard Reference was measured by NanoDrop (ThermoScientific 2010) in wavelengths of 350 nm and 355 nm. The standard stock dilution 1 mM was diluted accordingly to concentration measured by NanoDrop..



Appendix 4. Results of System Capacity and Linearity

Results of 55 minutes measurement with eleven AMC concentrations. Blank values are excluded as the fluorescence intensities are blank corrected values.

Dilution		Obtained Intensity values in 355nm												
No.	AMC [μ M]	0min	5min	10min	15min	20min	25min	30min	35min	40min	45min	50min	55min	
1	100	190178,5	191449,5	190630,5	189875,5	189281	188716	188362	187447,5	186839	186616	186018,5	185423,5	
2	50	123499,5	124034	123621,5	123197,5	122612,5	122104	121946,5	121490,5	121314,5	121099,5	120782	119853	
3	25	71857,5	72091	71654	71352	71051,5	70842,5	70722	70333,5	70216,5	69959,5	69790,5	69279,5	
4	12,5	39225	39394	39068,5	38987	38730	38629	38546,5	38333,5	38197,5	38075,5	37933	37759,5	
5	6,25	20889,5	20982,5	20845,5	20701	20556,5	20402	20343,5	20203	20158,5	20120	20021,5	19872,5	
6	3,125	11105	11191,5	11051,5	11000,5	10904,5	10816	10775	10719	10660,5	10636,5	10581	10491,5	
7	1,5625	5839,5	5859	5823	5778	5715,5	5679	5649	5623,5	5577,5	5571	5546,5	5508,5	
8	0,78125	1555,5	1567	1543,5	1537	1530,5	1518,5	1503	1498	1490,5	1493	1486,5	1469,5	
9	0,390625	1475,5	1476,5	1467,5	1453,5	1442,5	1424,5	1413,5	1409,5	1406,5	1399	1386,5	1381	
10	0,195313	752	758	751	747,5	742,5	736,5	729,5	723	715,5	717,5	712	704,5	
11	0,097656	388	385,5	384	383	382	377,5	376,5	374,5	369	368,5	362	362	

Appendix 5. Best-fit values for Michaelis-Menten

Results of five measurements with 95 % confidence intervals and standard error.

Michaelis-Menten					
Best-fit values					
Vmax	398,6	357,4	395,3	304,2	281,2
Km	14,78	13,27	17,45	16,22	16,53
Std. Error					
Vmax	36,18	43,68	33,09	48,92	45,36
Km	4,729	5,852	4,962	9,011	9,169
95% Confidence Intervals					
Vmax	324,1 to 473,1	267,4 to 447,3	327,1 to 463,4	203,4 to 405,0	187,8 to 374,6
Km	5,041 to 24,52	1,222 to 25,33	7,228 to 27,67	0,0 to 34,78	0,0 to 35,41
Goodness of Fit					
Degrees of Freedom	25	25	25	25	25
R square	0,8167	0,6959	0,8538	0,6004	0,6053
Absolute Sum of Squares	115119	182994	83447	194496	164491
Sy.x	67,86	85,56	57,77	88,20	81,11
Constraints					
Km	Km > 0,0	Km > 0,0	Km > 0,0	Km > 0,0	Km > 0,0
Number of points Analyzed	27	27	27	27	27

Michaelis-Menten	
Best-fit values	
Vmax	187,0
Km	17,76
Std. Error	
Vmax	15,15
Km	5,964
95% Confidence Intervals	
Vmax	149,9 to 224,1
Km	3,170 to 32,36
Goodness of Fit	
Degrees of Freedom	6
R square	0,9092
Absolute Sum of Squares	2669
Sy.x	21,09
Constraints	
Km	Km > 0,0
Number of points Analyzed	8

